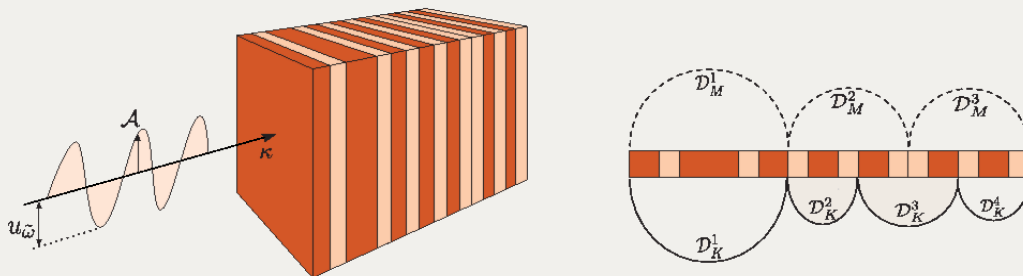




**NATIONAL AND KAPODISTRIAN
UNIVERSITY OF ATHENS**

SCHOOL OF SCIENCE - DEPARTMENT OF PHYSICS

**STUDY OF SCATTERING FROM APERIODIC
SET-UPS WITH THE USE OF LOCAL PARITY**



PANAYOTIS A. KALOZOUIMIS

Ph.D. THESIS
ATHENS 2014

This research has been co-financed by the European Union (European Social Fund – ESF) and Greek national funds through the Operational Program “Education and Lifelong Learning” of the National Strategic Reference Framework (NSRF) - Research Funding Program: Heracleitus II. Investing in knowledge society through the European Social Fund.



European Union
European Social Fund



MINISTRY OF EDUCATION & RELIGIOUS AFFAIRS, CULTURE & SPORTS
M A N A G I N G A U T H O R I T Y



Co-financed by Greece and the European Union

To Agapi and Alexandros...

ABSTRACT

We study the breaking of global discrete symmetries -specifically inversion and translation- in one-dimensional scattering set-ups. We focus on the case where the broken global symmetry is retained locally, in arbitrary domains of finite spatial extent and we find a class of space invariant, non-local currents, which are remnants of the broken global symmetry. These currents provide a mapping of the wave function from an arbitrary spatial domain, considered as source, to a target domain. The two domains are linked through the corresponding symmetry transform. The derived mapping constitutes a generalization of the Bloch and parity theorems for arbitrary finite systems which can be aperiodic or non-inversion symmetric. The obtained invariant currents are identified as remnants of the respective global symmetry, providing a systematic approach to the breaking of discrete global symmetries. The proposed method addresses successfully any combination of translation and inversion symmetry and can be applied to the study of wave propagation in aperiodic and quasi-periodic media. The fact it lies on very general symmetry arguments, combined with the Helmholtz-Schrödinger isomorphism, provide a unified framework which can be applied to the quantum optical and acoustic systems, notwithstanding their essential differences. Focusing on the parity transformation when applied to finite mirror symmetric domains, we introduce the concept of local parity (LP) and the corresponding operator. We consider non-symmetric, aperiodic scattering set-ups which can be completely decomposed in space domains where the LP symmetry is satisfied and reveal its impact on their transport properties and particularly on perfect transmission resonances (PTRs). With emphasis on the PTR manifestation and by employing the aforementioned invariant currents, we propose a classification of PTRs, based on their geometric representation on the complex plane. This classification lifts certain overlaps of alternative approaches in the existing literature and provides an unambiguous distinction between resonances based on fundamental, local symmetry principles. Finally we develop a construction principle which utilizes the simultaneous existence of different LP symmetry scales in the same set-up for the design of aperiodic wave mechanical devices with prescribed PTR properties. The implementation of this construction principle on quantum, photonic and acoustic systems, reveals its applicability in diverse systems.

CONTENTS

PREFACE	vii
INTRODUCTION	vii
1 PERIODIC AND QUASI-PERIODIC 1-D SYSTEMS	13
1.1 Introduction	13
1.2 Waves in infinite periodic media	14
1.2.1 Quantum mechanical periodic potential	14
1.2.2 Periodic dielectric array - The photonic crystal	16
1.2.3 A generalized Kronig-Penney model	18
1.3 Waves in locally periodic media	20
1.4 Waves in disordered media	23
1.5 Waves in aperiodic and quasi-periodic media	23
1.5.1 Fractal structures - Cantor filters	25
1.5.2 Quasi-periodic structures - Fibonacci filters	25
1.5.3 Structures with hybrid order	26
2 DISCRETE SYMMETRY INDUCED INVARIANTS	29
2.1 Introduction	29
2.2 The Helmholtz equation	29
2.2.1 The Helmholtz equation for acoustic waves	30
2.2.2 The Helmholtz equation for thermal waves	34
2.2.3 The Schrödinger equation	34
2.2.4 Electromagnetic waves	36
2.3 Invariants of discrete symmetries	38
2.3.1 Invariant non-local currents	39
2.3.2 Generalization of Bloch and parity theorems for broken symmetries	42
2.3.3 Globally symmetric potentials	43
2.3.4 Retrieving the Bloch and parity theorems	44
2.3.5 Locally symmetric potentials	46

2.4	Matrix formulation of the non-local currents	47
2.5	Invariants in systems with losses	50
3	POTENTIAL SCATTERING	55
3.1	Introduction	55
3.2	The Transfer and \hat{S} - Matrix methods	56
3.2.1	The S-matrix	57
3.2.2	The Transfer Matrix	61
3.3	Q -Matrix formulation for scattering	66
3.4	Relation between the \hat{Q} and the transfer matrix	66
4	REFLECTIONS AND THE LOCAL PARITY FORMALISM	71
4.1	Introduction	71
4.2	Global Parity	72
4.2.1	Reflections in Classical Physics	72
4.2.2	Reflection transformations in one-dimension	73
4.2.3	Reflections in Quantum Physics	74
4.3	From Global to Local Parity	75
4.4	The Local Parity operator	75
4.4.1	Properties of the LP operator	78
5	LOCAL PARITY AND SCATTERING IN APERIODIC MEDIA	83
5.1	Introduction	83
5.2	Symmetry scales in aperiodic systems	84
5.2.1	Global properties emerging from local invariants	85
5.3	Scattering from piecewise constant setups	86
5.3.1	Scattering under SAC in locally symmetric media	87
5.3.2	Asymptotic conditions and symmetry breaking	88
5.3.3	Perfect transmission in locally symmetric media	89
5.3.4	Geometric interpretation and classification of PTRs	91
5.4	Transmission properties of an aperiodic set-up	96
5.4.1	PTRs in an aperiodic photonic multilayer	97
5.4.2	PTRs in an aperiodic quantum system	101
5.5	Relation to alternative approaches	103
6	PERFECT TRANSMISSION CONTROL: A LOCAL PARITY APPROACH	105
6.1	Introduction	105
6.2	Quantum, optical and acoustic engineering	105
6.3	Local parity based design of PTR states	106
6.3.1	s -PTR construction principle	106

CONTENTS

v

6.3.2	<i>a</i> -PTR construction principle	108
6.4	<i>s</i> -PTR construction in quantum mechanical systems	109
6.4.1	<i>s</i> -PTR construction in aperiodic photonic multilayers	112
6.4.2	PTR construction in aperiodic acoustic waveguides	116
7	CONCLUSIONS AND PERSPECTIVES	121
A'		125
B'		129
Γ		131
	ΠΕΡΙΛΗΨΗ	133
	BIBLIOGRAPHY	141

PREFACE

The present Thesis has been elaborated in the section of Nuclear Physics and Elementary Particles in the Physics department of the National and Kapodestrian University of Athens.

First and foremost I would like to thank my supervisor and Teacher, Prof. F.K. Diakonos for his invaluable and constant support in every level of this procedure. I have been fortunate enough to know Fotis from my undergraduate studies, when he introduced me to the fascinating world of quantum theory. Since then, he keeps inspiring and motivating me with his deep insight and enthusiasm for Physics. Without him, the realization of this Thesis would be unattainable. In any case, a simple thank you is not enough.

I would like to express my heartfelt thanks to Prof. Dr. P. Schmelcher for the close and fruitful collaboration during the last four years. His ideas and comments had a decisive role in the outcome of this Thesis. I also want to thank Peter for the warm hospitality every time I visited ZOQ (Zentrum für Optische Quantentechnologien) in Hamburg.

Additionally, I want to thank Prof. A.I. Karanikas for the elucidating discussions we had, his comments and his willingness to provide ideas and answers to every scientific question.

I would like to express my sincere thanks to the other members of the examination committee, Lect. N. Fytas, Prof. E. Manousakis, Prof. K. Sfetsos and Prof. N. Tetradis. Moreover, I want to thank Prof. X. Maintas for his helpful comments.

A special thanks goes to my friend and colleague Christian Morfonios. In the past three years we had a very close and constructive collaboration. I want to thank him for his ideas on the several projects constituting this work and for the time he dedicated to improve the appearance of the figures and the clarity of the text.

I would like also to thank Dr. G. Theocharis for his interest to implement the proposed

approach experimentally in acoustic waveguides, which has led to a very nice and promising collaboration. I also thank Giorgos for providing me with useful data and for revising part of the manuscript.

Moreover, I thank Maria Kalozoumi for her help in the graphic editing of several figures appearing in the manuscript.

Finally, I want to express my gratitude to my parents. Their continuous support has been instrumental, not only during my studies, but in every aspect of my life. I deeply thank them.

Athens
April, 2014

P.A. Kalozoumis

INTRODUCTION

Symmetry and Physics

Symmetry can be perceived in a twofold manner. The first is abstract and related to the beauty and the harmony of an object [1]. In this sense, the notion of symmetry can be traced back in Classical Greece where, apart from describing the geometrical regularities of an object, it generally denoted the aesthetic quality of an entity. Moreover, its dominance in art and nature influenced the evolution of Philosophy, with symmetry principles being embodied in the philosophical currents of Pythagoras, Aristotle and Leucippus.

The second way to realize symmetry is from a rigorous, mathematical viewpoint. Any transformation on the coordinates of a system caused by e.g. a rotation, a reflection or a translation, leads to a change in the system. If, however, a property of the system remains invariant, then this constitutes a symmetry. Such a transformation can be either active when the change occurs on the system or passive when the system remains fixed and the change occurs on the reference frame.

The ubiquitous presence of symmetries in nature reveals their important role in physical sciences. Physics are dominated by symmetry principles which are either obvious as in the geometric description of an object or hidden in the physical laws. Newton's laws and Maxwell equations incorporate symmetry principles as the Galilean and Lorentz invariance, respectively. However, the emerging conservation laws were attributed to the corresponding dynamical laws overlooking their underlying symmetries [2]. It was Einstein's perspective which brought symmetry to the foreground, with the identification of Lorentz invariance as a means to determine the transformation properties of the electromagnetic field and subsequently dictate the form of the Maxwell equations.

A straightforward way to realize the power of symmetry in the physical laws is the ability to perform experiments at different times and at different places which yield the same results. This trivial consequence emerges from the invariance of physical laws under space and time translations. It becomes clear that in the absence of symmetry the discovery of physical laws would not be feasible. In fact, without the symmetry induced

regularities the notion of “law” would not make sense.

In modern Physics symmetry is prominently displayed. It has been realized that symmetry principles not only reduce the extent of information which are required for the description of a system but also dictate the form of the physical laws. Under this prism, the endeavour to extend the frontiers of our knowledge about nature is significantly based on the discovery of higher symmetry principles.

Types of symmetry

In Physics several types of symmetry are met. In general, a symmetry transformation can act either on the coordinates of a system, affecting accordingly the involved fields or directly to the fields without transforming the coordinates.

Symmetry transformations of the first kind, namely *space-time* symmetries, affect the spatiotemporal coordinates of the system. The spatial transformations, described by the $SO(3)$ group, belong to this category. In relativistic theories, space-time symmetry transforms include Lorentz boosts and spatial rotations, constituting Lorentz invariance. If spatiotemporal translations are also taken into consideration, then the Poincaré group is formed. The latter is of great significance in Physics since it preserves distances in Minkowski spacetime. It is also non-compact in the sense that the endpoints of the relevant parameters are not included in the range of values that they can actually take [3]. Particularly, the velocity of a particle with mass $m \neq 0$ can never reach the endpoint of light speed c .

The aforementioned space-time symmetry transformations are valid under any infinitesimal change of a relevant parameter e.g. the change $d\theta$ in the angle of a spatial rotation. Therefore, we refer to them as *continuous* symmetries, described mathematically by Lie groups.

On the other hand, if the space-time coordinates of the system change in a non-continuous manner, then the symmetry is *discrete* and it is described by a finite group. Parity, which inverts all spatial components of the position vector ($\vec{r} \rightarrow -\vec{r}$):

$$P : (t, \vec{r}) \rightarrow (t, -\vec{r})$$

and time-reversal

$$T : (t, \vec{r}) \rightarrow (-t, \vec{r})$$

are both discrete space-time symmetries.

Following our initial distinction, we now turn to *internal* symmetries, where the respective transformations act on the fields of the theory, in a certain way, transforming them in an abstract space, without referring to their spatiotemporal dependence. Internal symmetries, in turn, can be classified as *global* or *local*. The action of the former on

the corresponding fields does not depend on space-time coordinates. For instance, a transform described by

$$\Phi' = e^{i\alpha}\Phi,$$

where α is space independent is considered to be global.

On the contrary, the effect of local symmetry transformations on the corresponding fields, vary in each space-time point. Thus, in a local transform of the form

$$\Phi' = e^{i\alpha(x)}\Phi,$$

the parameter $\alpha(x)$ is depends on the point of space-time. Local symmetries and particularly *gauge* invariance possess a fundamental role in Physics, as we shall see in the following paragraphs.

Symmetry in classical Physics

Let us consider a classical system described by the generalized coordinates $q(t)$, $\dot{q}(t)$. The influence of symmetries in such systems can be studied using Hamilton's action principle which states that:

A particle which starts its motion from A at time t_A and arrives at B at t_B , follows the path which renders the action stationary.

The action is a functional of the path $q(t)$ and is defined as

$$S[q(t)] = \int_{t_A}^{t_B} L[q(t), \dot{q}(t), t] dt \quad (1)$$

where L is the Lagrangian. From the Hamilton's principle stems that if the generalized coordinates $q(t)$ describe the motion of the particle then it holds that

$$S[q(t) + \delta q(t)] = S[q(t)] \quad (2)$$

for any infinitesimal change $\delta q(t)$ in $q(t)$ which leaves the starting and final value, at t_A and t_B , unaffected.

A symmetry of a system which can be described in the above manner exists when there is a transformation of $q(t)$ which leaves the action invariant. If the symmetry transform is described by:

$$q(t) \rightarrow \mathcal{F}[q(t)], \quad (3)$$

it follows that the equations of motion remain invariant under the symmetry operation shown in Eq. (3). In other words, if the generalized coordinates render the action stationary and $\mathcal{F}[q(t)]$ is a symmetry operation, then $\mathcal{F}[q(t)]$ will also lead to a stationary

action. This, in principle, can lead to new solutions which emerge from the considered symmetry of the system.

Symmetry in Physics is also inextricably linked to the existing conservation laws. From a continuous, global symmetry which acts in the same manner at every space point and time, emerges a time invariant quantity. The relation between symmetry and conservation laws was identified by Emmy Noether and was formulated in her famous theorem. Thereby, the momentum and energy conservation stem from the symmetry of laws of nature under spatial and time translational invariance, respectively, as well as, charge is conserved due to the invariance under phase transformations in the wave function of charged particles.

To be more concrete, Noether's theorem states that if the Lagrangian $\mathcal{L}(\varphi, \delta\varphi, x^\mu)$ is invariant under continuous transformations with N parameters ω_i ($i = 1, 2, \dots, N$), so that for the action S holds $\delta S = 0$, then there exist N conserved currents J_i^μ . The conservation is expressed as $\partial_\mu J_i^\mu = 0$. The corresponding transformation affects the *coordinates* as:

$$x^\mu \rightarrow (x^\mu)' = \mathcal{F}(x^\mu) \quad (4)$$

and the *fields* $\varphi_\alpha(x)$ (where we use for notational simplicity x for x^μ) as:

$$\varphi_\alpha(x) \rightarrow \varphi'_\alpha(x') = \mathcal{F}(\varphi_\alpha(x)). \quad (5)$$

For an infinitesimal change we can write

$$(x^\mu)' = x^\mu + \delta x^\mu = x^\mu + X_i^\mu(x) \delta\omega^i \quad (6)$$

and

$$\varphi'_\alpha(x') = \varphi_\alpha(x) + \delta\varphi_\alpha(x) = \varphi_\alpha(x) + \Psi_{\alpha i}(x, \varphi) \delta\omega^i, \quad (7)$$

where we have analysed δx^μ to the directions of the parameters $\delta\omega^i$ of the transformation. If under the above transformation it holds for the action that $\delta S = 0$ then it can be proved (using also the equations of motion) that the current J_i^μ is given by:

$$J_i^\mu = -X_i^\mu \mathcal{L} + \frac{\partial \mathcal{L}}{\partial(\partial_\mu \varphi_\alpha)} (\Psi_{\alpha i} - \partial_\nu \varphi_\alpha X_i^\nu) \quad (8)$$

As an example, we consider the classical Lagrangian of a free particle, given by

$$\mathcal{L} = \frac{1}{2} m \dot{x}^2 \quad (9)$$

and the external symmetry, expressed by the following transformations for the fields and the coordinates, respectively:

$$x \rightarrow x' = x + \delta\omega \quad (10)$$

$$t \rightarrow t' = t, \quad (11)$$

where obviously $\Psi = 1$ and $X = 0$. Note that here holds the correspondence

$$x(t) \rightarrow \varphi(x). \quad (12)$$

Therefore, x corresponds to the field and t to the coordinates. Then Eq. (8) yields for the current:

$$J = \frac{\partial \mathcal{L}}{\partial \dot{x}} = m\dot{x} = P_x. \quad (13)$$

Then, $J^\mu = (J_0, \vec{J})$ and

$$\partial_\mu J^\mu = \partial_0 J^0 - \vec{\nabla} \cdot \vec{J} \quad (14)$$

According to the theorem of Noether,

$$\partial_\mu J^\mu = 0 \quad (15)$$

which expresses the momentum conservation

$$\frac{dP_x}{dt} = 0. \quad (16)$$

Noether's theorem however restricts the existence of conserved quantities to continuous symmetries, since it requires the continuous variation of parameters so that an infinitesimally close approach to the identity transformation is feasible. In the next chapters we will study the breaking of global discrete symmetries so that they pertain in local spatial domains. We will show that under broken inversion and translation symmetries, a class of spatially invariant non-local currents emerges as remnants of the corresponding global symmetries.

Symmetry in quantum Physics

When we enter the realm of quantum mechanics, symmetry principles appear even more empowered, revealing new kinds of symmetry and allowing for the construction of new states.

A striking example of the former, is the symmetry which stems from the exchange of identical particles and leads to their classification to fermions and bosons, according to their statistical description. Indeed, if we introduce the exchange operator $\hat{\mathcal{P}}$ and a two-particle wave function $\Psi(x_1, x_2)$, then the act of $\hat{\mathcal{P}}$ on $\Psi(x_1, x_2)$ has the following possible outcomes:

$$\hat{\mathcal{P}}\Psi(x_1, x_2) = \Psi(x_2, x_1), \quad \text{bosons}$$

$$\hat{\mathcal{P}}\Psi(x_1, x_2) = -\Psi(x_2, x_1), \quad \text{fermions}$$

since for $\hat{\mathcal{P}}$ holds that $\hat{\mathcal{P}}^2 = \hat{\mathbf{1}}$. Thus, for bosons, the wave function remains invariant under the permutation of two particles whether for fermions the wave function changes sign and is described by the Slater determinant.

In classical mechanics a symmetry transformation $\phi \rightarrow \mathcal{F}[\phi]$ can be used to construct new allowed states of a system. Respectively, this also holds in quantum mechanics. A state $|\Psi\rangle$ which is described by a vector in Hilbert space can be transformed by a linear operator F which acts on $|\Psi\rangle$ and transforms it to a new $|\Psi'\rangle$. Up to this point there is an equivalence between classical and quantum mechanics. It is the combination of the superposition principle with the corresponding symmetry transformations which allows the emergence of new states, which classically would not emerge. If the operator \hat{F} corresponds to the symmetry transformation \mathcal{F} the state $\hat{F}|\Psi\rangle$ is also allowed as the state $|\Psi\rangle$. Contrary to the classical case, we can now superimpose states $|\Psi\rangle$ and $\hat{F}|\Psi\rangle$ so that we construct a new -only quantum mechanically allowed- state $|\tilde{\Psi}\rangle = |\Psi\rangle + \hat{F}|\Psi\rangle$.

The existence of symmetry in quantum mechanical systems, combined with the superposition principle, is tightly related to the emergence of degeneracies in their energy spectra. Let $|\Psi\rangle$ be an eigenstate of the Hamiltonian so that

$$\hat{\mathcal{H}}|\Psi_n\rangle = \varepsilon_n|\Psi_n\rangle. \quad (17)$$

If \hat{O}_F is the operator which performs a symmetry transformation F , then the transformed state $\hat{O}_F|\Psi_n\rangle$ is also an eigenstate of the Hamiltonian with the same energy:

$$\hat{\mathcal{H}}\left(\hat{O}_F|\Psi_n\rangle\right) = \hat{O}_F\hat{\mathcal{H}}|\Psi_n\rangle = \hat{O}_F\varepsilon_n|\Psi_n\rangle = \varepsilon_n\left(\hat{O}_F|\Psi_n\rangle\right). \quad (18)$$

However, the states $|\Psi_n\rangle$ and $\hat{O}_F|\Psi_n\rangle$, in general, are not the same and since they share the same energy eigenvalue ε_n , the energy spectrum is degenerate (usually this is possible in higher dimensions). In this sense, the quantum mechanical possibility for new, superimposed states which have emerged under a symmetry transform F leads to degeneracies in the energy spectrum. In general, the observation of degeneracies in the spectrum, implies the existence of symmetries.

Finally, in relativistic quantum mechanics symmetry implications have also significant impact. In this case the analysis of the representations of the Poincare group -which apart from the rotations and boosts of the Lorentz group also involves space-time translations- yields another classification of the elementary particles, based on their mass. Thereby, the irreducible representations of the Poincare group can be classified to (i) massive representations, which are labelled by a finite mass $m \neq 0$ and the spin J and (ii) massless representations, where $m = 0$. This outcome which emerges from a group theoretic argumentation reveals a fundamental difference between massive and massless particles.

Local internal symmetries and gauge invariance

A global symmetry affects the system in the same manner everywhere. For example, a (global) rotation rotates the whole set-up, involving the laboratory and the observer. Thus, all observations will remain invariant. On the other hand, as it has been mentioned, local symmetries induce a different symmetry transformation at each space-time point.

Gauge symmetries are local, continuous symmetries which depend on space and time. Gauge symmetries may act on internal degrees of freedom, belonging to the class of internal symmetries, or on space-time, belonging to symmetries of coordinate invariance. Gauge invariance first appeared in electromagnetism where it was discovered that Maxwell's equations could be simplified by adding a four-vector potential $A_\mu = (\Phi, \vec{A})$ where Φ is a scalar potential and \vec{A} a vector, so that the electric and magnetic fields, \mathbf{E} and \mathbf{B} , could be expressed in terms of A_μ . However, this vector potential is not unique since under a gauge transformation:

$$A_\mu(x) \rightarrow A_\mu(x) + \partial_\mu\theta(x), \quad (19)$$

the fields \mathbf{E} and \mathbf{B} remain unaffected. If we consider the Lagrangian density of the electromagnetic field:

$$\mathcal{L} = -\frac{1}{4}F_{\mu\nu}F^{\mu\nu} \quad (20)$$

we can see that it is invariant under the gauge transform in Eq. (19), for any function $\theta(x)$.

Even though gauge symmetries were considered to be artificial, in the last 40 years there has been a radical change in this point of view, upgrading their role in Physics. In the first place, it has been understood that the vector potential which is used to the Maxwell's equations may have direct consequences which can be observed, contrary to the long-standing belief of being artificial. Namely, in the Bohm-Aharonov effect an electrically charged particle moving in a region where the electromagnetic field is excluded, it is affected by the corresponding vector potential, which is non-vanishing due to the geometry of the set-up. The Bohm-Aharonov effect demonstrates in a straightforward way that the electromagnetic vector potential is an existing and fundamental quantity in quantum mechanics.

The first example of gauge invariance was introduced in the formulation of the general relativity, where the space-time symmetry under local changes of coordinates led Einstein to the description of gravitation. Gauge theories also provide the framework to develop a theory for the electromagnetic, weak and strong interactions which, in turn, establishes the standard model. Gauge invariance also dictates the emergence of mediating gauge bosons which are massless particles with spin 1 and are the carriers

of the fundamental interactions in nature. Hence, the significance of gauge symmetries is revealed, in the sense that their existence comes prior of the system's dynamics. In the standard model the relevant gauge symmetry is the $SU(3) \times SU(2) \times U(1)$. This symmetry implies the existence of one massless particle, namely the photon, from the $U(1)$ symmetry of the electromagnetic field and three massive gauge bosons, W^\pm and Z , from the spontaneous symmetry breaking of the $SU(2)$ symmetry of the weak interactions. Also 8 massless gluons emerge as carriers of the strong interaction and stem from the $SU(3)$ symmetry.

Symmetry breaking

Even though symmetry possesses such a significant role in Physics, it is not always evident. In most cases, particularly when one searches for more profound types of symmetry, their identification becomes a cumbersome task. This happens because in a multitude of cases symmetry is broken. There are two kinds of symmetry breaking. The first is explicit, appearing at the level of the action of the system. In this case the physical laws are only approximately invariant under the corresponding symmetry transformation. If the deviation from symmetry is small then it can be treated as a small correction. The second is commonly referred as spontaneous symmetry breaking and is met both in classical and quantum physics. The term "spontaneous" characterizes the situation where the symmetry is not explicitly broken from the existence of asymmetric contributions to the Lagrangian, but it breaks due to the non-invariance of the ground state. Therefore, for invariant Lagrangians under a symmetry operation, there exist non-invariant solutions which emerge spontaneously, without any term to break explicitly the symmetry. When a suitable tuning parameter reaches a critical value, then the symmetric ground state is no longer stable under small fluctuations and breaks to new, degenerate ground states which are no longer symmetric. The whole set of the asymmetric solutions maintains the symmetry of the theory.

Spontaneous symmetry breaking, rigorously can occur only in systems with infinite degrees of freedom. In a quantum mechanical system with finite degrees of freedom spontaneous symmetry breaking is not feasible, as the superposition principle of all possible states combined with the tunnelling possibility leads to an always symmetric ground state. However, in systems with infinite degrees of freedom, where the volume is infinite, all degenerate ground states are inaccessible to each other, since tunnelling cannot occur.

The concept of spontaneous symmetry breaking is widespread in condensed matter physics and particularly in systems which undergo a continuous, thermal phase transition, from a high to a low symmetry phase. A typical example of such a phase transition is exhibited in ferromagnets. There the tuning of temperature drives the system from

the rotationally invariant high temperature, zero mean magnetization ($\langle M \rangle = 0$) state to the low temperature, $\langle M \rangle \neq 0$ state. The symmetry breaking occurs at a specific, critical temperature T_c and then the system undergoes a second order phase transition. The magnetization in this case is the order parameter of the system, namely a quantity being zero in the symmetric state and non-zero in the non-symmetric state. By increasing the temperature, the rotational symmetry can be restored.

It is believed that a similar procedure describes the symmetries of the fundamental interactions in nature. As the universe cooled down, they were broken, undergoing phase transitions. In very high temperatures, reaching those existing in the first moments of the universe, these symmetries are likely to be restored.

Other examples of symmetry breaking are met in superconductors where the relevant symmetry which breaks is the phase invariance of the charged particles or even the formation of crystals which results from the broken translational symmetry.

A viewpoint on a different symmetry case

In real physical systems global symmetry constitutes an idealized scenario, usually met in models, approximative schemes or structurally simple isolated systems. On the other hand, local gauge symmetries underlie the emergence of fundamental interactions and accurately describe particle physics.

Between these two symmetry classes, one acting in every point of space (or space-time) and the other acting in a single point, another category can be defined, where symmetry is fulfilled in localized domains of finite extent. Physical systems possessing the latter dominate in several length scales (e.g. nm, μm) and usually emerge due to the physical mechanism of a global symmetry breaking. The symmetry breaking, in turn, gives rise to new symmetries which manifest in the extensively diverse structures which are met in nature [4].

Spatially localized discrete symmetries can be intrinsic in complex systems like large molecules [5–7], in quasi-crystals [8–11] or disordered matter [12]. On the other hand they can be present by design in multilayered photonic devices [13–18], in quantum semiconductor superlattices [19] and acoustic waveguides [20]. Technological advances often require the global breaking of discrete symmetries in order to exploit structures suitable for applications.

Although systems which belong to these classes have been thoroughly studied, mainly spatial symmetries acting on the total extent of the device have been addressed. On a local level, structural features which affect spectral and localization properties has been carried out [61], for instance in hybrid systems which are comprised of domains each one with different quasi-periodic structure. However, little attention has been paid to the impact of explicit *local symmetries*, although they are obviously present. There-

fore, when the respective symmetry scales of a system do not allow their treatment in a global manner, nor the mean [22, 23] description is valid -as it would be the case in disordered media- then, obviously, a new point of view needs to be introduced.

Here we take a step towards this direction, by introducing a systematic approach to the breaking of global, discrete symmetries in one-dimensional systems, namely translation and inversion.

In Chapter 1 we summarize the basic properties of wave propagation in periodic, finite periodic and quasi-periodic one-dimensional systems. Starting from the electronic case, we describe the quantum propagation in crystals, using the Kronig-Penney model. Next, based on the same model, we refer to the photonic crystal concept. We turn then to the description of systems which retain periodicity, although they are finite. Thus, the global translational symmetry is broken, pertained though in the extent of the system. We close this chapter with an overview of aperiodic structures with emphasis on fractal and quasi-periodic geometries.

In Chapter 2 we address set-ups where the broken global symmetry is retained locally, in arbitrary spatial domains, aiming to describe the wave mechanical properties of aperiodic and quasi-periodic systems. We find a class of symmetry induced, space invariant, non-local currents, which can be considered to be remnants of the broken global symmetry. These currents, in turn, provide a mapping of the wave function between two symmetry-related domains (source and target domain respectively). This constitutes a generalization of the Bloch and parity theorems for finite systems and in the generic case, non-symmetric, aperiodic systems.

Chapter 3 begins with an overview of scattering theory focused on the transfer and the scattering matrices methods. Utilizing the symmetry-induced invariant currents from Chapter 2 we develop an alternative approach to the transfer matrix method.

The proposed method addresses successfully any combination of translation and inversion symmetry and can be applied to the study of wave propagation in aperiodic and quasi-periodic media. The fact it lies on very general symmetry arguments, combined with the Helmholtz-Schrödinger isomorphism, provide a unified framework which can be applied to the quantum optical and acoustic systems, notwithstanding their essential differences. In Chapter 4 we focus on the parity transformation when applied to finite mirror symmetric domains, we introduce the concept of local parity (LP) and the corresponding operator.

In Chapter 5 We consider non-symmetric, aperiodic scattering set-ups which can be completely decomposed in space domains where the LP symmetry is satisfied and reveal the its impact on their transport properties and particularly on perfect transmission resonances (PTRs). With emphasis on the PTR manifestation and by employing the aforementioned invariant currents, we propose a classification of PTRs, based on their geometric representation on the complex plane. This classification lifts certain overlaps of alternative approaches in the existing literature and provides an unambiguous

distinction between resonances based on fundamental, local symmetry principles.

Finally, in Chapter 6 we develop a construction principle which utilizes the simultaneous existence of different LP symmetry scales in the same set-up for the design of aperiodic wave mechanical devices with prescribed PTR properties. The implementation of this construction principle on quantum, photonic and acoustic systems, reveals its applicability in diverse systems.

CHAPTER 1

PERIODIC AND QUASI-PERIODIC 1-D SYSTEMS

1.1 Introduction

In this Chapter we will investigate how the wave transport is affected by the geometry of the set-up's underlying structure. Particularly, we will focus on three classes of systems: periodic, random and quasi-periodic. Periodic systems are well understood and give rise to interference phenomena which accurately describe the basic properties of solids. On the other hand, random systems with no regularities even though seem intractable by not following any geometry rule, have well-defined propagation properties due to methods of random scattering. Between these two extremes lie the class of aperiodic structures which are constructed in a deterministic manner and involve definite geometrical regularities. Such fractal and quasi-periodic media yield a complex and rich behaviour, regarding the wave interference properties.

The analysis begins with the study of waves in one-dimensional periodic media. The periodicity, as we shall see, leads to the emergence of *Bloch waves* and *band structure*. Particularly we will refer to the quantum mechanical and optical versions of a periodic system, describing the electronic behaviour of the a solid and the concept of the photonic crystal, respectively, even though the procedure can be extended to involve mechanical, acoustic or even oceanographic [24] waves. In order to treat in conjunction wave systems in periodic media, we will describe the *Kronig-Penney* model [25], adopting a generalized notation,. The more realistic case of locally periodic systems i.e. systems possessing periodicity without extending to infinity, will be considered afterwards and next a brief reference will be made to the concept of 1-D systems with randomness and to their basic properties. Finally, an overview of quasi-periodic systems will be presented as the intermediate state for the transition from periodicity to randomness.

1.2 Waves in infinite periodic media

In this section, we will make an overview on the effect of periodicity in an infinite array of scatterers. In an arbitrary finite system, scattering states are characterized by a continuous spectrum, while the spectrum becomes discrete when we refer to bound states. The former, in the classical wave motion, corresponds to travelling waves and the latter to standing waves. However, for an infinite system with scatterers, placed periodically, the propagating waves become Bloch waves and *band structure* occurs. In this sense, the propagating wave modes are concentrated to continuous frequency (energy) *bands* separated by *gaps* denoting frequencies (energies) which are forbidden to propagate.

1.2.1 Quantum mechanical periodic potential

The electron theory in solids is based on the assumption that the ions are placed in a perfectly periodic manner on the lattice sites of a Bravais lattice, depending on the geometry of the material. Even though this problem is, in general, a many body problem, involving both electron-ion and electron-electron interactions, we can confront it qualitatively as a single electron problem, by treating each ion as an individual atomic potential [26]. The following analysis refers to 1-D systems, nevertheless the generalization to 3-D is straightforward. We begin by considering the Schrödinger equation:

$$-\frac{\hbar^2}{2m} \frac{d^2}{dx} \Psi(x) + V(x)\Psi(x) = \varepsilon\Psi(x) \quad (1.1)$$

or

$$\frac{d^2}{dx} \Psi(x) + \frac{2m}{\hbar^2} [\varepsilon - V(x)] \Psi(x) = 0 \quad (1.2)$$

with

$$k_{QM} = \left(\frac{2m}{\hbar^2} [\varepsilon - V(x)] \right)^{1/2} = 0. \quad (1.3)$$

The translational symmetry of the potential is expressed via the relation:

$$V(x) = V(x + nL) \quad (1.4)$$

with $n \in \mathbb{Z}$ and L being the lattice constant. The translational invariance of the system suggests that the substitution $x \rightarrow x + L$ leads to the translated wave function $\Psi(x + L)$, which accordingly satisfies the same Schrödinger equation:

$$\frac{d^2}{dx} \Psi(x + L) + \frac{2m}{\hbar^2} [\varepsilon - V(x)] \Psi(x + L) = 0. \quad (1.5)$$

This means that $\Psi(x)$ either it is exactly periodic so that $\Psi(x) = \Psi(x + L)$, or it differs from a periodic function $u(x)$ by a phase. The latter case, expresses essentially the *Floquet* theorem [27], which was derived in 1883 by G. Floquet. In solid state physics often we refer to it as *Bloch* [28] theorem, even though the Bloch theorem consists the generalization to three-dimensions. Mathematically, the Floquet theorem reads:

$$\Psi(x) = e^{ikx}u_k(x) \quad ; \quad u_k(x) = u_k(x + L). \quad (1.6)$$

This kind of solutions, namely *Bloch waves*, have the form of plane waves with amplitude which is modulated by the periodicity of $V(x)$. In the limiting case of zero potential, $\Psi(x)$ becomes a regular plane wave in accordance to free propagation. The k index in $u_k(x)$ refers to the fact that its value depends to the corresponding wave number.

The Bloch wave of Eq. (1.6), apart from the real space periodicity, it also implies the periodicity of the wave number k in the reciprocal space. Indeed, the substitutions:

$$x \rightarrow x + L$$

$$k \rightarrow k + \frac{2\pi}{L}$$

lead to the original wave $\Psi(x)$. Thereby, the translational symmetry induces also the property that, wave-numbers which differ by an integer number times the reciprocal lattice constant $2\pi/L$, are equivalent. Each set of equivalent wave-number k constitute a *Brillouin zone*. Since the Brillouin zone is defined in the reciprocal space, its boundaries are positioned at:

$$k_n = \frac{\pi}{L}n \quad ; \quad n = \pm 1, \pm 2, \dots \quad (1.7)$$

The form of Eq. (1.7) induces discontinuities in the dispersion relation $E(k)$, indicating the energy regions where wave propagations is allowed (bands) and those where no wave propagation is allowed (gaps). This behaviour can be assigned to the formation of standing waves due to multiple reflections from the periodic structure.

The wave number which characterizes Bloch electrons that move in a periodic potential is not proportional to the momentum as in the case of the free electron propagation. This occurs due to the space non-homogeneity, since the presence of the periodic potential causes that the Hamiltonian eigenstates are not simultaneous eigenstates of the momentum operator. However, the quantity $\hbar k$, to which we refer to as *quasi* or *crystal* momentum, can be regarded as the momentum extension in the case of the translational invariance of a periodic system. Thereby, k is the corresponding quantum number for the periodic translational invariance, whereas p corresponds to the full translational invariance of the free space. In other words crystal momentum is conserved in “steps” of $2\pi\hbar/L$.

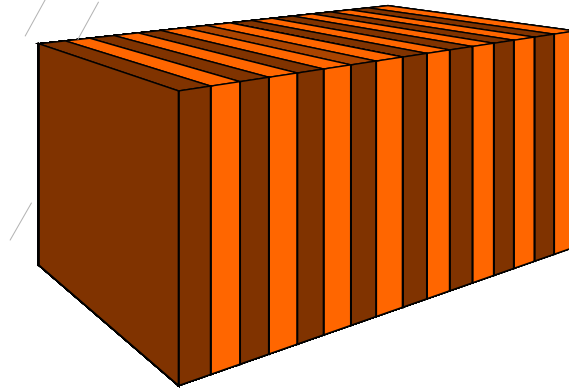


FIGURE 1.1: Schematic of a one-dimensional photonic crystal. Even though each slab is three-dimensional, the dielectric function $\epsilon(x)$ varies only in the x -direction, where also the light propagation occurs. In the $y - z$ -plane each slab is homogeneous.

1.2.2 Periodic dielectric array - The photonic crystal

The *photonic crystal* [29] is a periodic structure analogous to the periodic potential in the quantum mechanical case. Particularly, a photonic crystal is an inhomogeneous medium, with periodically alternating refractive index, while the periodic change may occur in one, two or three dimensions [30, 31]. In fact, the 1-D photonic crystal is a multilayer film which acts as a Bragg mirror for a particular range of frequencies. This idea originates back to 1917 when Lord Rayleigh [32, 33] published a relevant study on the optical properties of a periodically layered, dielectric medium. The similarity to the quantum mechanical electron propagation in a periodic potential, leads to a multitude of common features, as propagation of Bloch waves instead of plane waves, the existence of Brillouin zones and the emergence of band structure and photonic band gaps. A schematic of a photonic crystal is shown in Fig. 1.1. The dielectric function $\epsilon(x) = n^2(x)$ changes periodically in the x -direction. In the $y - z$ -plane each slab is homogeneous. However, in our analysis we will consider purely 1-D propagation in the x -direction and we will ignore the other two.

The main properties of the 1-D photonic crystal can be derived by considering the wave equation for the electric field $E(x, t)$:

$$\partial_{xx}E(x, t) + \frac{\epsilon(x)}{c^2}\partial_{tt}E(x, t) = 0. \quad (1.8)$$

with

$$E(x, t) = E(x)e^{i\omega t}. \quad (1.9)$$

After the substitution of Eq. (1.9) into Eq. (1.8) and by considering only the spatial part which is satisfied by $E(x)$, we are led to the Helmholtz equation for the electric field:

$$\frac{d^2}{dx^2}E(x) + \left(\frac{n(x)\omega}{c}\right)^2 = 0, \quad (1.10)$$

where the refraction index $n(x)$ is related to the dielectric function $\epsilon(x)$ as $n(x) = \sqrt{\epsilon(x)}$. Taking the translated, by the lattice constant α , electric field and following a procedure similar to the quantum mechanical case of the periodic potential, we arrive at the Bloch form of the electric field:

$$E(x) = \mathcal{E}_k(x)e^{ikx} \quad (1.11)$$

where $\mathcal{E}_k(x) = \mathcal{E}_k(x + L)$ is the periodic function which modulates the field and k is the Bloch wave number. The band structure also emerges in the photonic crystal case, as a consequence of the equivalence of states which differ by a wave number value

$$k_n = k + \frac{2\pi}{L}n, \quad n = \pm 1, \pm 2, \dots \quad (1.12)$$

The periodicity of the medium is strongly reflected in its dispersion relation $\omega(k)$. For an electromagnetic wave propagating in the vacuum the dispersion is

$$\omega = ck, \quad (1.13)$$

while for a continuum medium with refraction index n , becomes:

$$\omega = \frac{c}{n}k, \quad (1.14)$$

which implies propagation with decreased velocity. In these cases the E-M wave modes lie on the *light line*. The periodicity of the refraction index, however affects more radically the dispersion relation in a 1-D multilayer. The periodicity of the wave number in the reciprocal space, expressed in Eq. (1.12), implies the occurrence of breaks in the dispersion whenever the wave number satisfies the condition

$$k_n = n\frac{\pi}{L}, \quad n = \pm 1, \pm 2, \dots \quad (1.15)$$

Similarly to the electron motion in a periodic potential, this property leads to the Brillouin zones. At the boundaries of the Brillouin zone we have the formation of standing waves, which in turn yield the *photonic band gap*.

1.2.3 A generalized Kronig-Penney model

The periodicity and concurrent symmetry arguments gives the general picture for the band and gap formation, independently of the exact form of the potential. The Kronig-Penney model [25] provides the simplest quantitative description of a 1-D periodic potential, by considering piece-wise constant i.e. rectangular barriers, where the solutions are plane waves. Despite its simplicity it has proved very successful for the description of the electron properties in solids. The implementation of several variations on the basic concept renders the Kronig-Penney model a powerful tool with wide applicability. Thereby, apart from being textbook material, it is also used in research for the study of graphene [34–36], semiconductor superlattices [37], disordered systems [38,39] and relativistic electron propagation [40]. Along with the electronic properties of solids, the Kronig-Penney model can be employed for the theoretical study the properties of light in periodically ordered photonic multi-layered materials, i.e. a photonic crystal. Finally, in periodically layered acoustic waveguides [41,42] the Kronig-Penney model is employed for the study of the sound behaviour and the corresponding band and gap structure. Based on the its interdisciplinary nature, we will formulate a generalized Kronig-Penney model, applicable both to all the preceding and also to physically similar cases.

We consider an infinite array of periodically positioned stepwise potential units. In Fig. 1.2 we show a schematic of a rectangular barrier periodic array and the photonic crystal equivalent, comprised of dielectric slabs, each one with constant refraction index. The constancy of the potential unit (barrier or dielectric slab), implies that, within it, the corresponding field is a plane wave. Indeed, from the Helmholtz equation

$$\frac{d^2}{dx^2} \mathcal{A}(x) + \kappa \mathcal{A}(x) = 0 \quad (1.16)$$

we find that the solutions are of the form

$$\mathcal{A}_I(x) = A_I e^{i\kappa_I x} + B_I e^{-i\kappa_I x}, \quad (1.17)$$

when the wave is into the barrier area or into the corresponding slab (I), and

$$\mathcal{A}_{II}(x) = A_{II} e^{i\kappa_{II} x} + B_{II} e^{-i\kappa_{II} x}, \quad (1.18)$$

when the wave is in the zero potential area or slab (II) area. The fact that the propagation occurs into a periodic structure, entails however that the waves behave as Bloch, instead of plane waves. Thereby, they can be written as:

$$\mathcal{A}_I(x) = e^{iqx} \left(A_I e^{i(\kappa_I - q)x} + B_I e^{-i(\kappa_I + q)x} \right), \quad (1.19)$$

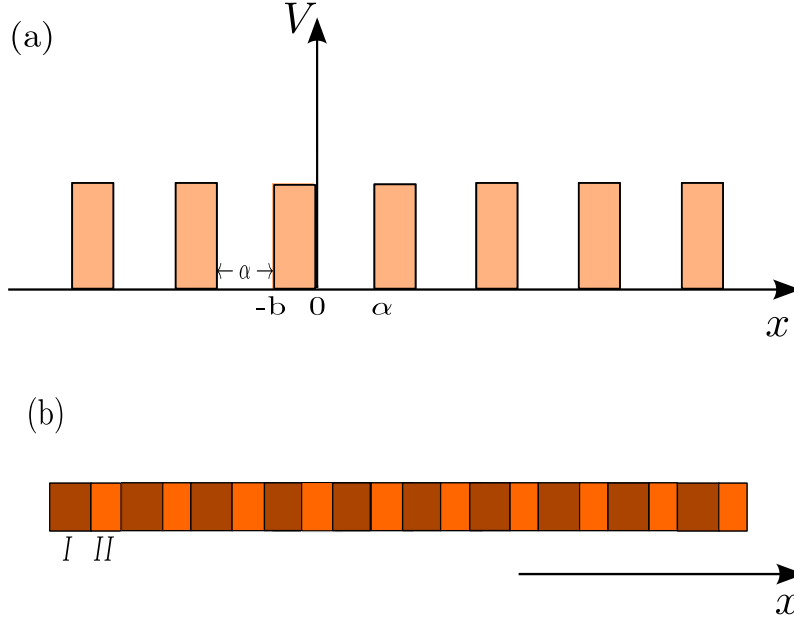


FIGURE 1.2: a) A periodic array of rectangular barriers. This configuration constitutes the basic Kronig-Penney model. Between two barriers, a potential free region intervenes. b) Periodic arrangement of slabs with alternating refractive index. Note that here, regions equivalent to those with zero potential do not exist.

where the “wave-number” q determines the crystal momentum and specifies the Bloch phase. Then the term:

$$u_I(x) = A_I e^{i(\kappa_I - q)x} + B_I e^{-i(\kappa_I + q)x}, \quad (1.20)$$

is a periodic function as stated by the Bloch theorem. Accordingly, we find that for the region (II) it holds that:

$$\mathcal{A}_{II}(x) = e^{iqx} u_{II}(x), \quad (1.21)$$

where

$$u_{II}(x) = A_{II} e^{i(\kappa_{II} - q)x} + B_{II} e^{-i(\kappa_{II} + q)x}. \quad (1.22)$$

Both the functions $\mathcal{A}(x)$ and their derivatives should obey the continuity condition in boundaries of each barrier (or slab). For simplicity reasons we implement them at $x = 0$, so that it holds:

$$\mathcal{A}(0^-) = \mathcal{A}(0^+) \quad (1.23)$$

and

$$\mathcal{A}'(0^-) = \mathcal{A}'(0^+). \quad (1.24)$$

Moreover, the periodicity imposes two extra conditions for $u(x)$ and $u'(x)$:

$$u(-b) = u(a - b) \quad (1.25)$$

and

$$u'(-b) = u'(a - b). \quad (1.26)$$

The above conditions yield the following matrix equation:

$$\begin{pmatrix} 1 & 1 & -1 & -1 \\ e^{i(\kappa_I - q)(a-b)} & e^{-i(\kappa_I + q)(a-b)} & -e^{-i(\kappa_{II} - q)b} & -e^{i(\kappa_{II} + q)b} \\ (\kappa_I - q)e^{i(\kappa_I - q)(a-b)} & -(\kappa_I + q)e^{i(\kappa_I + q)(a-b)} & -(\kappa_{II} - q)e^{i(\kappa_{II} - q)b} & (a - b)(\kappa_{II} + q)e^{i(\kappa_{II} + q)b} \end{pmatrix} \begin{pmatrix} A_I \\ B_I \\ A_{II} \\ B_{II} \end{pmatrix} = \begin{pmatrix} 0 \\ 0 \\ 0 \\ 0 \end{pmatrix} \quad (1.27)$$

This is a homogeneous system and for a non-trivial solution the determinant of the matrix must be zero. This finally yields the Kronig-Penney equation which reads:

$$\cos(qa) = \cos(\kappa_{II}b) \cos[\kappa_I(a - b)] - \frac{\kappa_I^2 + \kappa_{II}^2}{2\kappa_I\kappa_{II}} \sin(\kappa_{II}B) \sin[\kappa_I(a - b)]. \quad (1.28)$$

This result has a significant consequence. The left side of Eq (1.28) is always bounded by the values ± 1 . As a result, there are restrictions imposed on the possible values of κ_I , κ_{II} so that the right hand side of Eq (1.28) lies between ± 1 . When this term exceeds unity then Eq (1.28) is not fulfilled and κ_I , κ_{II} correspond to forbidden energies.

It should be mentioned here, that it is remarkable how this very simple model of a 1-D periodic crystal, predicts and describes quantitatively the concept of band structure. This is one of the model's great successes.

1.3 Waves in locally periodic media

In the previous section we focused on the behaviour of waves in fully periodic media, exhibiting the feature of band and gap structure. Now we turn to the more realistic situation of a medium comprised of scatterers positioned periodically, within a finite spatial extent. Particularly, in such systems the unit cell of the corresponding infinite system, is repeated N times in an equidistant manner. Their finite size renders the handling of these systems more cumbersome, in comparison to their infinite counterparts and this difficulty stems from the inapplicability of Bloch's theorem. Nevertheless, the problem is tractable and there exists an analytical solution for arbitrary number N of scatterers [24,43]. In this analysis, which is presented in detail in Ref. [24], one considers the plane wave propagation only from a single scatterer (unit cell) of the periodic structure and writes the corresponding transfer matrix \hat{M} . Due to the multiplicativity of \hat{M} (as we will see in detail in Chapter 5) and the periodicity of the potential, the transfer matrix for the whole array can be expressed as the N^{th} power of \hat{M} (\hat{M}^N).

With the use of the Caley-Hamilton theorem, which states that any matrix satisfies its own characteristic equation, we finally find that the transmission probability for a finite periodic system, comprised of N cells, is given by:

$$T_N = \frac{1}{1 + [|z|U_{N-1}(\xi)]^2}, \quad (1.29)$$

where z is a transfer matrix element, $U_N(\xi)$ is the N -th, second order Chebychev polynomial [44] and $\cos^{-1}(\xi)$ is the Bloch phase of the respective infinite system [24,43]. In this point it should be noted that the transmission calculation involves $|z|$, thereby it presupposes the knowledge of the transfer matrix of the single cell.

The preceding analysis yields [24] that the cosine of the Bloch phase ξ ($\xi = \cos\varphi_{Bloch}$) is related to the wave number of the incident wave and general characteristics of the potential via the relation:

$$\xi = \text{Re}(w) \cos(\kappa a) + \text{Im}(w) \sin(\kappa a), \quad (1.30)$$

where k is the wave number of the incident wave, a is the distance between each cell and w a transfer matrix element of the single cell, carrying information for the geometric characteristics of the cell. A detailed analysis for the transfer matrix is presented in Chapter 3

As an example we will examine how Eq. (1.30) becomes for the case of finite periodic array consisted of rectangular barriers. The transfer matrix of a rectangular barrier of width b and strength V has the form:

$$\begin{pmatrix} \left(\cos(\kappa' b) - i \frac{\kappa + \kappa'}{2\kappa\kappa'} \sin(\kappa' b) \right) e^{i\kappa b} & i \frac{\kappa - \kappa'}{2\kappa\kappa'} \sin(\kappa' b) \\ -i \frac{\kappa + \kappa'}{2\kappa\kappa'} \sin(\kappa' b) & \left(\cos(\kappa' b) - i \frac{\kappa + \kappa'}{2\kappa\kappa'} \sin(\kappa' b) \right) e^{-i\kappa b} \end{pmatrix} \quad (1.31)$$

with

$$\kappa' = \frac{\sqrt{2m(\varepsilon - V)}}{\hbar} ; \quad \kappa = \frac{\sqrt{2m\varepsilon}}{\hbar} \quad (1.32)$$

and ε the incident energy. Thus, Eq. (1.30) becomes:

$$\xi = \cos(\kappa' b) \cos[\kappa(a - b)] - \frac{\kappa + \kappa'}{2\kappa\kappa'} \sin(\kappa' b) \sin[\kappa(a - b)]. \quad (1.33)$$

The comparison with Eq. (1.28) interestingly shows that the equations for the infinite and the finite systems have the same form. This suggests that the transmission behaviour of the finite system is determined by the Bloch phase of its infinite counterpart. The cosine of φ_{Bloch} , ξ , has an important role on the determination of the transmission

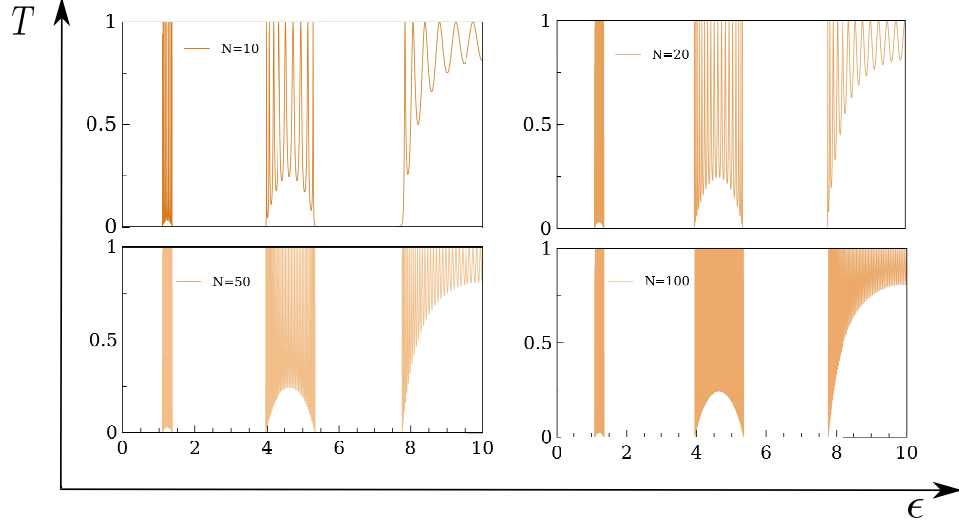


FIGURE 1.3: Transmission spectrum for a periodic rectangular barrier array, involving $N = 5, 20, 50, 100$ barriers. The characteristics of each barrier: width $b = 1$ and strength $V = 6$. The inter-barrier distance is $a = 2$.

properties of the finite periodic system. If we consider a periodic array of N barriers and impose *periodic boundary conditions* then we effectively create band structure properties even if it is not infinite. The more barriers we have, the denser each band will become. The level in each band are determined according to the number N of barriers and specifically each band involves $N - 1$ levels. This emerges from the form of ξ which due to boundary conditions becomes

$$\xi = \cos\left(\frac{n\pi}{N+1}\right), \quad n = 1, 2, \dots, N. \quad (1.34)$$

It is obvious that as N increases and tends to infinity, the more perfect transmission resonances appear in a certain energy extent of the transmission spectrum followed by energy regions of low transmission which accordingly become deeper. Clearly, these are precursors of the band structure which appears in the infinite, fully periodic system. Figure 1.3 illustrates the evolution towards the band structure formation for a locally periodic rectangular barrier array, for $N = 10, 20, 50, 100$ rectangular barriers. It is worth mentioning that the band formation becomes evident even for a very small number of barriers i.e. $N = 10$.

1.4 Waves in disordered media

As we have seen, the properties of propagating waves in periodic media are well understood, both in the case of the theoretical infinite model and when the more realistic case of finite periodicity is regarded. Our understanding and the mathematical description are significantly hindered when the translational invariance breaks and also in a random manner. Consider, for instance, a system with randomly distributed static scatterers, i.e. a conductor with a certain concentration of impurities. A single particle, which moves in such a medium, undergoes multiple scattering processes and this, in turn, lead to the phenomena as the *Anderson localization* (strong localization) [45, 46] and *coherent back-scattering* [47] (weak localization). Analogous phenomena, in appropriate systems, can be met in light wave scattering [48–51], even though the experimental realization is significantly more cumbersome [52]. In quantum systems the disorder-induced localization is followed by a phase transition, from the conducting phase to the insulating phase, usually referred to as metal-insulator transition [53].

Anderson localization describes the physical process that a single particle wave function will be spatially localized, by a time-independent potential. In particular, P.W. Anderson found that certain and sufficiently disordered random lattices, are characterized by the absence of electronic diffusion. On the other hand, coherent back scattering emerges in quantum transport, when the conditions for strong localization are not met, however they lie on the vicinity of its occurrence.

1.5 Waves in aperiodic and quasi-periodic media

The gap between perfect periodic crystals and amorphous media is covered by a large class of systems with geometry which belongs to the general framework of *aperiodic order* [54–60]. The theoretical study of such systems, i.e. systems with order but without periodicity [61], has been increasingly developed, involving semiconductor heterostructures [62], photonic multilayers [63], acoustic waveguides [20] or even DNA macromolecules [64] and extends from physical properties, such as transmission spectra [65–67] to more mathematical concepts as tiling theory and crystallography [68,69]. The increased experimental and theoretical interest render the study of systems with aperiodic order a dynamic and promising research field, especially concerning the design of devices with new functionalities and increased control on their transport properties. Therefore, in this section we will examine in what aspects such systems outmatch their periodic and random counterparts. In other words, whether and how aperiodically designed devices can be equipped with properties which impel their efficiency.

An aperiodically ordered structure is generated according to a deterministic rule. This is usually a substitution rule, which acts on a set of building blocks A , B , ..., each

one with long range order but without translational symmetry [70]. A single building block is then replaced by a composite one, following the pattern dictated by a certain rule, e.g. $A \rightarrow AB$.

A possible way to classify aperiodically ordered systems is to separate them to *self-similar* and *non-self-similar* patterns [61]. The former emerge from the application of a substitution rule while the latter no. Furthermore, systems with self-similarity can be split to those exhibiting long range quasi-periodic order like the *Fibonacci* and those which don't, including *fractal Cantor*, *Rudin-Shapiro* [71], *Thue-Morse* [72,73] and *period doubling* [74]. Materials with long range quasi-periodic order are known as *quasi-crystals* the discovery of which [8,9] in 1984, prompted significantly solid state physics. The reason for this boost was the surprising result from X-ray diffraction experiments showing that quasi-crystals, even though lacking translational symmetry, can possess X-ray diffraction patterns as sharp as those of periodic materials [8]. The reason for this similarity has been attributed to their long-range order [9].

Another characteristic property of quasi-crystals is the existence of two different kinds of order in two different length scales [61]. Particularly, order exists in the atomic level, following periodic arrangement, but also there is long-range aperiodic order determined by the apposition of the different layers. The flexibility in the manipulation of the latter length scale, according to the substitution rule, may enhance or suppress the emergence of physical properties which appear to a specific length scale, allowing for new applications [13].

The special geometric structure of systems with aperiodic order lead to theoretical results of great interest and with promising experimental implementations. Due to the Helmholtz-Schrödinger isomorphism [52] the theoretical treatment of quantum and classical waves follows the same pattern. However, in the quantum mechanical case, even though theory predicts the existence of special quantum states associated to the reflection of the geometry to the transmission spectrum [75–78], the experimental results are hindered by electron-phonon and electron-electron interactions or lattice structural defects [79–81]. Therefore, experimental application based is such geometries prove to be more valid when implemented to systems which support classical wave propagation, i.e. photonic quasi-crystals [55].

In the aforementioned examples of aperiodic order, the corresponding systems were constructed with the use of some substitution rule which determined the spatial arrangement of the different units i.e. potential barriers or dielectric slabs. However, it is possible to modify, extend or even ignore the substitution sequences in order to design systems with prescribed properties [82–84] or modulate the already existing properties of a material. We refer to systems tailored this way as systems *aperiodic by design* [61].

1.5.1 Fractal structures - Cantor filters

Aperiodic media with fractal structure [85,86] are basically characterized by the geometrical self-similarity and their fractional dimensionality. A self-similar object is exactly or approximately similar to a part of itself. When self-similarity is exact, so that at any magnification of the object there is a smaller part similar to the whole, then the system is scale invariant. Systems comprised of two different materials, organized in a fractal manner are referred to as *fractal filters* [87–93]. A commonly used fractal structure for the design of fractal filters is the Cantor set, which is generated by iteratively substituting the middle 1/3 portion from a linear segment into another linear segment [52]. Systems possessing Cantor structure have fractal dimensionality given by:

$$D(G) = \frac{\ln[(G+1)/2]}{\ln G}, \quad (1.35)$$

where G is the generator of the corresponding Cantor set. For a triadic Cantor set with $G = 3$, the dimensionality is $D(3) = \ln 2 / \ln 3$. In a Cantor fractal filter, the transmission spectrum of any given generation $N > 2$ of the substitution sequence which constructs it, involves all the transmission spectra of the preceding generations, from $m = 1, \dots, N-1$. In turn, the spectrum of all the embedded generations is suppressed by a factor G^{N-m} .

Devices with design based on the Cantor substitution rule usually possess a global parity symmetry axis. Such symmetrical filters exhibit splitting of the resonant transmission peaks. The number of split resonances increase as the generation N increases, in the same manner that the energy levels split in coupled quantum wells or as the precursors of band structure begin to form in locally periodic media. In optical devices, the emerging narrow transmission peaks result from the localization of light waves in cavities which behave as defects to a periodic structure. For the triadic Cantor case, with $N = 2$, we have $ABA|BBB|ABA$. In this symmetric structure the middle part BBB has the role of the defect/cavity, while the parts ABA behave as mirrors.

1.5.2 Quasi-periodic structures - Fibonacci filters

Rigorously, a function is quasi-periodic if it can be expanded in a sum of periodic functions with incommensurate periods [52]. The Fibonacci sequence offers a substitution sequence to construct quasi-periodic devices in 1-D. The Fibonacci rule is based on the regularities of the Fibonacci numbers F_N , which are dictated by the formula

$$F_N = F_{N-2} + F_{N-1} \quad ; \quad F_0 = 1, \quad F_1 = 1. \quad (1.36)$$

The limit of the ratio of two neighbouring terms in the Fibonacci sequence is the well known *golden mean*:

$$\lim_{N \rightarrow \infty} \frac{F_N}{F_{N-1}} = \frac{\sqrt{5} - 1}{2} = 0.6180339... \quad (1.37)$$

The Fibonacci quasi-crystal has been used in both in photonic [55] and in quantum [94] systems and it can be constructed as follows: A and B are the generating material units and form the first two generations. Each next generation is constructed by the sum of the two previous terms:

$$A, B, AB, BAB, ABBAB, BABABBAB$$

and so on. Studies on the electron propagation in a piecewise constant potential array, with barriers placed according to the Fibonacci sequence [95–97] revealed that the corresponding electron wave-function exhibited strong spatial fluctuations, deviating from the concept both of Bloch waves and of localized states. We refer such wave-functions as *critical* [52]. This peculiarity stems from the properties of the energy spectrum of quasi-periodic potentials which is neither continuous nor discrete. The energy can take an infinite number of discrete values forming a Cantor set, without developing however to a continuous band. We refer to this kind of spectra as *singular continuous* [98].

The novel properties characterizing the quantum transport in quasi-periodic barrier arrays, stimulated analogous studies for the propagation of classical waves in quasi-periodic photonic media, which often proved to be an advantageous field with respect to the experimental confirmation of the theoretical predictions. Indeed, as in their quantum counterparts, classical waves, when propagate to quasi-periodic media, exhibit both similar spectra and critical wave fields. Transmission spectra of photonic Fibonacci filters do show scalability, as in the Cantor case, however these properties become apparent in arrays produced from larger generations, that is when the array contain more layers compared to the Cantor counterpart [52].

1.5.3 Structures with hybrid order

Aperiodically designed structures, as we have seen, yield increased possibilities to control certain features of wave propagation and give rise to unique phenomena, absent in periodic systems. The question which is posed here is whether one can exploit more complex designs to manipulate propagation properties in a more efficient way. This can be achieved with *mixed structures* which are composed of both quasi-periodic and periodic components. Such systems with *hybrid* order [63], acquire new and easily tunable properties. As an example consider the critical states found in quasi-periodic set-ups and the Bloch states of media with perfect periodic order. A hybrid system consisted of Fibonacci/periodic/Fibonacci materials, may demonstrate localized modes in a selective manner [63,99]. This kind of flexibility in modulating the properties of a device, is often requested in technological applications.

In Fibonacci quasi-periodic devices the transmission spectrum doesn't, in general, demonstrate perfect transmitting resonances. This fact is attributed to the lack of parity symmetry, which until recently was regarded to be the essential structural requirement

for the existence of perfect transmission. Using however hybrid structures it possible to create parity symmetric devices, based on quasi-periodic order. For instance, studies which considered appropriately symmetrized Fibonacci (or other) structures [100], reported on finding perfectly transmitting resonances.

Quasi-periodic designs exhibiting mirror symmetry can be constructed by reversing the letters in the original sequence and then add the outcome to the original [101]. For the fifth Fibonacci generation $BABABBAB$ the reversed counterpart is $BABBABAB$ and the final symmetrized outcome is

$$BABABBAB|BABBABAB$$

Other ways to construct quasi-periodic structures with mirror symmetry is to embed the corresponding substitution rule to the iterative formula

$$S_{j+1} = S_{j-1}S_jS_{j-1}.$$

This kind of structure possesses dimer-like positional correlations between layers, which enhances the emergence of perfect transmission resonances [82].

However, as we shall see in detail in Chapters 5, 6, the *local parity* concept allows for perfect transmission in aperiodic set-ups and as a matter of fact the multitude of scales where it exist, offers the possibility to appear at desired frequencies [66,67].

Aperiodic lattices in 1-D, which are generated by substitution sequences, have been associated to the concept of local parity in yet another one manner, as it has been shown [102] that there exists a unified view of different classes of aperiodic lattices, according to the distribution of their maximal local parity symmetries.

CHAPTER 2

DISCRETE SYMMETRY INDUCED INVARIANTS

2.1 Introduction

In this chapter we focus on the concept of wave propagation in one dimensional media. The discussion begins with the derivation of the Helmholtz equation as the static limit of the acoustic wave and light equations, the heat and finally the Schrödinger equations. Due to the isomorphism of the resulting static equations, a unified treatment for one-dimensional systems is considered, which facilitates the link between this class of (time-independent) systems and the concept of local symmetries. Particularly, we consider global discrete symmetries i.e. parity and translational invariance and derive a set of symmetry induced *spatially invariant non-local currents* as a consequence of their breaking. These currents allow the determination of the field in the respective symmetric domain and subsequently leads to the *generalization of Bloch and parity theorems*, which hold in the case of non-broken translational and reflection invariance. Their emergence under the global symmetry breaking provides a systematic way to the comprehension and quantification of the discrete symmetry breaking process.

2.2 The Helmholtz equation

The Helmholtz equation is a linear, time-independent partial differential equation, named after Hermann von Helmholtz (1821 – 1894). The mathematical form of the Helmholtz equations is:

$$(\nabla^2 + k^2) \mathcal{A}(x) = f(x) \quad , \quad x \in \mathbb{R}^d \quad (2.1)$$

where $\mathcal{A}(x)$ is a scalar field and ∇^2 is the Laplacian operator. The parameter d determines the dimensionality of the problem and k is a real or complex constant. When $f(x) \neq 0$ the equation is inhomogeneous. We will consider here exclusively the homogeneous case $f(x) = 0$

Most commonly the Helmholtz equation models the propagation of both classical waves i.e. sound or light and matter waves in the quantum mechanical regime. Thus, in such problems the parameter k is interpreted as the wavenumber and the field $A(x)$ is the wave or the wave function amplitude, respectively.

The Helmholtz equation can be regarded as the static limit of the original time-dependent equation which describes a certain problem and emerges when *the separation of variables method* or the equation transform from the time to the frequency domain is applied. The latter is achieved by the replacement of the time derivative $\frac{\partial}{\partial t}$ with $-i\omega$. In the following we will examine several different physical problems which are successfully described in the static regime by the Helmholtz equation. Its applicability, partly is due to the absence of time-dependence. In fact, in the wave equation we have a second time derivative, while in the Schrödinger or the heat equations the time derivatives are of first order. In the Helmholtz equation this information is explicitly absent, even though, the type of time dependence of the original equation is implicitly revealed by the dispersion relation.

Our analysis will begin with the classic case of acoustic waves, for which both the wave and the Helmholtz equations will be derived. The treatment of all the other cases will have as a starting point the corresponding time-dependent equation.

2.2.1 The Helmholtz equation for acoustic waves

We assume a homogeneous, isotropic medium i.e. a fluid, with density $\varrho(\mathbf{r}, t)$, pressure $p(\mathbf{r}, t)$ and velocity $u(\mathbf{r}, t)$. In a fluid with no viscosity an acoustic wave can be regarded as a small perturbation. If ϱ_0, p_0 and u_0 are the respective values of the density, pressure and velocity for the unperturbed fluid and $\tilde{\varrho}, \tilde{p}, \tilde{u}$ are the small perturbations ($\tilde{\varrho} \ll \varrho_0, \tilde{p} \ll p_0$), then it holds that:

$$\varrho = \varrho_0 + \tilde{\varrho} \quad (2.2)$$

$$p = p_0 + \tilde{p}. \quad (2.3)$$

We will consider that the unperturbed fluid is at rest ($u_0 = 0$), so that the velocity is determined only by the perturbation \tilde{u} . Thus, the velocity of the fluid is significantly smaller than the speed of sound c . Consequently:

$$\tilde{u} \ll c \sim \left(\frac{p_0}{\varrho_0} \right)^{1/2}. \quad (2.4)$$

The motion of the fluid is then governed by the Euler equation [103] which expresses the momentum conservation:

$$\frac{\partial u}{\partial t} + (u \nabla) u + \frac{1}{\varrho} \nabla p = 0, \quad (2.5)$$

the continuity equation corresponding to the mass conservation:

$$\frac{\partial \varrho}{\partial t} + \nabla(\varrho u) = 0, \quad (2.6)$$

and the equation of state:

$$p = f(\varrho, \dot{\varrho}, \dots) \quad (2.7)$$

The above equations, after linearization become:

$$\frac{\partial \tilde{u}}{\partial t} + \frac{1}{\varrho_0} \nabla \tilde{p} = 0, \quad (2.8)$$

$$\frac{\partial \tilde{\varrho}}{\partial t} + \varrho_0 \nabla \tilde{u} = 0. \quad (2.9)$$

The differentiation of Eq. (2.9) with respect to t and the substitution $\frac{\partial \tilde{u}}{\partial t}$ from Eq. (2.8), yields an equation which links the perturbations $\tilde{\varrho}$, \tilde{p} of density and pressure, respectively:

$$\frac{\partial^2 \tilde{\varrho}}{\partial t^2} = \nabla^2 \tilde{p}. \quad (2.10)$$

Acoustic waves in barotropic fluids

To simplify the calculations we restrict ourself to the case of barotropic fluids, where the pressure is only a function of density $p = p(\varrho)$. This idealization can often adequately describe fluid behavior within a certain frequency range.

The procedure to derive the wave and subsequently the Helmholtz equations for the barotropic case starts by Taylor expanding p in the vicinity of ϱ_0 which denotes the unperturbed state:

$$p = p(\varrho_0) + (\varrho - \varrho_0) \left. \frac{dp}{d\varrho} \right|_{\varrho=\varrho_0} + \mathcal{O}\left((\varrho - \varrho_0)^2\right), \quad (2.11)$$

while we take into account that $p(\varrho_0) = p_0$ and also neglect higher order terms. Under these conditions it holds that:

$$p - p_0 = c^2(\varrho - \varrho_0) \Rightarrow p' = c^2 \varrho' \quad (2.12)$$

$$c^2 = \left. \frac{dp}{d\varrho} \right|_{\varrho=\varrho_0}.$$

The speed of sound c refers to the unperturbed fluid and is a real, positive quantity depending on the nature of the fluid. The final step for the derivation of the wave

equation is to insert Eq. (2.12) into Eq. (2.10), which results to the wave equation for pressure:

$$\nabla^2 p' - \frac{1}{c^2} \frac{\partial^2 p'}{\partial t^2} = 0. \quad (2.13)$$

The velocity perturbation u' will also satisfy the wave equation

$$\nabla^2 \mathbf{u}' - \frac{1}{c^2} \frac{\partial^2 \mathbf{u}'}{\partial t^2} = 0, \quad (2.14)$$

however, since the velocity is a vector, it will satisfy the vector wave equation. Apart from the velocity, Eq. (2.14) implies the existence of the so called velocity potential; a scalar function for which it holds that $u' = \nabla U$ and also satisfies the wave equation:

$$\nabla^2 U - \frac{1}{c^2} \frac{\partial^2 U}{\partial t^2} = 0. \quad (2.15)$$

Note here that the wave equation is linear and has solutions which are periodic in time. For harmonic time-dependence, the velocity potential has the form

$$U(\mathbf{r}, t) = \text{Re} (e^{i\omega t} \psi(\mathbf{r})) \quad (2.16)$$

where the temporal term is harmonic with circular frequency ω and $\psi(\mathbf{r})$ is the space dependent component which is a scalar complex function. Since in acoustics the velocity potential is real, we consider only the real part of the expression. The expression Eq. (2.16) satisfies Eq. (2.15) if the spatial field $\psi(\mathbf{r})$ satisfies the reduced wave equation or the *Helmholtz* equation:

$$\nabla^2 \psi(\mathbf{r}) + k^2 \psi(\mathbf{r}) = 0. \quad (2.17)$$

The parameter $k = \frac{\omega}{c}$ is the wavenumber and is real for real ω . The wavenumber k is related to the wavelength through the relation $\lambda = \frac{2\pi}{k}$. Thus, for a plane wave k expresses the number of waves per 2π units of length. The dependence of k on the frequency ω implies that the Helmholtz equation retains for monochromatic waves. Superposition of waves with different frequencies i.e. wave-packets, can also be treated within the context of the Helmholtz equation, nonetheless the Fourier transforms of the velocity potential $U(\mathbf{r}, t)$ has to be employed.

Acoustic waves in complex fluids

In very high frequencies, where chemical reactions or molecular relaxation occur, the barotropic approximation is rendered inadequate. In such media, referred as *complex*, internal processes occur as a result of some external action. These processes are induce relaxational effects which need for their description the inclusion of density time derivatives. Mathematically, the deviation from the barotropic case can be expressed through

the equation of state which no longer maintains its simple form $p = p(\varrho)$ but now also depends on the time derivative of the density $p = p(\varrho, \dot{\varrho})$. In this sense, the response of density to pressure changes is not immediate as the equation of state of the barotropic fluid implies, but rather involves a relaxation mechanism to the equilibrium state [103]. The linearization of the latter state equation yields:

$$\tilde{p} = c^2 \left(\tilde{\varrho} + \tau_\varrho \frac{\partial \tilde{\varrho}}{\partial t} \right), \quad (2.18)$$

where τ_ϱ , measured in time units, is the *density relaxation time*. The replacement of the new linearised equation of state in Eq. (2.10) yields the respective wave equation for this case, which accepts similar solutions as Eq. (2.16). The Helmholtz equation will be derived if we make a transform from the time to the frequency domain, via the replacement

$$\frac{\partial}{\partial t} \rightarrow -i\omega. \quad (2.19)$$

The spatially dependent field $\psi(\mathbf{r})$ satisfies the Helmholtz equation, however in this case with a complex wavenumber:

$$\nabla^2 \psi(\mathbf{r}) + k^2 \psi(\mathbf{r}) \quad ; \quad k^2 = \frac{\omega^2}{c^2(1 - i\omega\tau_\varrho)}. \quad (2.20)$$

At low frequencies, where the relaxation time τ_ϱ is very small ($\omega\tau_\varrho \ll 1$) we recover the barotropic case with real k .

In complex media the state equation can be more complicated, depending on density time derivatives of higher order $p = p(\dot{\varrho}, \ddot{\varrho}, \dots)$. Such media may possess, apart from relaxation dynamics, more complicated behaviour leading, for instance, to memory effects [103]. The equation of state then determines in what functional manner $k^2 = k^2(\omega)$, the wavenumber depends on the circular frequency, that is the dispersion relation. Finally, the actual functional form of the dispersion relation is determined from the physical properties of the medium.

In complex media, contrary to barotropic, the speed of sound $c = \frac{\omega}{k}$ can take complex values, since k is complex. If we isolate the real part of k we can define the *phase velocity*

$$c_p = \frac{\omega}{\text{Re}(k)}, \quad (2.21)$$

which is the rate that the phase of the wave propagates in space. The imaginary part, respectively, describes the attenuation of the waves in the medium.

2.2.2 The Helmholtz equation for thermal waves

The heat conduction equation is a partial differential equation which describes the temperature variation in a given region over time. It can be considered as a sub-case of the diffusion equation which also describes chemical or mass diffusion and other relevant cases. The mathematical form of the heat equation is:

$$\frac{\partial T}{\partial t} - \kappa \nabla^2 T = 0, \quad (2.22)$$

where T is the temperature perturbation and the parameter κ is the *thermal diffusivity*. The latter is defined as the ratio of the thermal conductivity d over the the density ρ times the heat capacity c_p under constant pressure, that is $\kappa = \frac{d}{\rho c_p}$.

To obtain the corresponding Helmholtz equation we implement the rule expressed in Eq. (2.19), transforming the heat equation from the time to the frequency domain. Then the Helmholtz equation is satisfied by the spatially dependent part of the solution $\psi(\mathbf{r})$:

$$\nabla^2 \psi(\mathbf{r}) + k^2 \psi(\mathbf{r}) \quad ; \quad k^2 = \frac{i\omega}{\kappa}, \quad (2.23)$$

where k^2 is purely imaginary.

As in the acoustic wave case, in the high frequency regime, relaxational procedures begin to occur, resulting to more complicated forms of dispersion relations, i.e. Eq. (2.20), to describe the propagation of thermal waves .

2.2.3 The Schrödinger equation

In Physics, the Helmholtz equation usually describes the propagation of classical waves, as previously demonstrated. Nonetheless, the time-independent Schrödinger equation, mathematically is equivalent to the Helmholtz equation. This equivalence, often referred to as *Helmholtz-Schrödinger isomorphism* [52], allows a similar treatment for classical and matter waves, even though the latter belong to the quantum regime.

The general form of the Schrödinger equation is:

$$i\hbar \frac{\partial \Psi(\mathbf{r}, t)}{\partial t} = \nabla^2 \Psi(\mathbf{r}, t) + V(\mathbf{r}) \Psi(\mathbf{r}, t), \quad (2.24)$$

with $V(\mathbf{r})$ being the potential which influences the motion of a quantum particle with mass m and \hbar the Planck constant. The solution $\Psi(\mathbf{r}, t)$ of Eq. (2.24) is the *wave function* which determines the probability to find the particle in the vicinity of \mathbf{r} at time t . From this probabilistic interpretation emerges the normalization condition which expresses the fact that the particle has to exist within volume V :

$$\int_V |\Psi(\mathbf{r}, t)|^2 = 1 \quad (2.25)$$

with $|\Psi(\mathbf{r}, t)|$ being the probability density.

In the Schrödinger equation case, instead of transformation from the time to the frequency domain, we will use the variable separation method. If $V(\mathbf{r})$ is time-independent, the wave function $\Psi(\mathbf{r}, t)$ can be written in the form

$$\Psi(\mathbf{r}, t) = \psi(\mathbf{r})T(t). \quad (2.26)$$

By inserting this equation to Eq. (2.24) we get:

$$i\hbar \frac{\dot{T}}{T} = \frac{H\psi}{\psi} = E. \quad (2.27)$$

From a mathematical point of view E is the *separation constant*. However, it has a significant physical meaning since it represents the energy of the particle. From Eq. (2.27) emerge the following two equations:

$$i\hbar \dot{T} = ET, \quad (2.28)$$

$$\mathcal{H}\psi = E\psi \quad (2.29)$$

where the solution of the first is $T(t) = e^{iEt/\hbar}$ and the second is a typical eigenvalue problem, with E being eigenvalue of the Hamiltonian operator

$$\hat{\mathcal{H}} = \nabla^2 + V(\mathbf{r}). \quad (2.30)$$

The spatial term $\psi(\mathbf{r})$ is a stationary state of the particle which described by the Schrödinger equation. If we rearrange the Eq. (2.29) using the Hamiltonian expression (2.30) we arrive at:

$$\nabla^2\psi(\mathbf{r}) + (E - V(\mathbf{r}))\psi(\mathbf{r}), \quad (2.31)$$

which, in turn, is the familiar Helmholtz equation:

$$\nabla^2\psi(\mathbf{r}) + k^2\psi(\mathbf{r}) ; \quad k^2 = (E - V(\mathbf{r})), \quad (2.32)$$

where now the corresponding wave vector k becomes a function of \vec{r} . In general the Schrödinger equation, depending on the boundary conditions dictated by physical problem, accepts certain quantized values for the energy E , thus being a PDE eigenvalue problem. These discretized solutions correspond to bound states. Nevertheless, for large values of energy, if $\lim_{r \rightarrow \infty} V(\vec{r})$ is finite, there exist a solution ψ for every E , rendering it an eigenvalues problem with a continuous spectrum. Moreover, depending on whether the E is smaller or larger than $V(\mathbf{r})$, the wavenumber k becomes imaginary or real, respectively.

2.2.4 Electromagnetic waves

Let us consider an electromagnetic (EM) field which is described by the following four vectors:

- the electric field vector \mathbf{E}
- the magnetic field vector \mathbf{H}
- the electric displacement vector \mathbf{D}
- the magnetic induction vector \mathbf{B}

The link between the vectors \mathbf{D} , \mathbf{B} and the vectors \mathbf{E} , \mathbf{H} is provided by the material equations:

$$\mathbf{D} = \varepsilon\varepsilon_0\mathbf{E} = \varepsilon_0\mathbf{E} + \mathbf{P}, \quad (2.33)$$

$$\mathbf{B} = \mu\mu_0\mathbf{H} = \mu_0\mathbf{H} + \mathbf{M}. \quad (2.34)$$

The parameters ε (relative dielectric permittivity) and μ (relative magnetic permeability) are dimensionless and characterize the medium where the wave propagation occurs. Respectively, ε_0 and μ_0 correspond to the permittivity and permeability of the vacuum. These parameters for anisotropic media are tensors and reduce to scalars in the isotropic case. The vectors \mathbf{P} and \mathbf{M} represent the electric and magnetic polarization, respectively. The set of vectors \mathbf{E} , \mathbf{H} , \mathbf{D} , \mathbf{B} satisfy the Maxwell's equations:

$$\nabla \times \mathbf{E} = -\frac{\partial \mathbf{B}}{\partial t}, \quad (2.35)$$

$$\nabla \times \mathbf{H} = \frac{\partial \mathbf{D}}{\partial t} + \mathbf{J}, \quad (2.36)$$

$$\nabla \cdot \mathbf{D} = \rho, \quad (2.37)$$

$$\nabla \cdot \mathbf{B} = 0. \quad (2.38)$$

The vector \mathbf{J} corresponds to the electric current density and ρ to the electric charge density, with units $\frac{A}{m^2}$ and $\frac{Cb}{m^3}$, respectively.

We consider now the case where no currents or charges exist ($\mathbf{J} = 0$, $\rho = 0$). The substitution of the Eqs. (2.33), (2.34) into the Maxwell equations yield:

$$\nabla \times \mathbf{E} = -\mu\mu_0 \frac{\partial \mathbf{H}}{\partial t}, \quad (2.39)$$

$$\nabla \times \mathbf{H} = \varepsilon\varepsilon_0 \frac{\partial \mathbf{E}}{\partial t}, \quad (2.40)$$

$$\nabla \cdot \mathbf{E} = 0, \quad (2.41)$$

$$\nabla \mathbf{H} = 0. \quad (2.42)$$

The curl of Eq. (2.39) combined with Eq. (2.40) gives:

$$\nabla \times \nabla \times \mathbf{E} = -\mu\mu_0 \frac{\partial}{\partial t} (\nabla \times \mathbf{H}) = -\mu\mu_0 \varepsilon \varepsilon_0 \frac{\partial^2 \mathbf{E}}{\partial t^2}. \quad (2.43)$$

Due to the following identity:

$$\nabla^2 E = \nabla (\nabla E) - \nabla \times \nabla \times \mathbf{E} \quad (2.44)$$

we obtain the wave equation for the electric field:

$$\nabla^2 E - \mu\mu_0 \varepsilon \varepsilon_0 \frac{\partial^2 \mathbf{E}}{\partial t^2} = 0, \quad (2.45)$$

which is satisfied by the plane wave solution

$$\mathbf{E}(\mathbf{r}, t) = e^{i(\omega t - \mathbf{k}\mathbf{r})}. \quad (2.46)$$

The wave number and the phase velocity then are

$$k = \omega (\mu\mu_0 \varepsilon \varepsilon_0)^{-\frac{1}{2}} \quad (2.47)$$

$$v = \frac{\omega}{k} = (\mu\mu_0 \varepsilon \varepsilon_0)^{-\frac{1}{2}}. \quad (2.48)$$

Note that when the wave propagation occurs in the vacuum, the dielectric permittivity and magnetic permeability are respectively $\varepsilon = 1$ and $\mu = 1$, defining in this manner the speed of light in the vacuum as:

$$c = (\mu_0 \varepsilon_0)^{-\frac{1}{2}} \approx 3 \times 10^8 \text{ m/s}. \quad (2.49)$$

Otherwise, it holds that

$$v = \frac{c}{n}, \quad (2.50)$$

where n is the refraction index of the material, defined as

$$n = \sqrt{\varepsilon \mu}. \quad (2.51)$$

Inserting now the definitions c and n in Eq. (2.45) we get the wave equation which governs the dynamics of the electric field within a material of refraction index n :

$$\nabla^2 E - \frac{n^2}{c^2} \frac{\partial \mathbf{E}}{\partial t^2} = 0. \quad (2.52)$$

Following a similar procedure, one can obtain the wave equation that corresponds to the propagation of the magnetic field \mathbf{H} :

$$\nabla^2 H - \frac{n^2}{c^2} \frac{\partial \mathbf{H}}{\partial t^2} = 0. \quad (2.53)$$

If $\mathbf{p}_{1,2}$ are unit vectors in the direction of the field, we can express the vector fields $\mathbf{E}(\mathbf{r}, t)$, $\mathbf{H}(\mathbf{r}, t)$ via the scalar fields $E(\mathbf{r}, t)$, $H(\mathbf{r}, t)$ [52]

$$\mathbf{E}(\mathbf{r}, t) = \mathbf{p}_1 E(\mathbf{r}, t) \quad ; \quad \mathbf{H}(\mathbf{r}, t) = \mathbf{p}_2 H(\mathbf{r}, t). \quad (2.54)$$

For plane, monochromatic waves the scalar fields can be written so as to separate the temporal and spatial parts:

$$E(\mathbf{r}, t) = E(\mathbf{r})e^{i\omega t} \quad ; \quad H(\mathbf{r}, t) = H(\mathbf{r})e^{i\omega t}. \quad (2.55)$$

Therefore, by inserting Eq. (2.55) to the wave Eqs. (2.52), (2.53), we get their time independent version

$$\nabla^2 E(\mathbf{r}) + k^2 E(\mathbf{r}) = 0 \quad ; \quad \nabla^2 H(\mathbf{r}) + k^2 H(\mathbf{r}) = 0, \quad (2.56)$$

where $k = \frac{n(\mathbf{r})}{c}\omega$. These equations are the *Helmholtz equations* for EM waves and describe the space distribution of the electric or magnetic field when an EM wave propagates in a material of refraction index $n(\mathbf{r})$.

2.3 Invariants of discrete symmetries

Here we attempt to link the concept of local, discrete symmetries i.e. parity and translational invariance to the propagation of waves in media which, in their time independent version, are described by the Helmholtz equation. Based on the fact that these symmetries in their *global* version can be broken either by violating the boundary conditions, while the potential still retains the corresponding symmetry property, or when the potential does not exhibit the corresponding symmetry $\forall x \in \mathbb{R}$. In the latter case the symmetry can be either completely absent or maintained in spatially restricted domains.

Global translation invariance describes a system which is fully periodic and extends to infinity or it is equipped with periodic boundary conditions. Even though in nature, perfect periodicity cannot be met due to defects, models which exhibit perfect translation symmetry are the cornerstone for the description of crystals. In such periodic structures, the description of electronic propagation is greatly facilitated by the Bloch theorem [28] which, in turn, leads to the description of *band structure*. On the other hand, a quantum system, the potential of which has a *global reflection symmetry*, leads to the classification of

the eigenstate spectrum of the bound quantum systems in even and odd wavefunctions. We use here the term *parity theorem* for the well known theorem of quantum mechanics concerning the commutation of the global parity operator with the Hamiltonian and the existence of common eigenstate spectrum for the two operators [104].

The common case, however, in realistic physical systems, is that discrete global symmetries are broken and replaced either by others which are valid in a finite spatial extent (finite periodic systems) or by different symmetries which coexist at different spatial scales (aperiodic and quasi-periodic systems). Despite this fact, a rigorous theoretical treatment of global discrete symmetry breaking for the translation and the parity invariance is still lacking. To this aim we develop a formalism which describes the wave propagation in media with inversion or translation symmetry in finite spatial domains while globally these symmetries are broken and show how the parity and Bloch theorems can be generalized for globally broken symmetries [105]. Such systems are characterized by a generalized potential $\mathcal{W}(x)$ which is homogeneous in the zy -plane, and varies only in the x -direction, $\mathcal{W}(\vec{r}) = \mathcal{W}(x)$. The generalized potential $\mathcal{W}(x)$ is generated by the effective wave vector $\kappa(x)$ which describes the inhomogeneity of the medium. We also restrict the wave to normal incidence on the zy -plane, so that it propagates along the x -axis. Then the field can be written $\mathcal{A}(\vec{r}, t) = \mathcal{A}(x)e^{-i\omega t}\hat{x}$, where $\mathcal{A}(x)$ is the complex field amplitude. Therefore, the developed formalism applies directly not only to quantum mechanical but also to optical, acoustic or any wave system described by the Helmholtz equation. For instance, in the quantum mechanical case, $\mathcal{A}(x)$ is the wavefunction in x -representation, $\mathcal{W}(x) = \frac{2m}{\hbar^2}(\varepsilon - V(x))$ (m being the mass and ε the energy of the quantum particle in the potential $V(x)$) while for electromagnetic waves with frequency ω , the function $\mathcal{A}(x)$ could represent the electric field and $\mathcal{W}(x) = \frac{\omega^2 n^2(x)}{c^2}$ ($n(x)$ being the refractive index of the medium of propagation).

Of special interest is the case of systems which can be completely decomposed in units within each -in general a different- reflection or translation symmetry is exactly fulfilled. Such systems form a special class of *completely locally symmetric materials* which extend the notion of periodicity or global parity symmetry. In the following chapters we will extensively study such systems, revealing their intriguing properties.

2.3.1 Invariant non-local currents

We proceed showing first the existence of non-local currents which are spatially constant within the finite domain(s) in which the medium obeys the symmetry. Subsequently we show how these currents can be used to partially determine the solution of the associated wave equation in the symmetry domain(s). In this sense our approach generalizes parity and Bloch theorems for systems which obey reflection or translation symmetry in restricted spatial domains. To make the last statement more transparent we demonstrate, in the case of translation symmetry, how our formalism leads to the Bloch theorem when

the symmetry domain becomes infinite i.e. it covers the entire space and the symmetry is globally restored. The analysis and the presentation of our theory is performed in one dimension assuming the wave propagation to be described by the Helmholtz equation. However, it is straightforward to extend our treatment in higher dimensions. In the latter case the translation symmetry is trivially extended while the parity symmetry is replaced by the inversion with respect to some center.

In order to treat wave propagation in inhomogeneous media within a unified framework we employ the Helmholtz equation:

$$\mathcal{A}''(x) + \mathcal{W}(x)\mathcal{A}(x) = 0. \quad (2.57)$$

where the prime denotes differentiation with respect to x . We consider the following linear transform

$$F(x) = \sigma x + \rho \quad ; \quad \text{with} \quad \begin{cases} \sigma = -1 & ; \quad \rho = 2\alpha \quad (\text{parity}) \\ \sigma = +1 & ; \quad \rho = L \quad (\text{translation}) \end{cases} \quad (2.58)$$

which acts on the generalized potential of Eq. (2.57) in the following manner:

$$\mathcal{W}(x) = \mathcal{W}(F(x)), \quad (2.59)$$

$\forall x$ in the domain \mathcal{D} . The transform in Eq. (2.58) describes a reflection about the point α when $\sigma = -1$ and a translation by L when $\sigma = +1$.

Particularly, the translation operator \hat{T}_L , which causes a translation by L is defined from the relation :

$$\hat{T}_L \mathcal{A}(x) = \mathcal{A}(x + L). \quad (2.60)$$

This can be straightforwardly shown by expanding $\mathcal{A}(x + L)$ to get

$$\mathcal{A}(x + L) = \mathcal{A}(x) + \mathcal{A}'(x)L + \frac{1}{2}\mathcal{A}''(x)L^2 + \dots \quad (2.61)$$

$$\mathcal{A}(x + L) = \sum_{n=0}^{\infty} \frac{L^n}{n!} \frac{d^n \mathcal{A}(x)}{dx^n} \quad (2.62)$$

$$\mathcal{A}(x + L) = e^{L \frac{d}{dx}} \mathcal{A}(x) \quad (2.63)$$

$$\mathcal{A}(x + L) = \hat{T}_L \mathcal{A}(x) \quad (2.64)$$

where $\hat{T}_L \equiv e^{L \frac{d}{dx}}$. In the quantum mechanical case the translation operator has the form

$$\hat{T}_L \equiv e^{iL \frac{\hat{P}}{\hbar}} \quad (2.65)$$

and $\hat{P} = i\hbar \frac{d}{dx}$ is the momentum operator. If $\mathcal{A}(x)$ is an eigenfunction of \hat{T}_L , then we can write:

$$\hat{T}_L \mathcal{A}(x) = \lambda_T \mathcal{A}(x). \quad (2.66)$$

When the set-up extends to infinity then from the Bloch theorem we have:

$$\mathcal{A}(x + L) = e^{ikL} \mathcal{A}(x), \quad (2.67)$$

where k is the quasi wave number, associated with the crystal momentum $\hbar k$. Obviously then, we can write:

$$\hat{T}_L \mathcal{A}(x) = e^{ikL} \mathcal{A}(x) \quad (2.68)$$

and therefore the eigenvalues of \hat{T}_L are phases $\lambda_T = e^{ikL}$, lying on the unit circle.

Similarly, the parity operator Π acting on $\mathcal{A}(x)$ yields:

$$\Pi \mathcal{A}(x) = \mathcal{A}(-x). \quad (2.69)$$

If $\mathcal{A}(x)$ is an eigenfunction of Π then:

$$\Pi \mathcal{A}(x) = \lambda_\Pi \mathcal{A}(x) \quad (2.70)$$

$$\Pi^2 \mathcal{A}(x) = \lambda_\Pi^2 \mathcal{A}(x). \quad (2.71)$$

The parity operator is Hermitian $\Pi = \Pi^\dagger$ and unitary $\Pi^\dagger = \Pi^{-1}$ (see Chapter 4) and as a result it is involutory $\Pi^2 = \hat{1}$. Therefore, the parity eigenvalues are $\lambda_\Pi = \pm 1$ corresponding to even and odd eigenfunctions.

Since Eq. (2.57) is valid for every x in \mathbb{R} it must also hold for the images of x under the transform F :

$$\mathcal{A}''(F(x)) + \mathcal{W}(F(x))\mathcal{A}(F(x)) = 0. \quad (2.72)$$

Now we multiply Eq. (2.57) by $\mathcal{A}(F(x))$ and Eq. (2.72) by $\mathcal{A}(x)$. Subsequently, we subtract the resulting equations from each other, taking into account the symmetry of the generalized potential $\mathcal{W}(x)$ (valid only for $x \in \mathcal{D}$), expressed by Eq. (2.59). The outcome is:

$$\mathcal{A}(F(x))\mathcal{A}''(x) - \mathcal{A}(x)\mathcal{A}''(F(x)) = 0 \quad (2.73)$$

Equation (2.73) (for $\sigma = \pm 1$) has the form of a total derivative:

$$\frac{d}{dx} [\mathcal{A}(F(x))\mathcal{A}'(x) - \sigma \mathcal{A}(x)\mathcal{A}'(F(x))] = 0 \quad ; \quad \forall x \in \mathcal{D} \quad (2.74)$$

which in turn implies that the complex quantity:

$$Q = \frac{1}{2i} [\sigma \mathcal{A}(x)\mathcal{A}'(F(x)) - \mathcal{A}(F(x))\mathcal{A}'(x)] \quad (2.75)$$

is spatially invariant within the domain \mathcal{D} .

In the same manner, we can use the complex conjugate of Eq. (2.57) (or Eq. (2.72)) and repeat the same procedure. Then we obtain another independent, spatially invariant quantity in the domain \mathcal{D} :

$$\tilde{Q} = \frac{1}{2i} [\sigma \mathcal{A}^*(x) \mathcal{A}'(F(x)) - \mathcal{A}(F(x)) \mathcal{A}'^*(x)] \quad (2.76)$$

The quantities defined by Eqs. (2.75), (2.76) have the form of a *non-local current*, involving points connected by the corresponding symmetry transform. Since we refer to a real generalized potential $\mathcal{W}(x)$ in Eq. (2.57), apart from the constants Q and \tilde{Q} , also exists the globally conserved local current J given by:

$$J = \frac{1}{2i} [\mathcal{A}'(x) \mathcal{A}^*(x) - \mathcal{A}'^*(x) \mathcal{A}(x)] \quad (2.77)$$

which represents the probability current in the quantum mechanical case or the $1 - D$ analogue of the Poynting vector in the electromagnetic case. The invariants Q , \tilde{Q} , J are not independent due the relation

$$\sigma (|\tilde{Q}|^2 - |Q|^2) = J^2, \quad (2.78)$$

which provides the relevant link. Equation (2.78) can be directly obtained by taking the moduli of Q , \tilde{Q} from Eqs. (2.75), (2.76) and subtract them.

2.3.2 Generalization of Bloch and parity theorems for broken symmetries

In its most general form, the transform $F(x)$ maps a domain \mathcal{D} to a different domain \mathcal{D}' , as long as these domains are related with each other with the corresponding symmetry operation. These domains don't need to be connected and they can be separated by any distance, as long as the symmetry is preserved. In the usual case of parity, where the mirror axis at α belongs to the domain, the mapping occurs from \mathcal{D} to itself and particularly from the rhs of the mirror axis to the lhs, or vice-versa.

The image of the wave field $\mathcal{A}(F(x))$, can be expressed in terms of $\mathcal{A}(x)$, $\mathcal{A}^*(x)$ and the invariants Q , \tilde{Q} by solving the system of Eqs. (2.75), (2.76) with respect to $\mathcal{A}(F(x))$ and $\mathcal{A}'(F(x))$. This, in turn, yields:

$$\mathcal{A}(F(x)) = \frac{\tilde{Q}}{J} \mathcal{A}(x) - \frac{Q}{J} \mathcal{A}^*(x) \quad (2.79)$$

and

$$\mathcal{A}'(F(x)) = \sigma \left(\frac{\tilde{Q}}{J} \mathcal{A}'(x) - \frac{Q}{J} \mathcal{A}'^*(x) \right) \quad (2.80)$$

Equation (2.79) is of central importance. One can directly determine the image $\mathcal{A}(F(x))$ in the target domain \mathcal{D}' from $\mathcal{A}(x)$ in \mathcal{D} only by using the constant non-local currents Q and \tilde{Q} , which result from the symmetry expressed in Eq. (2.59) of the potential $\mathcal{W}(x)$ relating the domains \mathcal{D} and \mathcal{D}' . In this sense, it constitutes the generalization of Bloch and parity theorems in the case of potential $\mathcal{W}(x)$ with broken global symmetry. As it will be shown in the following paragraphs the non-vanishing invariant current Q expresses the manifestation of the broken discrete symmetry.

2.3.3 Globally symmetric potentials

In order to explain transparently the mechanism of symmetry breaking we define the linear operator \hat{O}_F which acts in the x -representation on an arbitrary function $\Phi(x)$ and transforms it according to the respective symmetry operation:

$$\hat{O}_F \Phi(x) = \Phi(F(x)) \quad ; \quad \forall x \in \mathbb{R}. \quad (2.81)$$

Global symmetry with respect to the transform \hat{O}_F is realized when $\mathcal{W}(x) = \mathcal{W}(F(x))$ for all $x \in \mathbb{R}$. In this case the Helmholtz operator

$$\hat{\Omega} = \frac{d^2}{dx^2} + \mathcal{W}(x) \quad (2.82)$$

commutes with \mathcal{O}_F and $\mathcal{A}(x)$ is an eigenstate of \hat{O}_F :

$$\hat{O}_F \mathcal{A}(x) = \lambda_F \mathcal{A}(x), \quad (2.83)$$

λ_F being an eigenvalue of \hat{O}_F . The simplest scenario to break the global \hat{O}_F -symmetry is when $\hat{\Omega}$ still commutes with \hat{O}_F , i.e.

$$\mathcal{W}(x) = \mathcal{W}(F(x)) \quad \forall x \in \mathbb{R}$$

but the function $\mathcal{A}(x)$ ceases to be an eigenfunction of \hat{O}_F violating Eq. (2.83) due to its asymptotic behaviour, which is typically the case in a scattering problem. Remarkably, within the present framework, even if the symmetry is broken due the asymptotic conditions the conserved quantities Q and \tilde{Q} are constant in the entire space (and Eq. (2.79) applies for all x in \mathbb{R}) due to the global underlying symmetry of the potential. Using Eqs. (2.79) and (2.81) we can write:

$$\hat{O}_F \mathcal{A}(x) = \frac{\tilde{Q}}{J} \mathcal{A}(x) - \frac{Q}{J} \mathcal{A}^*(x) \quad ; \quad \forall x \in \mathbb{R} \quad (2.84)$$

which clearly shows that $Q \neq 0$ manifests as a remnant of the broken global translation or inversion symmetry.

2.3.4 Retrieving the Bloch and parity theorems

To set $Q = 0$ has interesting consequences on the field $\mathcal{A}(x)$. One can integrate Eq. (2.75) and get

$$\mathcal{A}(F(x)) = c\mathcal{A}(x) \quad (2.85)$$

where $c \in \mathbb{C}$ is an integration constant. If however we set $c = \lambda_F = \frac{\tilde{Q}}{J}$ we recover Eq. (2.83), which is consistent with our interpretation of the invariant Q as a symmetry breaking term. Based on a vanishing Q value, we will show rigorously how parity and Bloch theorems are retrieved in the limit of global symmetry restoration. This constitutes an argumentation on how Eqs. (2.75), (2.76), (2.79) generalize the parity and Bloch theorems for the case of broken global symmetry.

Inversion ($\sigma = -1$)

Starting from the inversion case we integrate Eq. (2.75) assuming $Q = 0$ which, as previously discussed, is a necessary condition for a global discrete symmetry to hold. This yields:

$$\mathcal{A}(2\alpha - x) = c\mathcal{A}(x) \quad ; \quad \mathcal{A}'(2\alpha - x) = -c\mathcal{A}'(x) \quad (2.86)$$

where c is an integration constant. One can determine c by setting in Eq. (2.75) $x = \alpha$ since for the case of global parity the symmetry axis necessarily belongs to the domain of mirror symmetry which is the entire space. This leads to $\mathcal{A}(\alpha)\mathcal{A}'(\alpha) = 0$. Assuming $\mathcal{A}(\alpha) \neq 0$ and $\mathcal{A}'(\alpha) = 0$ we find $c = 1$ while assuming $\mathcal{A}(\alpha) = 0$ and $\mathcal{A}'(\alpha) \neq 0$ we get $c = -1$. Thus for $Q = 0$ the wave function $\mathcal{A}(x)$ becomes an eigenfunction of the global parity operator $\hat{O}_F \equiv \hat{\Pi}_\alpha$ which performs mirror reflection around the axis located at α . Note that for $Q = 0$, Eq. (2.78) becomes:

$$|\tilde{Q}|^2 = -J^2,$$

which, in turn implies that $\tilde{Q} = J = 0$. Therefore, for parity, the global symmetric scenario is realized either in bound state problems where the asymptotic conditions are symmetric and $J = 0$ or in scattering problems if incoming waves arrive at the potential $\mathcal{W}(x)$ from both sides in a certain, symmetric manner so that $J = 0$. The latter are actually the zero current states discussed in [66]. In Chapter 5 *zero current states* will be introduced, demonstrating that in this scattering scenario it is possible to have $Q = 0$, which in turn denotes that the symmetry is restored in the whole space.

Translation ($\sigma = 1$)

Going over to the global translational symmetry, where $\sigma = 1$, we set $Q = 0$ in Eq. (2.84) which becomes an eigenvalue equation. Then, from Eq. (2.78) it follows that:

$$\left| \frac{\tilde{Q}}{J} \right| = 1 \quad (2.87)$$

and consequently, $\frac{\tilde{Q}}{J}$ becomes a phase which is in agreement with the fact that it is an eigenvalue of the translation operator $\hat{O}_F \equiv \hat{T}_L$.

Global translation symmetry implies infinite periodicity for the potential $\mathcal{W}(x)$, i.e. $\mathcal{W}(x) = \mathcal{W}(x + L)$ for all x in \mathbb{R} . Thus, the property $\mathcal{W}(x) = \mathcal{W}(x + nL)$ with $n \in \mathbb{Z}$ applies too. This in turn implies that Eqs. (2.75), (2.76), (2.79) can be written replacing the translation parameter L with nL . For global translation symmetry $Q = 0$ must hold for all n in \mathbb{Z} . However the \tilde{Q} 's would in general differ for various n 's. It is therefore useful to introduce an index noticing \tilde{Q}_{nL} the constant \tilde{Q} corresponding to displacement nL . Equation (2.79) generalizes accordingly in a trivial way as:

$$\begin{aligned} \mathcal{A}(x + L) &= e^{i\theta(L)} \mathcal{A}(x) & ; & & \theta(L) &= \theta_{\tilde{Q}_L} \\ \tilde{Q}_L &= \pm |J| e^{i\theta_{\tilde{Q}_L}} \end{aligned} \quad (2.88)$$

Then, due to the infinite periodicity we expect that \tilde{Q}_L will be the same for every x in \mathbb{R} . Using Eq. (2.79) we can relate $\mathcal{A}(x + nL)$ with $\mathcal{A}(x)$ either by performing n translations by L or one translation by nL . The uniqueness of the wave function value requires:

$$\begin{aligned} \mathcal{A}(x + nL) &= e^{i\theta(nL)} \mathcal{A}(x) = (e^{i\theta(L)})^n \mathcal{A}(x) \\ \Rightarrow \theta(nL) &= n\theta(L) \end{aligned} \quad (2.89)$$

which means that $\theta(L) = kL$ with k a constant of inverse length dimension. In addition one obtains a relation for the phases of the different \tilde{Q} 's:

$$\theta_{\tilde{Q}_{nL}} = n\theta_{\tilde{Q}_L}. \quad (2.90)$$

Equation (2.89) can be written as

$$\mathcal{A}(x + L) = e^{ikL} \mathcal{A}(x), \quad (2.91)$$

where k is the *quasi wave number*, associated with the crystal momentum $\hbar k$. Multiplying both sides of this relation with $e^{-ik(x+L)}$ leads to

$$e^{-ikx} \mathcal{A}(x) = e^{-ik(x+L)} \mathcal{A}(x + L), \quad (2.92)$$

which is exactly the periodic function $u(x) = u(x + L)$, with period L , which appears in the Bloch theorem

$$\mathcal{A}(x) = e^{ikx}u(x) \ ; \ u(x) = u(x + L). \quad (2.93)$$

Thus we have shown that Eqs. (2.75), (2.76), (2.79) contain the parity and Bloch theorems as the special limit of global symmetry restoration.

2.3.5 Locally symmetric potentials

We turn now to the second and more demanding scenario of symmetry breaking. Contrary to the above discussed case where the symmetry of the potential $\mathcal{W}(x) = \mathcal{W}(F(x))$ was retained in its total spatial extent, here we consider potentials $\mathcal{W}(x)$ which do not exhibit globally such symmetry. Since, in this case, \hat{O}_F does not commute with the Helmholtz operator Ω , it is not possible to seek for stationary eigenstates as in Eq. (2.83), unless the action of \hat{O}_F is partitioned as was done in Ref. [66], for parity symmetry. However, here we will consider the local symmetry properties according to the invariants Q , \tilde{Q} , which relate in an explicit manner the effects of symmetry on the wave field amplitudes, through Eq. (2.79).

In the extreme case of complete breaking of the global symmetry, i.e. when there is no domain \mathcal{D}_i for which a remnant of the global symmetry is present in $\mathcal{W}(x)$, then, as expected, there is also no domain in which Q and \tilde{Q} are constant. Although, one can still define the spatially dependent function $Q(x)$, $\tilde{Q}(x)$, their non-constancy brings no advantage to the representation of the scattering problem.

Nevertheless, when there are one or several domains \mathcal{D}_n ($n = 1, 2, \dots, N$ for N domains) in the x -space for which Eq. (2.59), which denotes the existence of the symmetry in the specific domain as remnant of the global symmetry, is valid. Then the global symmetry is partially broken and the previous analysis is applicable leading to the existence of a pair of complex spatially constant quantities (Q_n, \tilde{Q}_n) in each domain \mathcal{D}_n . These constant quantities allow the determination of the image $\mathcal{A}(F(x))$ from $\mathcal{A}(x)$ for all x in \mathcal{D}_n through the Eq. (2.79). In addition the relation of these constants to the globally conserved current J gives a constraint between their magnitudes in different domains:

$$|\tilde{Q}_1|^2 - |Q_1|^2 = |\tilde{Q}_2|^2 - |Q_2|^2 = \dots = |\tilde{Q}_N|^2 - |Q_N|^2 \quad (2.94)$$

Among the different set-ups which support the partial breaking of the \hat{O}_F -symmetry, of greatest interest is the case of systems possessing a potential $\mathcal{W}(x)$ which can be completely decomposed in locally symmetric domains each one characterized by a different remnant of the broken symmetry. Then the domains \mathcal{D}_n cover the extent of the entire set-up and the corresponding symmetry is fulfilled in each $\mathcal{W}_n(x)$

$$\mathcal{W}_n(x) = \mathcal{W}_n(F_n(x)) \quad \forall \ x \in \mathcal{D}_n. \quad (2.95)$$

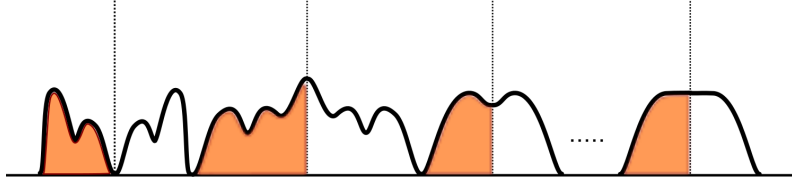


FIGURE 2.1: Schematic of a completely locally symmetric set-up, with each barrier being parity symmetric. The colored parts of the barriers indicate the part of the potential where we need to know the field $\mathcal{A}(x)$ in order to determine $\mathcal{A}(F(x))$, if the invariants $\{Q_n, \tilde{Q}_n\}$ for each symmetry domain, are known.

We refer to such a potential as a *completely locally symmetric (CLS)* potential.

To be more concrete we consider a potential which is the sum of terms defined in non-overlapping domains each one characterized by a different mirror symmetry [66,67] as those shown in Chapters 5, 6. Assume that in each domain the axis of mirror symmetry lies at the center of the domain. As already discussed the domain is mapped to itself in this case. Using Eq. (2.79) in each domain one can obtain the wave function in the right part of a domain from the wave function of the left part (or the opposite), by employing the invariants Q_n, \tilde{Q}_n of the corresponding potential $\mathcal{W}(x)$ in the sub-domain \mathcal{D}_n . Thus we need only to know the wave function in the half space in order to obtain it for the remaining half space, as shown in Fig 2.1. If the total potential is comprised by N LP, non-overlapping domains \mathcal{D}_n , each one characterized by a potential $\mathcal{W}_n(x)$, then there will exist N couples of $\{Q_n, \tilde{Q}_n\}$. In the case of the global symmetry restoration the situation is similar, though simplified since the rhs of the field can be calculated from the lhs by a multiplication with ± 1 . What differs in the case of broken symmetry is that the half-intervals where we need to know the wave function are disconnected forming an array and not a simply connected region. The aforementioned analysis suggests a characteristic class of CLS material structures, which generalize the notion of aperiodic and quasi-periodic systems.

2.4 Matrix formulation of the non-local currents

In this section we will reformulate the developed formalism for the introduced invariant non-local currents, so as to facilitate an analogous study for systems with losses, which will be presented in the next section. Moreover, the matrix formulation for the invariants will be used in Chapter 5 in order to allow their connection with the transfer matrix of any system which supports their existence. Adding Eqs. (2.75), (2.76), we get:

$$\frac{Q + \tilde{Q}}{2} = \frac{1}{2i} [\sigma \mathcal{A}'(F(x)) \mathcal{A}_R(x) - \mathcal{A}(F(x)) \mathcal{A}'_R(x)] \quad (2.96)$$

which turns to the following real invariants after the separation of real and imaginary parts:

$$q_1 = \frac{1}{2i} [\sigma \mathcal{A}'_R(F(x)) \mathcal{A}_R(x) - \mathcal{A}_R(F(x)) \mathcal{A}'_R(x)], \quad (2.97)$$

and

$$q_2 = \frac{1}{2i} [\sigma \mathcal{A}'_I(F(x)) \mathcal{A}_R(x) - \mathcal{A}_I(F(x)) \mathcal{A}'_R(x)], \quad (2.98)$$

where we have used that $\mathcal{A}(x) = \mathcal{A}_R(x) + i\mathcal{A}_I(x)$. The quantities q_1 and q_2 are still spatially invariant and have the form of non-local currents, though now they are pure imaginary. Note, that we refer to a general domain \mathcal{D} where the potential changes under the linear transform $F(x)$. The following procedure holds both when \mathcal{D} constitutes the whole set-up and when \mathcal{D} is part of the total set-up, as long as the symmetry transform $F(x)$ is valid within its extend.

The same procedure is followed by subtracting Q and \tilde{Q} to obtain two more imaginary invariants:

$$q_3 = \frac{1}{2i} [\sigma \mathcal{A}'_R(F(x)) \mathcal{A}_I(x) - \mathcal{A}_R(F(x)) \mathcal{A}'_I(x)], \quad (2.99)$$

and

$$q_4 = \frac{1}{2i} [\sigma \mathcal{A}'_I(F(x)) \mathcal{A}_I(x) - \mathcal{A}_I(F(x)) \mathcal{A}'_I(x)]. \quad (2.100)$$

The connection between the complex invariants Q , \tilde{Q} and q_1 , q_2 , q_3 , q_4 can be straightforwardly obtained by the equations:

$$Q = q_1 - q_4 + i(q_2 + q_3) \quad (2.101)$$

$$\tilde{Q} = q_1 + q_4 + i(q_2 - q_3). \quad (2.102)$$

When $F(x)$ is a parity transform and the position α of the symmetry axis is within the domain then it holds that $q_2 = q_3$ and since these are constant quantities, this equality holds for any $x \in \mathcal{D}$. Therefore, Eqs. (2.101), (2.102) become:

$$Q = q_1 - q_4 + i2q_2 \quad (2.103)$$

$$\tilde{Q} = q_1 + q_4. \quad (2.104)$$

Equations (2.97), (2.99) form a system, with solution:

$$\mathcal{A}_R(F(x)) = \frac{2i}{J} (q_3 \mathcal{A}_R(x) - q_1 \mathcal{A}_I(x)) \quad (2.105)$$

$$\mathcal{A}'_R(F(x)) = \frac{2i}{J\sigma} (q_3\mathcal{A}'_R(x) - q_1\mathcal{A}'_I(x)), \quad (2.106)$$

where we have used that the denominator is equal to the probability current J . This is easily shown from the definition of J :

$$\begin{aligned} \mathcal{A}^*(x)\mathcal{A}'(x) - \mathcal{A}(x)\mathcal{A}'^*(x) &= 2iJ \Rightarrow \\ \mathcal{A}_R(x)\mathcal{A}'_I(x) - \mathcal{A}_I(x)\mathcal{A}'_R(x) &= J. \end{aligned} \quad (2.107)$$

Equations (2.98), (2.100) also form a system with solution:

$$\mathcal{A}_I(F(x)) = \frac{2i}{J} (q_4\mathcal{A}_R(x) - q_2\mathcal{A}_I(x)) \quad (2.108)$$

$$\mathcal{A}'_R(F(x)) = \frac{2i}{J\sigma} (q_4\mathcal{A}'_R(x) - q_2\mathcal{A}'_I(x)). \quad (2.109)$$

Expressing J at $F(x)$ as

$$\mathcal{A}_R(F(x))\mathcal{A}'_I(F(x)) - \mathcal{A}_I(F(x))\mathcal{A}'_R(F(x)) = J \quad (2.110)$$

and substituting Eqs. (2.105), (2.106), (2.108), (2.109), we obtain the following relation

$$J^2 = q_1q_4 - q_2q_3 \quad (2.111)$$

which indicates that the current can be expressed exclusively with the use of the invariants q_i .

The solutions of the first and second system can be written compactly in the following matrix equation:

$$\begin{pmatrix} \mathcal{A}_R(F(x)) \\ \mathcal{A}_I(F(x)) \\ \mathcal{A}'_R(F(x)) \\ \mathcal{A}'_I(F(x)) \end{pmatrix} = \frac{2i}{J} \hat{Q} \begin{pmatrix} \mathcal{A}_R(x) \\ \mathcal{A}_I(x) \\ \mathcal{A}'_R(x) \\ \mathcal{A}'_I(x) \end{pmatrix}. \quad (2.112)$$

with \hat{Q} :

$$\hat{Q} = \begin{pmatrix} q_3 & -q_1 & 0 & 0 \\ q_4 & -q_2 & 0 & 0 \\ 0 & 0 & \frac{q_3}{\sigma} & \frac{-q_1}{\sigma} \\ 0 & 0 & \frac{q_4}{\sigma} & \frac{-q_2}{\sigma} \end{pmatrix}. \quad (2.113)$$

Let us consider now a completely LP symmetric setup, which is comprised of N LP symmetric domains \mathcal{D}_m , $m = 1, 2, \dots, N$ and in each domain a \hat{Q}_m -matrix can be assigned. \hat{Q}_m -matrix can be written more compactly in the following form:

$$\hat{Q}_m = \sigma_z \otimes \hat{T}_m \quad ; \quad \hat{T}_m = \begin{pmatrix} q_3 & -q_1 \\ q_4 & -q_2 \end{pmatrix}, \quad (2.114)$$

where

$$\gamma = \begin{pmatrix} 1 & 0 \\ 0 & \frac{1}{\sigma} \end{pmatrix} \quad (2.115)$$

is the third Pauli matrix. The total \hat{Q} -matrix would be:

$$\begin{aligned} \hat{Q} &= \prod_{m=1}^N \hat{Q}_m \Rightarrow \\ \hat{Q} &= \prod_{m=1}^N \gamma_z \otimes \hat{T}_m \end{aligned} \quad (2.116)$$

and finally,

$$\hat{Q} = \gamma_z^N \otimes \prod_{m=1}^N \hat{T}_m. \quad (2.117)$$

This is an alternative way to express the findings of the previous section. The reason we followed this pathway will be revealed in the next section where symmetry induced, spatially invariant quantities will be derived for systems with losses. There, the relevance of the imaginary non-local currents q_i is more transparent.

2.5 Invariants in systems with losses

The previous analysis on the existence of invariant quantities, emerging from local or global symmetric linear transforms $F(x)$, concerned idealized systems, where the effects of losses were absent. However, in real systems losses are inevitable and their theoretical description is necessary to accurately describe or predict the expected outcome. To this aim, the developed theory should be enriched in order to incorporate losses.

Losses may emerge either due to friction effects or due to radiation. In the former case, they are described with the addition of an imaginary part in the (generalized) energy ($\epsilon = \epsilon_R + i\epsilon_I$). The complex energy eigenvalues and particularly the imaginary part ϵ_I leads to exponentially decaying terms, which describe the effect of friction. On the other hand, energy loss due to radiation is described with the addition of an imaginary potential part. In fact from the continuity equation it can be shown that a complex potential of the form $V(x) = V_R(x) + iV_I(x)$ describes particle or radiation loss.

In the following we will attempt to incorporate both the aforementioned lossy cases in the previously developed theory, trying to elucidate the manner that the invariants q_1, q_2, q_3, q_4 are affected. As previously we will consider the Helmholtz equation and a general wave field $\mathcal{A}(x)$. The losses in this case are described by a complex wave-number κ . The substitution of:

$$\kappa = \kappa_R(x) + i\kappa_I(x)$$

$$\mathcal{A}(x) = \text{Re}[\mathcal{A}(x)] + i \text{Im}[\mathcal{A}(x)]$$

into the Helmholtz equation yields:

$$\text{Re}[\Psi''(x)] + \kappa_R(x) \text{Re}[\Psi(x)] - \kappa_I(x) \text{Im}[\Psi(x)] = 0 \quad (2.118)$$

$$\text{Im}[\mathcal{A}''(x)] + \kappa_R(x) \text{Im}[\mathcal{A}(x)] + \kappa_I(x) \text{Re}[\mathcal{A}(x)] = 0, \quad (2.119)$$

where we have separated the real and imaginary parts of the emerged equation. We multiply Eq. (2.118) with $\text{Re}[\mathcal{A}(F(x))]$:

$$\begin{aligned} \text{Re}[\mathcal{A}(F(x))] \text{Re}[\mathcal{A}'(x)] - \kappa_R(x) \text{Re}[\mathcal{A}(F(x))] \text{Re}[\mathcal{A}(x)] + \\ \kappa_I(x) \text{Re}[\mathcal{A}(F(x))] \text{Im}[\mathcal{A}(x)] = 0 \end{aligned} \quad (2.120)$$

and afterwards we take the parity transformed Schrödinger equation and multiply it with $\text{Re}[\mathcal{A}(x)]$:

$$\begin{aligned} \text{Re}[\mathcal{A}'(F(x))] \text{Re}[\mathcal{A}(x)] - \kappa_R(F(x)) \text{Re}[\mathcal{A}(x)] \text{Re}[\mathcal{A}(F(x))] + \\ \kappa_I(F(x)) \text{Re}[\mathcal{A}(x)] \text{Im}[\mathcal{A}(F(x))] = 0. \end{aligned} \quad (2.121)$$

By subtracting Eq. (2.121) from Eq. (2.120), provided that both the real and the imaginary parts of the potential are symmetric with respect to the transformation $F(x)$,

$$\kappa_R(x) = \kappa_R(F(x))$$

$$\kappa_I(x) = \kappa_I(F(x))$$

we get:

$$\text{Re}[\mathcal{A}(F(x))] \text{Re}[\mathcal{A}'(x)] - \text{Re}[\mathcal{A}'(F(x))] \text{Re}[\mathcal{A}(x)] = 0. \quad (2.122)$$

In the lhs of this equation we identify the derivative of the quantity q_1 which is invariant in the lossless case and Eq. (2.122) becomes

$$\frac{dq_1}{dx} = -\kappa_I(x) (\text{Re}[\mathcal{A}(F(x))] \text{Im}[\mathcal{A}(x)] - \text{Re}[\mathcal{A}(x)] \text{Im}[\mathcal{A}(F(x))]). \quad (2.123)$$

Obviously, when losses are taken into consideration, the invariance of q_1 is lifted.

Similar treatment of Eq. (2.121) can lead to the respective equations for q_4 . Particularly, the multiplication of Eq. (2.121) and corresponding parity transformed with $\text{Im}[\mathcal{A}(F(x))]$ and $\text{Im}[\mathcal{A}(x)]$, respectively, followed by the subtraction of the resulting equations, yields:

$$\begin{aligned} \text{Im}[\mathcal{A}''(x)] \text{Im}[\mathcal{A}(F(x))] - \text{Im}[\mathcal{A}''(F(x))] \text{Im}[\mathcal{A}(x)] = \\ \kappa_I(x) (\text{Re}[\mathcal{A}(x)] \text{Im}[\mathcal{A}(F(x))] - \text{Re}[\mathcal{A}(F(x))] \text{Im}[\mathcal{A}(x)]) . \end{aligned} \quad (2.124)$$

In the lhs of this equation we identify the derivative of the quantity q_1 which is invariant in the lossless case and Eq. (2.122) becomes

$$\frac{dq_4}{dx} = \kappa_I(x) (\text{Re}[\mathcal{A}(x)] \text{Im}[\mathcal{A}(F(x))] - \text{Re}[\mathcal{A}(F(x))] \text{Im}[\mathcal{A}(x)]), \quad (2.125)$$

which also indicates that q_4 is not invariant in a lossy LP symmetric system. Nonetheless, the rhs of Eqs. (2.123), (2.125) are the same and consequently it holds that:

$$\begin{aligned} \frac{d}{dx} (q_1 - q_4) &= 0 \Rightarrow \\ q_1 - q_4 &= \text{const.} \end{aligned} \quad (2.126)$$

The construction of q_2 and q_3 follows the same pattern. In the first place we multiply Eq. (2.118) with $\text{Im}[\mathcal{A}(F(x))]$:

$$\begin{aligned} \text{Im}[\mathcal{A}(F(x))] \text{Re}[\mathcal{A}'(x)] - \kappa_R(x) \text{Im}[\mathcal{A}(F(x))] \text{Re}[\mathcal{A}(x)] + \\ \kappa_I(x) \text{Im}[\mathcal{A}(F(x))] \text{Im}[\mathcal{A}(x)] = 0. \end{aligned} \quad (2.127)$$

Then we consider the parity transform of Eq. (2.118), multiplied with $\text{Im}[\mathcal{A}(F(x))]$:

$$\begin{aligned} \text{Re}[\mathcal{A}'(F(x))] \text{Im}[\mathcal{A}(x)] - \kappa_R(F(x)) \text{Im}[\mathcal{A}(x)] \text{Re}[\mathcal{A}(F(x))] + \\ \kappa_I(F(x)) \text{Re}[\mathcal{A}(x)] \text{Im}[\mathcal{A}(F(x))] = 0. \end{aligned} \quad (2.128)$$

Similarly, we multiply Eq. (2.119) with $\text{Re}[\mathcal{A}(F(x))]$:

$$\begin{aligned} \text{Re}[\mathcal{A}(F(x))] \text{Im}[\mathcal{A}''(x)] - \kappa_R(x) \text{Im}[\mathcal{A}(x)] \text{Re}[\mathcal{A}(F(x))] + \\ \kappa_I(x) \text{Re}[\mathcal{A}(x)] \text{Re}[\mathcal{A}(F(x))] = 0 \end{aligned} \quad (2.129)$$

and its respective parity transform with $\text{Re}[\mathcal{A}(x)]$:

$$\begin{aligned} \text{Im}[\mathcal{A}''(F(x))] \text{Re}[\mathcal{A}(x)] \kappa_R(F(x)) \text{Im}[\mathcal{A}(F(x))] \text{Re}[\mathcal{A}(x)] + \\ \kappa_I(F(x)) \text{Re}[\mathcal{A}(x)] \text{Re}[\mathcal{A}(F(x))] = 0. \end{aligned} \quad (2.130)$$

The following steps for the q_2 , q_3 calculation is to subtract Eq. (2.130) from Eq. (2.127) which leads to:

$$\begin{aligned} \text{Re}[\mathcal{A}'(x)] \text{Im}[\mathcal{A}(F(x))] - \text{Im}[\mathcal{A}''(F(x))] \text{Re}[\mathcal{A}(x)] = \\ -\kappa_I(x) [\text{Re}[\mathcal{A}(F(x))] \text{Re}[\mathcal{A}(x)] + \text{Im}[\mathcal{A}(F(x))] \text{Im}[\mathcal{A}(x)]] \end{aligned}, \quad (2.131)$$

where we identify the derivative of the quantity q_2 in the lhs:

$$\frac{dq_2}{dx} = -\kappa_I(x) [\text{Re}[\mathcal{A}(F(x))] \text{Re}[\mathcal{A}(x)] + \text{Im}[\mathcal{A}(F(x))] \text{Im}[\mathcal{A}(x)]] \quad (2.132)$$

and subsequently to subtract Eq. (2.128) from Eq. (2.129)

$$\begin{aligned} \text{Im}[\mathcal{A}''(x)] \text{Re}[\mathcal{A}(F(x))] - \text{Re}[\mathcal{A}'(F(x))] \text{Im}[\mathcal{A}(x)] = \\ \kappa_I(x) [\text{Re}[\mathcal{A}(F(x))] \text{Re}[\mathcal{A}(x)] + \text{Im}[\mathcal{A}(F(x))] \text{Im}[\mathcal{A}(x)]] \quad , \end{aligned} \quad (2.133)$$

$$\frac{dq_3}{dx} = -(-\kappa_I(x)) [\text{Re}[\mathcal{A}(F(x))] \text{Re}[\mathcal{A}(x)] + \text{Im}[\mathcal{A}(F(x))] \text{Im}[\mathcal{A}(x)]] . \quad (2.134)$$

Finally, Eqs. (2.132), (2.134) lead to:

$$\begin{aligned} \frac{d}{dx} (q_2 + q_3) &= 0 \Rightarrow \\ q_2 + q_3 &= \text{const}, \end{aligned} \quad (2.135)$$

stating that, in the lossy case, even though q_2 and q_3 are not individually conserved, their sum $q_2 + q_3$ is an invariant quantity, within an LP symmetric domain.

Since both $q_1 - q_4$ and $q_2 + q_3$ are spatially constant, we conclude from Eqs. (2.101), (2.102) that in a system with attenuation, the quantity Q is still spatially invariant, even though the invariance now is lifted for \tilde{Q} . This prevents the straightforward generalization of the Bloch and parity theorems, for lossy systems with the corresponding symmetries broken. Nevertheless, the invariance of Q still allows for a generalization. By dividing Eq. (2.75) with $\mathcal{A}^2(x)$ we get

$$\frac{Q}{\mathcal{A}^2(x)} = \frac{1}{2i} \frac{\sigma \mathcal{A}(x) \mathcal{A}'(F(x)) - \mathcal{A}(F(x)) \mathcal{A}'(x)}{\mathcal{A}^2(x)}. \quad (2.136)$$

The second part of the Eq. (2.136) can be written as a total derivative:

$$\frac{Q}{\mathcal{A}^2(x)} = \frac{1}{2i} \left(\frac{\mathcal{A}(F(x))}{\mathcal{A}(x)} \right)'. \quad (2.137)$$

Then by integration we find:

$$\mathcal{A}(F(x)) = \frac{1}{2i} \left(C \mathcal{A}(x) - Q \mathcal{A}(x) \int \frac{1}{\mathcal{A}^2(x')} dx' \right), \quad (2.138)$$

where C is the integration constant. Equation (2.138) can be regarded as a generalization of the Bloch and parity theorems for the, even more general, case of a system with losses. Obviously it provides a - more complex - link for the wave field from a source domain to a target domain, which are related via the symmetry transformation $F(x)$.

An alternative way to express the invariants $q_1 - q_4$ and $q_2 + q_3$ in a compact form is to consider the polar representation of the wave function

$$\mathcal{A}(x) = u(x) e^{i\vartheta(x)} \quad ; \quad u(x) \equiv |\mathcal{A}(x)|, \quad (2.139)$$

with $u(x) \geq 0 \quad \forall x \in \mathbb{R}$. The real and imaginary parts of $\mathcal{A}(x)$, along with the respective derivatives are:

$$\operatorname{Re}[\mathcal{A}(x)] = u(x) \cos[\vartheta(x)] \quad ; \quad \operatorname{Re}[\mathcal{A}'(x)] = u'(x) \cos[\vartheta(x)] - u(x) \sin[\vartheta(x)]\vartheta'(x) \quad (2.140)$$

$$\operatorname{Im}[\mathcal{A}(x)] = u(x) \sin[\vartheta(x)] \quad ; \quad \operatorname{Im}[\mathcal{A}'(x)] = u'(x) \sin[\vartheta(x)] + u(x) \cos[\vartheta(x)]\vartheta'(x). \quad (2.141)$$

By substituting the above expressions to the equations for q_1, q_2, q_3, q_4 we can write the invariants $q_1 - q_4$ and $q_2 + q_3$ as:

$$q_1 - q_4 = (u(F(x))u'(x) + u'(F(x))u(x)) \cos[\vartheta(F(x)) + \vartheta(x)] - u(F(x))u(x) \sin[\vartheta(F(x)) + \vartheta(x)] (\vartheta'(F(x)) + \vartheta'(x)) \quad (2.142)$$

and

$$q_2 + q_3 = (u'(F(x))u(x) + u(F(x))u'(x)) \sin[\vartheta(F(x)) + \vartheta(x)] + u(F(x))u(x) \cos[\vartheta(F(x)) + \vartheta(x)] (\vartheta'(F(x)) + \vartheta'(x)). \quad (2.143)$$

Equations (2.142), (2.143) can be compactly expressed in matrix form, as:

$$\begin{pmatrix} Q_+ \\ Q_- \end{pmatrix} = \begin{pmatrix} u(x), & u'(x) \end{pmatrix} \left(\hat{\sigma}_x \cos[\Phi(x)] \pm \frac{\hat{\sigma}_z}{2} \sin[\Phi(x)]\Phi'(x) \right) \begin{pmatrix} u(F(x)) \\ u'(F(x)) \end{pmatrix} \quad (2.144)$$

where $Q_+ = q_2 + q_3, Q_- = q_1 - q_4, \Phi(x) = \vartheta(x) + \vartheta(F(x))$ and $\hat{\sigma}_x, \hat{\sigma}_z$ the Pauli matrices.

CHAPTER 3

POTENTIAL SCATTERING

3.1 Introduction

Scattering processes play a major role in our perception and understanding of nature. Scattered electro-magnetic waves in the visible spectrum provide the information of color, whereas deflected sound waves facilitate or prevent hearing. In quantum physics, scattering experiments is the main tool to extract information from physical systems, both in high energy physics where beam collisions are used for the discovery of sub-atomic particles [106] and in low energy physics where neutron [107] and x-ray [108] scattering constitute important tools for the study of the internal structures of solid state systems [109], in polymers [110] or even in structural biology [111].

Scattering phenomena can be studied from two different points of view, constituting the direct and the inverse scattering problem, respectively. In the direct problem, the characteristics of the scattering center are known and we are interested in the long distance detection of the transmitted and reflected particles after their interaction with the scatterer. Then, possible relevant quantities to be calculated or measured would be the transmission spectrum, the occurrence of resonances or the scattering cross sections. On the other hand, in the inverse problem, one takes into consideration the knowledge of certain characteristics of the scattered waves which are finally detected in long distances and attempt to extract information about the local structure of the scatterer.

In this chapter, we will discuss the standard mathematical framework for the study of scattering in 1-D, with emphasis on the transfer matrix (TM) [24, 112], the scattering matrix (S-matrix) [113] and their connection. The S-matrix can be generalized easily in three dimensions and also reveals transparently the scattering properties of a specific problem. However, the TM facilitates significantly the treatment of 1-D scattering from an arbitrary array of potential barriers. Therefore, it will be extensively used in the following chapters.

3.2 The Transfer and \hat{S} - Matrix methods

In order to confront stationary, wave scattering problems in a uniform manner we will use the notation introduced in the Chapter 3, in the frame of the Helmholtz equation.

$$\mathcal{A}''(x) + \kappa\mathcal{A}(x) = 0 \quad (3.1)$$

with \mathcal{A} being a plane wave of the form

$$\mathcal{A}(x) = Ae^{i\kappa x} + Be^{-i\kappa x}. \quad (3.2)$$

The scatterer is characterized by the generalized potential $\mathcal{W}(x)$ and may correspond e.g. to the potential in a quantum mechanical problem or to the refraction index in optics.

For simplicity we consider that the scatterer is located within a finite region, so that for $\mathcal{W}(x)$ it holds:

$$\mathcal{W}(x) = \begin{cases} w(x), & 0 \leq x \leq a \\ 0, & x > a. \end{cases} \quad (3.3)$$

When the wave approaches the target, a part of it is transmitted and a part is reflected. In the quantum mechanical regime, effects with no classical analogue, such as tunnelling, may emerge. We can assume that on either side of the scatterer the wave can be mathematically described by a superposition of plane waves:

$$\begin{aligned} \mathcal{A}_L(x) &= \mathcal{A}_L^+(x) + \mathcal{A}_L^-(x), \quad x \leq 0 \\ \mathcal{A}_R(x) &= \mathcal{A}_R^+(x) + \mathcal{A}_R^-(x), \quad x \geq a \end{aligned} \quad (3.4)$$

where

$$\begin{aligned} \mathcal{A}_L^+(x) &= Ae^{i\kappa x} \quad , \quad \mathcal{A}_L^-(x) = Be^{-i\kappa x} \\ \mathcal{A}_R^+(z) &= Ce^{i\kappa x} \quad , \quad \mathcal{A}_R^-(x) = De^{-i\kappa x}. \end{aligned} \quad (3.5)$$

Here, A, B, C, D are complex coefficients and κ is the wave vector which is linked to the energy ϵ through the dispersion relation $\epsilon = \epsilon(\kappa)$. The subscripts L and R refer to the position of the particle with respect to the position of the scatterer (left or right respectively). Accordingly, the superscripts \pm refer the direction of the wave propagation, with (+) denoting the propagation from left to right and (-) from right to left.

The scattering and the transfer matrices can be derived by taking into consideration the continuity conditions of the field $\mathcal{A}(x)$ and its derivative at the scatterer's boundaries:

$$\begin{aligned} \mathcal{A}_L(x = 0^-) &= \Psi(x = 0^+) \quad , \quad \mathcal{A}'_L(x = 0^-) = \Psi'(x = 0^+) \\ \mathcal{A}_R(x = a^-) &= \Psi(x = a^+) \quad , \quad \mathcal{A}'_R(x = a^-) = \Psi'(x = a^+) \end{aligned} \quad (3.6)$$



FIGURE 3.1: Wave scattered off an arbitrary scatterer. On either side of the scatterer the incoming and outgoing amplitudes are shown.

where $\Psi(x)$ denotes the field inside the scatterer and its functional form depends on the form of $\mathcal{W}(x)$. In general it can't be expressed as a superposition of plane waves, as $\mathcal{A}(x)$.

In principle, the solution of the Schrödinger equation provides all the necessary information needed for a scattering problem. However, in most cases the Schrödinger equation is not analytically solvable for a generic scatterer form $\mathcal{W}(x)$ and one would aim to relate the complex probability amplitudes A , B , C and D . Actually, these four amplitudes are not independent, but linked through linear relations. Depending on the coefficient pairs which are associated, we define the TM and the S-matrix.

3.2.1 The S-matrix

The S-matrix relates the incoming with the outgoing waves and this linear relation defines it:

$$\begin{pmatrix} \mathcal{A}_L^-(x=0) \\ \mathcal{A}_R^+(x=a) \end{pmatrix} = \mathbf{S} \begin{pmatrix} \mathcal{A}_L^+(x=0) \\ \mathcal{A}_R^-(x=a) \end{pmatrix} \Rightarrow$$

$$\begin{pmatrix} \mathcal{A}_L^-(x=0) \\ \mathcal{A}_R^+(x=a) \end{pmatrix} = \begin{pmatrix} S_{11}(\epsilon) & S_{12}(\epsilon) \\ S_{21}(\epsilon) & S_{22}(\epsilon) \end{pmatrix} \begin{pmatrix} \mathcal{A}_L^+(x=0) \\ \mathcal{A}_R^-(x=a) \end{pmatrix} \quad (3.7)$$

It is obvious that the S-matrix can be expressed in order to relate the amplitudes A , D of the incoming components of the field $\mathcal{A}(x)$, with the amplitudes B , C of the outgoing components.

To fully determine the S-matrix we need to calculate the four complex parameters S_{11} , S_{12} , S_{21} , S_{22} . However, the identification of symmetries which apply to a physical

problem can reduce the parameter space for the full determination of the scattering problem.

Current Density Conservation

For physical systems of time-independent wave propagation the current density has to be equal on either side of the scatterer:

$$J_{z<0} = J_{z>a}, \quad (3.8)$$

where the current density for this class of problems has the general form:

$$J(x) \sim \mathcal{A}(x) \frac{\partial \mathcal{A}^*(x)}{\partial z} - \mathcal{A}^*(x) \frac{\partial \mathcal{A}(x)}{\partial z}. \quad (3.9)$$

Then on the left side of the scatterer the density current is:

$$J_L \sim |\mathcal{A}_L^+|^2 - |\mathcal{A}_L^-|^2 = |A|^2 - |B|^2 \quad (3.10)$$

and on the right side:

$$J_R \sim |\mathcal{A}_R^+|^2 - |\mathcal{A}_R^-|^2 = |C|^2 - |D|^2 \quad (3.11)$$

The equality $J_R = J_L$, after a rearrangement of the terms yields:

$$|\mathcal{A}_R^+|^2 - |\mathcal{A}_R^-|^2 = |\mathcal{A}_L^+|^2 - |\mathcal{A}_L^-|^2. \quad (3.12)$$

It is convenient, for the forthcoming analysis, to express the above relation in vector notation:

$$(\mathcal{A}_L^{+*} \ \mathcal{A}_R^{-*}) \begin{pmatrix} \mathcal{A}_L^+ \\ \mathcal{A}_R^- \end{pmatrix} = (\mathcal{A}_L^{-*} \ \mathcal{A}_R^{+*}) \begin{pmatrix} \mathcal{A}_L^- \\ \mathcal{A}_R^+ \end{pmatrix}. \quad (3.13)$$

By substituting Eq. (3.7) to Eq. (3.13) we get:

$$(\mathcal{A}_L^{+*} \ \mathcal{A}_R^{-*}) \mathbf{S} \begin{pmatrix} \mathcal{A}_L^- \\ \mathcal{A}_R^+ \end{pmatrix} = (\mathcal{A}_L^{-*} \ \mathcal{A}_R^{+*}) \begin{pmatrix} \mathcal{A}_L^- \\ \mathcal{A}_R^+ \end{pmatrix}. \quad (3.14)$$

Subsequently, we insert in Eq. (3.14) the complex conjugate form of the Eq. (3.7):

$$(\mathcal{A}_L^{+*} \ \mathcal{A}_R^{-*}) = (\mathcal{A}_L^{-*} \ \mathcal{A}_R^{+*}) \mathbf{S}^\dagger, \quad (3.15)$$

with \mathbf{S}^\dagger being the Hermitian conjugate of \mathbf{S} (the complex conjugate of the transpose):

$$(\mathcal{A}_L^{-*} \ \mathcal{A}_R^{+*}) \mathbf{S}^\dagger \mathbf{S} \begin{pmatrix} \mathcal{A}_L^- \\ \mathcal{A}_R^+ \end{pmatrix} = (\mathcal{A}_L^{-*} \ \mathcal{A}_R^{+*}) \begin{pmatrix} \mathcal{A}_L^- \\ \mathcal{A}_R^+ \end{pmatrix}. \quad (3.16)$$

Equation (3.16) is valid if:

$$\mathbf{S}^\dagger \mathbf{S} = \mathbf{1}, \quad (3.17)$$

which renders the S -matrix *unitary*. Unitarity, in turn, leads to the following conditions among the S -matrix elements.

$$\begin{aligned} |S_{11}|^2 + |S_{21}|^2 &= 1 \\ |S_{22}|^2 + |S_{12}|^2 &= 1 \\ S_{11}^* S_{12} &= -S_{21}^* S_{22} \\ S_{12}^* S_{11} &= -S_{22}^* S_{21}. \end{aligned} \quad (3.18)$$

Finally, if the unitarity condition is expressed as:

$$\mathbf{S}^\dagger = \mathbf{S}^{-1}, \quad (3.19)$$

and take into consideration that $|\det \mathbf{S}| = 1$ (since \mathbf{S} is unitary), we obtain:

$$\begin{pmatrix} S_{11}^* & S_{21}^* \\ S_{12}^* & S_{22}^* \end{pmatrix} = \frac{1}{\det \mathbf{S}} \begin{pmatrix} S_{22} & -S_{21} \\ -S_{12} & S_{11} \end{pmatrix}, \quad (3.20)$$

which implies two more constraints for the S -matrix elements:

$$\begin{aligned} |S_{11}| &= |S_{22}| \\ |S_{12}| &= |S_{21}|. \end{aligned} \quad (3.21)$$

Time-Reversal Symmetry

When a system is invariant under time inversion it obeys the *time-reversal symmetry* and induces more constraints on the form of the S -matrix elements. Since the systems which are treated here are time-independent, the time-reversal symmetry is always valid and mathematically this is expressed through the fact that both the field $\mathcal{A}(x)$ and its complex conjugate $\mathcal{A}^*(x)$ are solutions of the Helmholtz equation. Under time reversal, the plane waves on either side of the scatterer change sign in the exponential term, changing effectively the direction of propagation. However, due to the change of every wave the physical problem remains invariant.

$$\begin{pmatrix} \mathcal{A}_L^{+*}(x=0) \\ \mathcal{A}_R^{-*}(x=a) \end{pmatrix} = \mathbf{S} \begin{pmatrix} \mathcal{A}_L^{-*}(x=0) \\ \mathcal{A}_R^{+*}(x=a) \end{pmatrix}. \quad (3.22)$$

Moreover, the complex conjugate of Eq. (3.7) gives:

$$\begin{pmatrix} \mathcal{A}_L^{+*}(x=0) \\ \mathcal{A}_R^{-*}(x=a) \end{pmatrix} = \mathbf{S}^* \begin{pmatrix} \mathcal{A}_L^{+*}(x=0) \\ \mathcal{A}_R^{-*}(x=a) \end{pmatrix}. \quad (3.23)$$

From the combination of Eqs. (3.22), (3.23) finally we get:

$$\begin{pmatrix} \mathcal{A}_L^{-*} \\ \mathcal{A}_R^{+*} \end{pmatrix} = \mathbf{S}\mathbf{S}^* \begin{pmatrix} \mathcal{A}_L^{-*} \\ \mathcal{A}_R^{+*} \end{pmatrix}, \quad (3.24)$$

leading, in turn, to the condition:

$$\mathbf{S}\mathbf{S}^* = 1 \quad (3.25)$$

which holds for any incoming wave.

The time-reversal symmetry also imposes constraints on the S-matrix elements:

$$\begin{aligned} |S_{11}|^2 + S_{21}S_{12}^* &= 1 \\ |S_{22}|^2 + S_{12}S_{21}^* &= 1 \\ S_{11}^*S_{12} &= -S_{12}^*S_{22} \\ S_{21}^*S_{11} &= -S_{22}^*S_{21}. \end{aligned} \quad (3.26)$$

From Eqs. (3.18), (3.26) we compare equations:

$$S_{11}^*S_{12} = -S_{12}^*S_{22} \quad ; \quad S_{11}^*S_{12} = -S_{21}^*S_{22}$$

and find that

$$S_{12} = S_{21}. \quad (3.27)$$

Thus, when both the conservation of the current density and the time reversal symmetry apply to a scattering problem, then the S-matrix is symmetric.

Transmission and Reflection

We consider now a more realistic scattering scenario where we send a plane wave from the right side of the scatterer. The wave is normalized so that the $|\mathcal{A}_R^-|^2 = 1$. From the right side of the scatterer there is no incoming wave, so that $\mathcal{A}_L^+ = 0$. The incoming wave \mathcal{A}_R^- is connected to the transmitted and reflected waves via the following relations which are imposed by the S-matrix:

$$\begin{aligned} \mathcal{A}_L^- &= S_{12} \mathcal{A}_R^- \\ \mathcal{A}_R^+ &= S_{22} \mathcal{A}_R^- \end{aligned} \quad (3.28)$$

Since the matrix elements S_{12} and S_{22} are related to the transmission and the reflection of the wave, we will refer to them as transmission and reflection amplitudes, respectively:

$$t = S_{12} \quad ; \quad r = S_{22}. \quad (3.29)$$

Similarly, if we consider the incident wave from the left side of the scatterer, we get the respective transmission and reflection amplitudes t' , r' :

$$t' = S_{21} \quad ; \quad r' = S_{11}. \quad (3.30)$$

The S-matrix then can be written in terms of the transmission and reflection amplitudes:

$$\mathbf{S} = \begin{pmatrix} r' & t \\ t' & r \end{pmatrix} \quad (3.31)$$

and the physical meaning of each parameter is:

- t , transmission of the wave coming from right to left
- r , reflection of the wave coming from right to left
- t' , transmission of the wave coming from left to right
- r' , reflection of the wave coming from left to right.

Nevertheless, as have shown above, the current conservation and the time reversal invariance impose the symmetry condition to the S-matrix, that is $S_{12} = S_{21}$ and consequently $t = t'$.

Now we can define the transmission and reflection coefficients T , R , which essentially are the magnitudes of the amplitudes t (t') and r (r'), respectively. Namely, $T = |t|^2$ and $R = |r|^2$. Equations (3.18, 3.26) imply also that

$$T + R = 1 \quad ; \quad T' + R' = 1, \quad (3.32)$$

which, combined with $t = t'$, yield the extra condition, $|r| = |r'|$.

3.2.2 The Transfer Matrix

The TM formalism has been developed to study a multitude of physical problems involving wave propagation, such as quantum particles [114], electromagnetic [115] and acoustic [116] waves. The usefulness of the TM can be detected at several levels which we will discuss subsequently. A major advantage is that it allows for a unified manipulation of all the above systems [117]. The TM is defined by the relation:

$$\begin{aligned} \begin{pmatrix} \mathcal{A}_R^+ \\ \mathcal{A}_R^- \end{pmatrix}_{x=a} &= \mathbf{M} \begin{pmatrix} \mathcal{A}_L^+ \\ \mathcal{A}_L^- \end{pmatrix}_{x=0} \Rightarrow \\ \begin{pmatrix} \mathcal{A}_R^+ \\ \mathcal{A}_R^- \end{pmatrix}_{x=a} &= \begin{pmatrix} M_{11}(\epsilon) & M_{12}(\epsilon) \\ M_{21}(\epsilon) & M_{22}(\epsilon) \end{pmatrix} \begin{pmatrix} \mathcal{A}_L^+ \\ \mathcal{A}_L^- \end{pmatrix}_{x=0} \end{aligned} \quad (3.33)$$

Similarly to the case of the S-matrix, TM can be expressed in order to relate the amplitudes C , D in the right side of the scatterer, with the amplitudes A , B in the left side.

A simple rearrangement in the relations which relate the incoming and the outgoing waves, in order to relate the waves on the right side of the potential to the those on the left side, give rise to the transfer matrix, which can be written in terms of the S-matrix elements, as:

$$\mathbf{M} = \begin{pmatrix} S_{21} - \frac{S_{22}S_{11}}{S_{12}} & \frac{S_{22}}{S_{12}} \\ -\frac{S_{11}}{S_{12}} & \frac{1}{S_{12}} \end{pmatrix}. \quad (3.34)$$

In a respective manner the S-matrix elements can be expressed in terms of the TM:

$$\mathbf{S} = \begin{pmatrix} \frac{M_{21}}{M_{22}} & \frac{1}{M_{22}} \\ M_{11} - \frac{M_{12}M_{21}}{M_{22}} & \frac{M_{12}}{M_{22}} \end{pmatrix}. \quad (3.35)$$

The symmetries of density current conservation and time-reversal can be also applied in the TM, so that the parameter space can be reduced in the same manner as in the S-matrix.

Current Density Conservation

As a x-independent quantity, the density current J is spatially constant and it holds:

$$J_{z<0} = J_{z>a} \Rightarrow |\mathcal{A}_R^+|^2 - |\mathcal{A}_L^-|^2 = |\mathcal{A}_L^+|^2 - |\mathcal{A}_R^-|^2. \quad (3.36)$$

This equation, which indicates the density current conservation, can be re-written in matrix notation, by inserting the σ_z Pauli matrix:

$$(\mathcal{A}_L^{+*} \ \mathcal{A}_L^{-*}) \sigma_z \begin{pmatrix} \mathcal{A}_L^+ \\ \mathcal{A}_L^- \end{pmatrix} = (\mathcal{A}_R^{+*} \ \mathcal{A}_R^{-*}) \sigma_z \begin{pmatrix} \mathcal{A}_R^+ \\ \mathcal{A}_R^- \end{pmatrix}, \quad (3.37)$$

or

$$(\mathcal{A}_L^{+*} \ \mathcal{A}_L^{-*}) \begin{pmatrix} 1 & 0 \\ 0 & -1 \end{pmatrix} \begin{pmatrix} \mathcal{A}_L^+ \\ \mathcal{A}_L^- \end{pmatrix} = (\mathcal{A}_R^{+*} \ \mathcal{A}_R^{-*}) \begin{pmatrix} 1 & 0 \\ 0 & -1 \end{pmatrix} \begin{pmatrix} \mathcal{A}_R^+ \\ \mathcal{A}_R^- \end{pmatrix}. \quad (3.38)$$

Next, we use the conjugate expression of Eq. (3.33), which is:

$$(\mathcal{A}_R^{+*} \ \mathcal{A}_R^{-*}) \sigma_z = \begin{pmatrix} \mathcal{A}_L^{+*} \\ \mathcal{A}_L^{-*} \end{pmatrix} \mathbf{M}^\dagger \quad (3.39)$$

and insert it in Eq. (3.38):

$$(\mathcal{A}_L^{+*} \mathcal{A}_L^{-*}) \begin{pmatrix} 1 & 0 \\ 0 & -1 \end{pmatrix} \begin{pmatrix} \mathcal{A}_L^+ \\ \mathcal{A}_L^- \end{pmatrix} = (\mathcal{A}_L^{+*} \mathcal{A}_L^{-*}) \mathbf{M}^\dagger \begin{pmatrix} 1 & 0 \\ 0 & -1 \end{pmatrix} \mathbf{M} \begin{pmatrix} \mathcal{A}_L^+ \\ \mathcal{A}_L^- \end{pmatrix}. \quad (3.40)$$

This holds if:

$$\begin{pmatrix} 1 & 0 \\ 0 & -1 \end{pmatrix} = \mathbf{M}^\dagger \begin{pmatrix} 1 & 0 \\ 0 & -1 \end{pmatrix} \mathbf{M} \quad (3.41)$$

and by substituting the explicit TM form,

$$\begin{pmatrix} 1 & 0 \\ 0 & -1 \end{pmatrix} = \begin{pmatrix} M_{11}^* & M_{21}^* \\ M_{12}^* & M_{22}^* \end{pmatrix} \begin{pmatrix} 1 & 0 \\ 0 & -1 \end{pmatrix} \begin{pmatrix} M_{11} & M_{12} \\ M_{21} & M_{22} \end{pmatrix}, \quad (3.42)$$

we arrive to the following constraints for the TM elements:

$$\begin{aligned} |M_{11}|^2 - |M_{21}|^2 &= 1 \\ |M_{22}|^2 - |M_{12}|^2 &= 1 \end{aligned} \quad (3.43)$$

$$\begin{aligned} M_{11}^* M_{12} &= M_{21}^* M_{22} \\ M_{12}^* M_{11} &= M_{22}^* M_{21} \end{aligned} \quad (3.44)$$

In the following, we will see that these constraints will be further reduced when we take the time-reversal symmetry into consideration.

Time-Reversal Symmetry

The effect of time-reversal symmetry in a time-independent scattering problem with incident and scattered plane waves, is to change the incoming waves to outgoing and the vice-versa. Thus, Eq. (3.33), under time-reversal can be written as:

$$\begin{pmatrix} \mathcal{A}_R^{-*} \\ \mathcal{A}_R^{+*} \end{pmatrix} = \mathbf{M} \begin{pmatrix} \mathcal{A}_L^{-*} \\ \mathcal{A}_L^{+*} \end{pmatrix}, \quad (3.45)$$

which with the use of the σ_x Pauli matrix becomes:

$$\sigma_x \begin{pmatrix} \mathcal{A}_R^{+*} \\ \mathcal{A}_R^{-*} \end{pmatrix} = \mathbf{M} \sigma_x \begin{pmatrix} \mathcal{A}_L^{+*} \\ \mathcal{A}_L^{-*} \end{pmatrix} \quad (3.46)$$

or

$$\begin{pmatrix} \mathcal{A}_R^{+*} \\ \mathcal{A}_R^{-*} \end{pmatrix} = \begin{pmatrix} 0 & 1 \\ 1 & 0 \end{pmatrix} \mathbf{M} \begin{pmatrix} 0 & 1 \\ 1 & 0 \end{pmatrix} \begin{pmatrix} \mathcal{A}_L^{+*} \\ \mathcal{A}_L^{-*} \end{pmatrix}. \quad (3.47)$$

The comparison of the above equation with the complex conjugate of Eq. (3.33):

$$\begin{pmatrix} \mathcal{A}_R^{+*} \\ \mathcal{A}_R^{-*} \end{pmatrix} = \mathbf{M}^* \begin{pmatrix} \mathcal{A}_L^{+*} \\ \mathcal{A}_L^{-*} \end{pmatrix} \quad (3.48)$$

leads finally to the TM relation:

$$\begin{pmatrix} 0 & 1 \\ 1 & 0 \end{pmatrix} \mathbf{M} \begin{pmatrix} 0 & 1 \\ 1 & 0 \end{pmatrix} = \mathbf{M}^*. \quad (3.49)$$

Evidently, the constraints imposed on the TM elements from the time-reversal symmetry are:

$$M_{11} = M_{22}^* \quad ; \quad M_{21} = M_{12}^*. \quad (3.50)$$

Equation (3.50) combined with the conditions in Eq. (3.43), yields that:

$$|M_{11}|^2 - |M_{12}|^2 = 1, \quad (3.51)$$

or, in other words:

$$\det \mathbf{M} = 1. \quad (3.52)$$

Note also, that the trace of the TM is a real number $\text{Tr} \mathbf{M} = M_{11} + M_{11}^*$. Based on all the above, we can conclude that when time reversal symmetry and current conservation are fulfilled, the TM is *unimodular* ($\det \mathbf{M} = 1$) and has the general form:

$$\mathbf{M} = \begin{pmatrix} M_{11} & M_{12} \\ M_{12}^* & M_{11}^* \end{pmatrix} \quad (3.53)$$

Transmission and Reflection

Previously it was shown that the S-matrix can be expressed via the transmission and reflection amplitudes as:

$$\mathbf{S} = \begin{pmatrix} r' & t \\ t' & r \end{pmatrix} \quad (3.54)$$

The TM is also possible to be expressed in the same manner if the t , t' , r , r' are substituted in Eq. (3.34):

$$\mathbf{M} = \begin{pmatrix} t' - rt^{-1}r' & rt^{-1} \\ -t^{-1}r' & t^{-1} \end{pmatrix}. \quad (3.55)$$

A further simplification in the above expression can be achieved with the use of equation $S_{11}^* S_{12} = S_{21}^* S_{22}$ (see Eq. (3.18), which becomes:

$$rt^{-1} = -(r't'^{-1})^*. \quad (3.56)$$

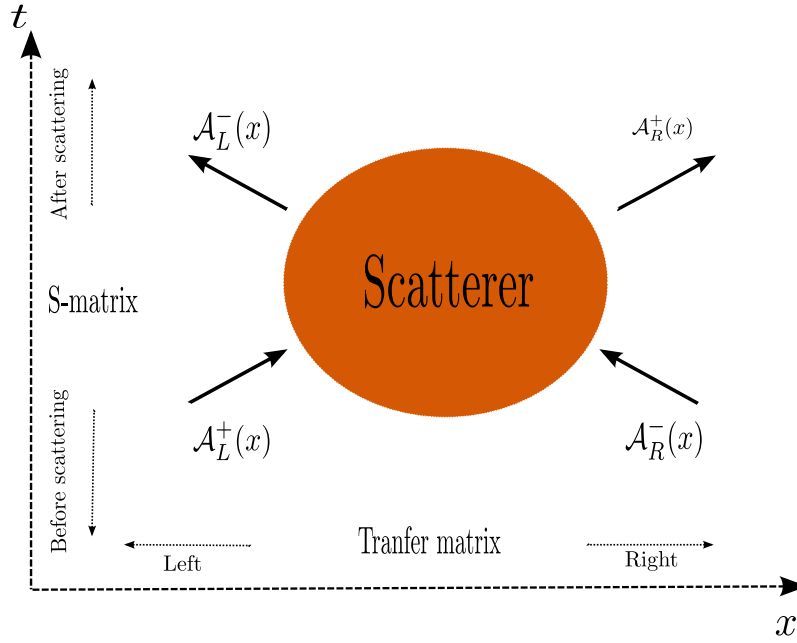


FIGURE 3.2: Wave scattered off an arbitrary scatterer. The S-matrix relates amplitudes before the scattering (incoming) with amplitudes after the scattering (outgoing). The transfer matrix relates amplitudes on the left and right side of the scatterer.

The matrix element M_{11} subsequently becomes:

$$M_{11} = t' - rt^{-1}r' = t + R'(t')^{*-1} = \frac{T' + R'}{(t')^*} = (t')^{*-1}.$$

Considering also that in the presence of time-reversal symmetry $t = t'$, the TM becomes:

$$\mathbf{M} = \begin{pmatrix} t^{*-1} & rt^{-1} \\ -t^{-1}r' & t^{-1} \end{pmatrix}. \quad (3.57)$$

3.3 \mathcal{Q} -Matrix formulation for scattering

Let us consider a plane wave scattered from an arbitrary barrier with global parity (GP). On left (lhs) and on the right (rhs) hand side of the barrier the plane waves are:

$$\Psi_L(x) = Ae^{ikx} + Be^{-ikx} \quad (3.58)$$

$$\Psi_R(x) = Ce^{ikx} + De^{-ikx} \quad (3.59)$$

The corresponding transfer matrix (TM) which describes the propagation from the lhs to the rhs is:

$$\begin{pmatrix} A \\ B \end{pmatrix} = \begin{pmatrix} w & z \\ z^* & w^* \end{pmatrix} \begin{pmatrix} C \\ D \end{pmatrix} \quad (3.60)$$

From the TM emerge the following two complex equations:

$$A = wC + zD \quad (3.61)$$

$$B = z^*C + w^*D, \quad (3.62)$$

which lead to the following 4×4 TM if real and imaginary parts are separated:

$$\begin{pmatrix} A_R \\ A_I \\ B_R \\ B_I \end{pmatrix} = \begin{pmatrix} w_R & -w_I & z_R & -z_I \\ w_I & w_R & z_I & z_R \\ z_R & z_I & w_R & w_I \\ -z_I & z_R & -w_I & w_R \end{pmatrix} \begin{pmatrix} C_R \\ C_I \\ D_R \\ D_I \end{pmatrix} \quad (3.63)$$

3.4 Relation between the $\hat{\mathcal{Q}}$ and the transfer matrix.

In Chapter 4 we introduced the \mathcal{Q} -matrix as an alternative expression of the generalized Bloch and parity theorems and showed how it relates the wave fields on either side of the potential $\mathcal{W}(x)$.

A common property between the TM and the $\hat{\mathcal{Q}}$ -matrix is that both can describe the propagation through several domains simply by multiplying the TM or $\hat{\mathcal{Q}}$ -matrices of the respective domains. Equation (2.112) connects the lhs of an LP symmetric domain with the rhs, in an equivalent manner to the TM. In this sense, it makes a transfer from a point on one side of the domain \mathcal{D}_m to its symmetric with respect to the corresponding symmetry axis. Also, the $\hat{\mathcal{Q}}$ -matrix links the wave-functions, on either side of the symmetric domain, in their general form and does not require plane wave boundary conditions. The close resemblance to the functionality of the transfer matrix, along with certain common properties as the unimodularity and the multiplicativity, raises the connection whether a connection between these two approaches exist.

By solving Eqs. (3.61), (3.62) with respect to ω , ω^* , respectively we get:

$$\omega = \frac{A - zD}{C} \quad ; \quad \omega^* = \frac{B - z^*C}{D}. \quad (3.64)$$

Having considered the complex conjugate of the latter, the equation of the two expressions for ω , yields:

$$z (|C|^2 - |D|^2) = B^*C - AD^*, \quad (3.65)$$

which combined with the expression for the probability current of a plane wave $J = k (|C|^2 - |D|^2)$, relates the matrix element z with the plane wave coefficients:

$$z = \frac{(B^*C - D^*A) k}{J}. \quad (3.66)$$

Similarly, the substitution of $\omega = \frac{A - zD}{C}$ into Eq. (3.66) leads to:

$$\omega = \frac{(C^*A - B^*D) k}{J}. \quad (3.67)$$

We consider now an LP symmetric domain \mathcal{D}_m , which may be part of a larger, completely LP symmetric setup. On either side of \mathcal{D}_m and on its boundaries, the wavefunctions are plane waves given by Eqs. (3.58), (3.59). The substitution of Eqs. (3.58), (3.59) into Eqs. (2.75), (2.76), leads to an equivalent expression for invariants Q and \tilde{Q} , namely:

$$Q = 2ik \left(ACe^{2ik\alpha} - BDe^{-2ik\alpha} \right) \quad (3.68)$$

and

$$\tilde{Q} = 2ik \left(AD^*e^{2ik\alpha} - BC^*e^{-2ik\alpha} \right) \quad (3.69)$$

The solution of Eqs. (3.68), (3.69) with respect to A and B ,

$$A = \frac{ie^{-2ik\alpha} (\tilde{Q}D - QC^*)}{2J} \quad (3.70)$$

$$B = \frac{ie^{2ik\alpha} (\tilde{Q}C - QD^*)}{2J} \quad (3.71)$$

and their substitution to Eqs. (3.66), (3.67) yields:

$$z = \frac{ike^{-2ik\alpha}}{2J^2} \left[Q^*CD + QC^*D^* - \tilde{Q} (|C|^2 - |D|^2) \right] \quad (3.72)$$

and

$$\omega = \frac{ike^{-2ik\alpha}}{2J^2} \left[2\tilde{Q}C^*D - Q(C^*)^2 - Q^*D^2 \right]. \quad (3.73)$$

For convenience we define:

$$U = \frac{k}{2J^2} \left[Q^*CD + QC^*D^* - \tilde{Q} (|C|^2 - |D|^2) \right], \quad R \in \mathbb{R}, \quad (3.74)$$

to facilitate the polar expression of the matrix element z , $z = iUe^{-2ik\alpha}$, or

$$z = Ue^{-i(2k\alpha - \frac{\pi}{2})}. \quad (3.75)$$

In the case where the center of the domain \mathcal{D}_m is at $\alpha_m = 0$, then $z \in \mathbb{I}$, as one would expect. This result is consistent with the fixed phase value $\phi_z = \frac{\pi}{2}$ of the matrix element z , in the case of a globally symmetric domain with its symmetry axis placed at $\alpha_m = 0$. Nevertheless, here it is shown that in the general case where the LP symmetric domain \mathcal{D}_m is part of an aperiodic, globally non-symmetric setup, the TM element z_m , corresponding to \mathcal{D}_m , has also fixed phase, equal to:

$$\phi = \frac{\pi}{2} - 2k\alpha_m, \quad (3.76)$$

where α_m is the position of the symmetry axis.

In order to relate the TM of the LP domain \mathcal{D}_m to the respective \hat{Q} -matrix, a direct correspondence between $z_R^{(m)}$, $z_I^{(m)}$, $\omega_R^{(m)}$, $\omega_I^{(m)}$ and $q_1^{(m)}$, $q_2^{(m)}$, $q_4^{(m)}$ should be derived. Equations (3.72), (3.73) involve coefficients C , C^* , D , D^* , rendering this direct correspondence impossible. Nonetheless, if we treat the domain \mathcal{D}_m individually instead as part of the total aperiodic setup, we have the following correspondence to the plane wave coefficients:

$$A \rightarrow 1, \quad B \rightarrow R, \quad C \rightarrow T, \quad D \rightarrow 0,$$

where 1 is the amplitude of the incident wave and R , T the reflection and the transmission amplitudes respectively. Under this assumption, Eq. (3.72) becomes:

$$z = -\frac{ike^{-2ik\alpha}}{2J^2} \tilde{Q}|T|^2 \quad (3.77)$$

and by substituting $|T|^2 = \frac{J}{k}$ we finally obtain:

$$z = \frac{\tilde{Q}}{2iJ} e^{-2ik\alpha}, \quad (3.78)$$

where the connection between z and \tilde{Q} is direct. Accordingly, Eqs. (3.67), (3.68) become,

$$\omega = \frac{kT^*}{J}, \quad (3.79)$$

and

$$\begin{aligned} Q &= 2ik e^{2ik\alpha} T \Rightarrow \\ T^* &= -\frac{Q^*}{2ik} e^{2ik\alpha}, \end{aligned} \quad (3.80)$$

respectively. Finally, we find that ω can be expressed only with Q and the position of the symmetry axis of the domain \mathcal{D}_m :

$$\omega = -\frac{Q^*}{2iJ} e^{2ik\alpha}. \quad (3.81)$$

As an example on how the TM can be expressed in terms of the imaginary invariants q_i , we turn to the case of parity, where the transform for a the LP symmetric domain \mathcal{D}_m is $F(x) = 2\alpha_m - x$. The complex invariants Q, \tilde{Q} can be trivially expressed via the real invariants q_1, q_2, q_4 by substituting in Eqs. (2.75), (2.76) the real and imaginary parts of the wave function ($\text{Re } \Psi_m(x), \text{Im } \Psi_m(x)$) and subsequently identifying the expressions of q_1, q_2, q_4 . The corresponding equations are:

$$Q = (q_1 - q_4) + 2iq_2 \quad (3.82)$$

and

$$\tilde{Q} = q_1 + q_4. \quad (3.83)$$

If we insert Eqs. (3.82), (3.83) into Eqs. (3.78), (3.81) and separate real and imaginary parts, we obtain a direct connection between the TM and the \hat{Q} -matrix elements:

TABLE 3.1: Transfer Matrix elements expressed with invariants q ($\alpha \neq 0$)

z	ω
$z_R = -\frac{q_1+q_4}{2J} \sin(2k\alpha)$	$\omega_R = -\frac{q_1-q_4}{2J} \sin(2k\alpha) + \frac{q_2}{J} \cos(2k\alpha)$
$z_I = -\frac{q_1+q_4}{2J} \cos(2k\alpha)$	$\omega_I = \frac{q_1-q_4}{2J} \cos(2k\alpha) + \frac{q_2}{J} \sin(2k\alpha)$

In the case where the set-up is globally parity symmetric, centred around $\alpha = 0$, the above expressions are greatly simplified:

TABLE 3.2: Transfer Matrix elements expressed with invariants q ($\alpha = 0$)

z	ω
$z_R = 0$	$\omega_R = \frac{q_2}{J}$
$z_I = -\frac{q_1+q_4}{2J}$	$\omega_R = \frac{q_1-q_4}{2J}$

CHAPTER 4

REFLECTIONS AND THE LOCAL PARITY FORMALISM

4.1 Introduction

A particularly relevant symmetry operation is the reflection of an object. Depending on the dimensionality of the system, the object can be reflected through a mirror axis, a plane or a hyperplane. The reflection operation performs a mapping from an Euclidean space to itself and can be regarded as an isometry with a hyperplane. The hyperplane type depends on the space dimensionality in one-dimension it is a point, in two-dimensions it is an axis and in three-dimensions it is a plane. In every case this hyperplane is a set of fixed points and with the term isometry we refer to a distance preserving mapping from a metric space to another metric space.

In this chapter we describe in detail the reflection symmetry, when acting both globally and in arbitrary, finite space domains in classical and quantum physical systems. We outline briefly its basic properties in both case and also show how translations in one-dimension emerge from reflections through certain axes. Then, our analysis turns to symmetries fulfilled in finite space domains and especially to *Local Parity (LP)*. The concept of Local Parity [66, 67], is of central importance in the following chapters. Therefore, we develop a mathematically consistent scheme for the description of this operation by defining the LP operator and its properties. This scheme can be considered as an alternative to the approach which utilizes the symmetry induced invariants Q , \tilde{Q} . Instead of using the pairs of $\{Q_m, \tilde{Q}_m\}$ for every locally symmetric domain, one can define local translation and parity operators which act as the regular operators within the relevant domains and as the identity operator on the rest of the set-up.

The link of the LP operator with quantum mechanical and classical wave scattering problems is provided by the commutation of the LP operator with a generalized Helmholtz operator of Eq. (2.82).

4.2 Global Parity

4.2.1 Reflections in Classical Physics

Consider a vector \mathbf{r} in the three-dimensional Euclidean space \mathbb{R}^3 with coordinates given by $r_i = \mathbf{e}_i \mathbf{r}$. A spatial reflection of \mathbf{r} can be seen either as a passive transformation $\mathbf{e}_i \rightarrow -\mathbf{e}_i$ which affects the coordinate system or an active transformation $\mathbf{r}_i \rightarrow -\mathbf{r}_i$, where the coordinate system remains unaffected and every component of \mathbf{r} is transformed. The reflection of \mathbf{r} can be understood as the result of the *parity operator* $\hat{\mathcal{P}}$ when acting on \mathbf{r} .

$$\hat{\mathcal{P}} \mathbf{r} = -\mathbf{r} \quad (4.1)$$

In classical mechanics usually we restrict ourselves in \mathbb{R}^3 . Then in matrix notation the parity operator $\hat{\mathcal{P}}$ can be written as:

$$\hat{\mathcal{P}} \rightarrow \mathcal{P} = \begin{pmatrix} -1 & 0 & 0 \\ 0 & -1 & 0 \\ 0 & 0 & -1 \end{pmatrix} \equiv -I \quad (4.2)$$

where I is the 3-D unit matrix. Under the prism of an eigenvalue problem, \mathbf{r} is an eigenvector of $\hat{\mathcal{P}}$ and the parity eigenvalue is $\lambda = -1$. The repeated action of the operator $\hat{\mathcal{P}}$ in Eq 4.1 yields:

$$\hat{\mathcal{P}}^2 \mathbf{r} = \lambda^2 \mathbf{r} = \mathbf{r} \quad (4.3)$$

Thus, the possible eigenvalues are $\lambda = \pm 1$. The vectors with negative parity $\lambda = -1$ are referred as “polar” vectors, while these with positive parity $\lambda = +1$ as “axial” or “pseudo” vectors [118]. Most vectors in kinematics, like the position vector ($\hat{\mathcal{P}}\mathbf{r} = -\mathbf{r}$), velocity, acceleration and momentum are polar. On the other hand, the cross product of polar vectors results in an axial vector. An illustrative example is the angular momentum $\mathbf{L} = \mathbf{r} \times \mathbf{p}$:

$$\begin{aligned} \hat{\mathcal{P}}\mathbf{L} &= \hat{\mathcal{P}}(\mathbf{r} \times \mathbf{p}) = \hat{\mathcal{P}}\mathbf{r} \times \hat{\mathcal{P}}\mathbf{p} \\ &\hat{\mathcal{P}}\mathbf{L} = \mathbf{L} \end{aligned} \quad (4.4)$$

Formally, a function $f(x, y, z)$ under a parity transformation becomes $f(-x, -y, -z)$ and in the simpler one-dimensional case $f(x) \rightarrow f(-x)$. The function $f(x)$ under parity inversion is:

- $f(-x) = f(x)$, symmetric
- $f(-x) = -f(x)$, antisymmetric

In the case where not all coordinates are transformed we have a partial reflection leading to a mirror image. For example, if $x \rightarrow -x$, $y \rightarrow y$ and $z \rightarrow z$, then a reflection through the $y - z$ -plane occurs.

4.2.2 Reflection transformations in one-dimension

Here we will show that any translation of an object in 1-D is equivalent to two reflections. Consider two points x_1 and x_2 lying in the x -axis. The translation of a point particle from x_1 to x_2 is equivalent to its reflection through the mirror axis lying in the center $\alpha = \frac{x_1+x_2}{2}$ of $[x_1, x_2]$. However, if the object is extended from a to b , then the translation by a distance L is equivalent to two reflections. To show this, let us denote with α' the center of $[a, b]$, which determines the position of the object prior to any transformation and α'' the center of the $[c, d]$ which determines the position of the object after has been translated by L . The parameters α' and α'' are linked via the relation:

$$\alpha'' = \alpha' + L \quad (4.5)$$

Next, we consider the positions of the object's center (α' , α'') prior and after the translation by L and denote the center of the region defined by α' and α'' as α :

$$\alpha = \frac{\alpha'' + \alpha'}{2}. \quad (4.6)$$

Eliminating α' from Eq. (4.5) yields:

$$2\alpha'' = 2\alpha + L \quad (4.7)$$

In the first place we will show that for an extended object the equivalence between a translation and a *single* reflection, leads to a contradiction. To this aim, let $x \in [a, b]$ with $a \leq x < \alpha'$ which, under a reflection with respect to mirror axis α , is transformed as:

$$x' = 2\alpha - x \quad (4.8)$$

By inserting Eq. (4.7) into Eq. (4.8) we get:

$$x' = 2\alpha'' - L - x \quad (4.9)$$

Since we impose that the translation and the reflection are equivalent, it should hold for x :

$$x' = x + L \quad (4.10)$$

Then, the combination of Eqs (4.9), (4.10) leads to:

$$x = \alpha'' - L \Rightarrow x = \alpha' \quad (4.11)$$

which is contradictory to the initial assumption that $x \in [a, \alpha']$. The same can be shown for $\alpha' < x \leq b$. However, if the first reflection is followed by a second with respect to the axis in α'' , the new position x'' will be:

$$x'' = 2\alpha'' - x' \quad (4.12)$$

Substituting Eq. (4.8) and subsequently Eq. (4.7) we finally obtain:

$$x'' = L + x, \quad (4.13)$$

which indicates that any translation of an object in one-dimension is equivalent to two reflections.

4.2.3 Reflections in Quantum Physics

The quantum parity operator \hat{I} essentially differs from its classical counterpart $\hat{\mathcal{P}}$ since the latter acts on vectors in \mathbb{R}^3 (or \mathbb{R} in the 1-D case) while the former acts on state vectors in Hilbert space. The link between \hat{I} and $\hat{\mathcal{P}}$ is provided by the relation:

$$\hat{I}|\mathbf{r}\rangle = |\hat{\mathcal{P}}\mathbf{r}\rangle = |-\mathbf{r}\rangle \quad (4.14)$$

In analogy with the classical case, if we act again with \hat{I} on both sides of Eq. (4.14) we obtain:

$$\hat{I}^2 = \hat{I}, \quad (4.15)$$

which in turn leads to the conclusion that the quantum parity operator is an involutory matrix, that is, it is its own inverse:

$$\hat{I}^{-1} = \hat{I}. \quad (4.16)$$

If $|b\rangle$ is an eigenstate of \hat{I} , the corresponding eigenvalue problem is

$$\hat{I}|b\rangle = \lambda_b|b\rangle. \quad (4.17)$$

A further action of \hat{I} on either side of Eq. (4.17) leads to

$$\hat{I}^2|b\rangle = \lambda_b^2|b\rangle \quad (4.18)$$

and by employing Eq. (4.16) we find that the eigenvalues are:

$$\lambda_b = \pm 1. \quad (4.19)$$

Consequently, the eigenvalues of \hat{I} are real and the respective eigenstates have either positive ($\lambda_b = 1$) or negative ($\lambda_b = -1$) parity.

Another property of the parity operator is that it is also Hermitian:

$$\langle \mathbf{r}|\hat{I}|\mathbf{r}'\rangle = \langle \mathbf{r}|-\mathbf{r}'\rangle = \delta(\mathbf{r} + \mathbf{r}') \quad (4.20)$$

$$\langle \mathbf{r}'|\hat{I}|\mathbf{r}\rangle^* = \langle \mathbf{r}'|-\mathbf{r}\rangle^* = \delta(\mathbf{r} + \mathbf{r}')^* \quad (4.21)$$

and since

$$\delta(\mathbf{r} + \mathbf{r}')^* = \delta(\mathbf{r} + \mathbf{r}'),$$

we arrive at:

$$\hat{\Pi} = \hat{\Pi}^\dagger \quad (4.22)$$

From Eqs. (4.15), (4.22) we conclude that the the $\hat{\Pi}$ is also unitary:

$$\hat{\Pi}^{-1} = \hat{\Pi}^\dagger \quad (4.23)$$

.

4.3 From Global to Local Parity

In Physics, commonly we refer to a system as “spatially symmetric” when the considered symmetry is global holding in the whole space. Nonetheless, as it has been mentioned global spatial symmetry in most cases pertains exactly to structurally simple isolated systems and idealized models. The treatment of symmetries which do not occur in the whole space either because they act only in restricted space domains or because they are approximate, is in principle not trivial. For example, in order to quantify the presence of approximate symmetries in certain systems, symmetry measures [119,120] have been proposed. These are constructed so that they reflect the degree to which the system remains unaffected under specific symmetry operations. Up to now, we have seen that when the symmetry of a system under spatial transformations is globally broken, remnants of it -expressed through non-vanishing invariants- can be preserved at new local scales. In such cases, the symmetry is not completely destroyed (as in a disordered system) and the invariance of certain physical properties under the new local symmetries is still able to affect the system’s behaviour. If a system can be completely covered by spatial domains where its structure exhibits such local symmetry, it can be regarded as *completely locally symmetric*. Since these domains can be of variable extent and at different locations within a single system, there is, in general, a multitude of possible local symmetry decompositions with different symmetry scales and axes [66,67], as demonstrated in Fig. 4.3.

4.4 The Local Parity operator

To quantify in a rigorous way the concept of LP, we introduce the LP operation, which performs the usual parity transform in a finite sub-domain \mathcal{D} of the configuration space (the x -axis in 1-D) and acts in the remaining part, up to a sign, as the identity operator. This definition of local parity preserves its spectral equivalence to global parity since

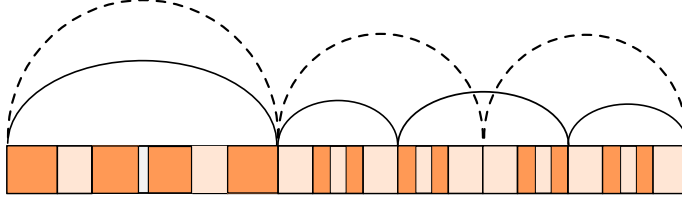


FIGURE 4.1: Local symmetries in 1D. Schematic of a completely local parity symmetric set-up. The arcs depict two different decompositions in LP symmetric domains.

its eigenvalues can be again ± 1 . Also we consider that \mathcal{D} begins at $x = a$ and ends at $x = b$. The single LP operator $\hat{\Pi}_s^{\mathcal{D}}$ ($s = \pm 1$ denotes even and odd parity transform) referring to \mathcal{D} , is parametrized by the location of its inversion point α and the size $L = b - a$ of \mathcal{D} . Note that the LP approach which we will follow is general and it can be applied to several wave-mechanical systems e.g. quantum, photonic, acoustic etc, which in the time-independent regime are described by the Helmholtz equation. The generalized wave-function will be denoted as $\mathcal{A}(x)$. Thus, the action of the LP operator $\hat{\Pi}_s^{\mathcal{D}}$ on an arbitrary, x -dependent field is:

$$\begin{aligned} \hat{\Pi}_s^{\mathcal{D}} \mathcal{A}(x) = & \Theta \left(\frac{L}{2} - |x - \alpha| \right) \mathcal{A}(2\alpha - x) \\ & + s \Theta \left(|x - \alpha| - \frac{L}{2} \right) \mathcal{A}(x), \quad s = \pm 1 \end{aligned} \quad (4.24)$$

where Θ is the Heaviside step function. That is, in addition to inverting the argument of $\mathcal{A}(x)$ within \mathcal{D} , $\hat{\Pi}_-^{\mathcal{D}}$ changes its sign outside \mathcal{D} , while $\hat{\Pi}_+^{\mathcal{D}}$ retains it.

When the spatial extent of the domain \mathcal{D} covers the entire x -space, that is $L \rightarrow \infty$, the LP operator reduces to the global parity operator. In this sense, the LP operation can be regarded as a generalization of global parity, describing a larger variety of more realistic physical systems. Since $(\hat{\Pi}_s^{\mathcal{D}})^2 = \hat{1}$, either one of the two operators has two eigenvalues, $\lambda_s = \pm 1$. The corresponding sets of eigenstates of the $\hat{\Pi}_s^{\mathcal{D}}$ each have two parts, one odd and one even, as shown schematically in Fig. 4.2. The even eigenstates of $\hat{\Pi}_-^{\mathcal{D}}$ as well as the odd of $\hat{\Pi}_+^{\mathcal{D}}$ necessarily vanish outside \mathcal{D} . Therefore they correspond to isolated bound states which possess *global* definite parity. On the contrary, even and odd eigenstates of $\hat{\Pi}_+^{\mathcal{D}}$ and $\hat{\Pi}_-^{\mathcal{D}}$, respectively, are arbitrary outside \mathcal{D} . In this case, *local* parity can be fulfilled in a non-trivial manner. The latter case is relevant for scattering, since it implies open boundary conditions.

By writing Eq. (4.24) in the form

$$\begin{aligned}\hat{\Pi}_s^{\mathcal{D}} \mathcal{A}(x) &= \Theta \left(x - \left(\alpha - \frac{L}{2} \right) \right) \mathcal{A}(2\alpha - x) \\ &+ s \Theta \left(x - \left(\alpha + \frac{L}{2} \right) \right) \mathcal{A}(x),\end{aligned}\quad (4.25)$$

it is straightforward to show that two different LP operators $\hat{\Pi}_{s_1}^{\mathcal{D}_1}, \hat{\Pi}_{s_2}^{\mathcal{D}_2}$ commute if the associated domains $\mathcal{D}_1, \mathcal{D}_2$ don't overlap. Subsequent application of $N = N_+ + N_-$ non-overlapping single LP transforms, where N_{\pm} is the number of acting $\hat{\Pi}_{\pm}^{\mathcal{D}_n}$ operators, thus corresponds to a *total* LP operator

$$\hat{\Pi} = \prod_{n=1}^N \hat{\Pi}_{s_n}^{\mathcal{D}_n}, \quad s_n = \pm 1 \quad (4.26)$$

having again two eigenvalues $\lambda = \prod_{n=1}^N \lambda_{s_n} = \pm 1$. As a consequence of the properties of the LP eigenstates, seen in Fig. 4.2, an eigenstate of $\hat{\Pi}$ can be non-vanishing only in a *single* subdomain \mathcal{D}_n if it is an eigenstate of $\hat{\Pi}_{\pm}^{\mathcal{D}_n}$ with *opposite* eigenvalue $\lambda_n = \mp 1$. Therefore, an eigenstate of $\hat{\Pi}$ (with eigenvalue $\lambda = (-1)^{N_-}$) is non-vanishing in multiple subdomains, and thereby relevant for scattering, only if it is a simultaneous eigenstate of each $\hat{\Pi}_{s_n}^{\mathcal{D}_n}$ with eigenvalue $\lambda_n = s_n$.

As we will see in the following, the transport properties of a system, in relation with the existence of LP, is provided by the commutation of the generalized Helmholtz operator $\hat{\Omega} = \frac{d^2}{dx^2} + \mathcal{W}(x)$ with the total LP operator of the set-up $\hat{\Pi}$. The commutation of $\hat{\Omega}$ explicitly lead to its commutation with each $\hat{\Pi}_{s_n}^{\mathcal{D}_n}$. The term $\mathcal{W}(x) = \kappa^2(x)$ is a real potential term generated by the effective wave vector $\kappa(x)$ and describes the inhomogeneity of the medium where the wave propagation takes place. In the case of a quantum system $\mathcal{A}(x)$ is the wavefunction in x -representation, $\mathcal{W}(x) = \frac{2m}{\hbar^2}(\varepsilon - V(x))$ with m being the mass, ε the incident energy of the quantum particle and $V(x)$ the potential. For electromagnetic waves with frequency ω , $\mathcal{A}(x)$ represents the electric field and $\mathcal{W}(x) = \frac{\omega^2 n^2(x)}{c^2}$, where $n(x)$ is the (x -dependent) refractive index of the medium of propagation. Consider a completely LP symmetric potential $\mathcal{W}(x)$, which can be decomposed in N LP symmetric domains $\mathcal{D}_n = [\alpha_n - \frac{L_n}{2}, \alpha_n + \frac{L_n}{2}]$, each one being symmetric about α_n

$$\mathcal{W}(x) = \mathcal{W}(2\alpha_n - x) \quad \forall x \in \mathcal{D}_n. \quad n = 1, \dots, N, \quad (4.27)$$

We remind the reader that the term ‘‘completely LP symmetric’’ refers to fact that the N non-overlapping domains of the decomposition, cover the entire extent of the set-up. The action of the commutator associated with the n -th subdomain then reads

$$\begin{aligned}
[\hat{\Omega}, \hat{\Pi}_{s_n}^{\mathcal{D}_n}] \mathcal{A}(x) &= \frac{1}{2} \Delta'(x) \{ \mathcal{A}(2\alpha_n - x) - s_n \mathcal{A}(x) \} - \\
&\Delta(x) \{ \mathcal{A}'(2\alpha_n - x) + s_n \mathcal{A}'(x) \}, \quad s_n = \pm 1
\end{aligned} \tag{4.28}$$

where $\Delta(x) = \delta(x - \alpha_n - \frac{L_n}{2}) - \delta(x - \alpha_n + \frac{L_n}{2})$ is a sum of boundary Dirac δ -functions and the prime denotes differentiation with respect to x . The detailed calculation of the commutator is presented in Appendix A'. Note that, whereas $[\hat{\Pi}_{s_n}^{\mathcal{D}_n}, \hat{\mathcal{W}}] \mathcal{A}(x) = [\mathcal{W}(x) - \mathcal{W}(2\alpha_n - x)] \mathcal{A}(2\alpha_n - x) = 0$ for $x \in \mathcal{D}_n$ by assumption, the kinetic term in $\hat{\Omega}$ leads to non-vanishing boundary terms. The commutation is then manifest in a weak sense, which indicates that the commutator acts on a state $\mathcal{A}(x)$ and becomes zero under certain conditions. In the same manner, $\hat{\Omega}$ will commute weakly also with the total LP operator $\hat{\Pi}$, since

$$\begin{aligned}
[\hat{\Omega}, \hat{\Pi}] \mathcal{A}(x) &= [\hat{\Omega}, \prod_{n=1}^{N-1} \hat{\Pi}_{s_n}^{\mathcal{D}_n}] \hat{\Pi}_{s_N}^{\mathcal{D}_N} \mathcal{A}(x) \\
&= \lambda_{s_N} [\hat{\Omega}, \prod_{n=1}^{N-2} \hat{\Pi}_{s_n}^{\mathcal{D}_n}] \hat{\Pi}_{s_{N-1}}^{\mathcal{D}_{N-1}} \mathcal{A}(x) \\
&= \left(\prod_{n=2}^N \lambda_{s_n} \right) [\hat{\Omega}, \hat{\Pi}_{s_1}^{\mathcal{D}_1}] \mathcal{A}(x) = 0.
\end{aligned} \tag{4.29}$$

The weak commutation relation $[\hat{\Omega}, \hat{\Pi}] \mathcal{A}(x) = 0$ imposes N conditions on the wave field $\mathcal{A}(x)$ in order to be LP definite in every LP symmetric domain:

$$\mathcal{A}(x) = s_n \mathcal{A}(2\alpha_n - x), \quad x \in \mathcal{D}_n, \quad n = 1, 2, \dots, N. \tag{4.30}$$

In polar representation where $\mathcal{A}(x) = \sqrt{\rho(x)} e^{i\varphi(x)}$, we get accordingly $2N$ conditions

$$\rho(x) = \rho(2\alpha_n - x) \tag{4.31}$$

$$\varphi(x) = \varphi(2\alpha_n - x) + \frac{(1-s_n)\pi}{2} \tag{4.32}$$

for the probability density $\rho(x)$ and for the phase $\varphi(x)$ defined up to $\text{mod}(2\pi)$. The violation of one of these two conditions implies a breaking of LP symmetry. In the next chapters we will see that a remnant of this breaking manifests in a class of perfect transmission resonances, where LP symmetry appears in the module of $\mathcal{A}(x)$.

4.4.1 Properties of the LP operator

The existence of the Heaviside Theta functions in the definition of the LP operator does not allow the direct generalization of the global parity operator properties to the case

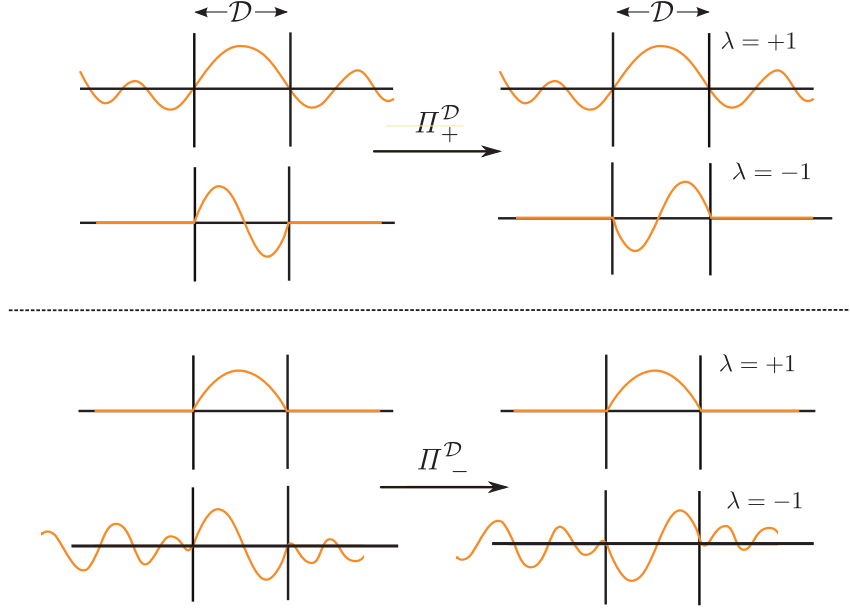


FIGURE 4.2: Real parts of local parity eigenstates, shown for a single sub-domain \mathcal{D} . The eigenstates of $\hat{\Pi}_+^{\mathcal{D}}$ with eigenvalue $\lambda = +1$ are even within \mathcal{D} and arbitrary outside. These allow open boundary condition and correspond to scattering states. The same holds for the eigenstates of $\hat{\Pi}_-^{\mathcal{D}}$ with $\lambda = -1$. These are odd within \mathcal{D} and arbitrary outside. Eigenstates of $\hat{\Pi}_+^{\mathcal{D}}$ with eigenvalue $\lambda = -1$ are odd within \mathcal{D} and zero outside, corresponding to bound states. The same situation holds respectively for $\hat{\Pi}_-^{\mathcal{D}}$ with eigenvalue $\lambda = 1$.

of local parity. Here we will show certain properties of the LP operator, namely the hermiticity and the unitarity.

Hermiticity of the LP operator

Considering the LP operator $\hat{\Pi}_{s_n}^{\mathcal{D}_n}$ which acts on the n -th subdomain \mathcal{D}_n (extending from a to b) as the parity operator and in the rest x -axis as the identity operator \hat{I} , we

calculate the integral:

$$\begin{aligned}
\langle \hat{H}_{s_n}^{\mathcal{D}_n} \mathcal{A}(x) | \mathcal{A}(x) \rangle &= \int_{-\infty}^{\infty} \left(\hat{H}_{s_n}^{\mathcal{D}_n} \mathcal{A}(x) \right)^* \mathcal{A}(x) dx & (4.33) \\
&= \int_{-\infty}^{\infty} \mathcal{A}^*(2\alpha - x) [\Theta(x - a) - \Theta(x - b)] \mathcal{A}(x) dx \\
&+ \int_{-\infty}^{\infty} \mathcal{A}^*(x) [\Theta(a - x) + \Theta(x - b)] \mathcal{A}(x) dx,
\end{aligned}$$

where we have used Eq. (4.24) with $s_n = 1$, denoting an even parity transform, $L = b - a$ and $\alpha = \frac{a+b}{2}$.

For the Hermiticity of the operator it must hold that:

$$\langle \hat{H}_{s_n}^{\mathcal{D}_n} \mathcal{A}(x) | \mathcal{A}(x) \rangle = \langle \mathcal{A}(x) | \hat{H}_{s_n}^{\mathcal{D}_n} \mathcal{A}(x) \rangle = (\langle \hat{H}_{s_n}^{\mathcal{D}_n} \mathcal{A}(x) | \mathcal{A}(x) \rangle)^*. \quad (4.34)$$

Then, we calculate the integral:

$$\begin{aligned}
\langle \mathcal{A}(x) | \hat{H}_{s_n}^{\mathcal{D}_n} \mathcal{A}(x) \rangle &= \int_{-\infty}^{\infty} \mathcal{A}^*(x) \hat{H}_{s_n}^{\mathcal{D}_n} \mathcal{A}(x) dx & (4.35) \\
&= \int_{-\infty}^{\infty} \mathcal{A}^*(x) [\Theta(x - a) - \Theta(x - b)] \mathcal{A}(2\alpha - x) dx \\
&+ \int_{-\infty}^{\infty} \mathcal{A}^*(x) [\Theta(a - x) + \Theta(x - b)] \mathcal{A}(x) dx,
\end{aligned}$$

where the second term is the same with the second term of Eq. (4.33). Therefore, for Eq. (4.34) to hold, we consider the first term of Eq. (4.33):

$$\int_{-\infty}^{\infty} \mathcal{A}^*(2\alpha - x) [\Theta(x - a) - \Theta(x - b)] \mathcal{A}(x) dx \quad (4.36)$$

Changing variables

$$\begin{aligned}
x' &= 2\alpha - x \\
dx &= -dx' \\
x = a &\rightarrow x' = b \\
x = b &\rightarrow x' = a.
\end{aligned}$$

we are led to:

$$\int_{-\infty}^{\infty} \mathcal{A}^*(x') [\Theta(b - x') - \Theta(a - x')] \mathcal{A}(2\alpha - x') dx'. \quad (4.37)$$

Based on the Heaviside Theta function property:

$$\Theta(-x) = 1 - \Theta(x), \quad (4.38)$$

for $\Theta(b - x')$ and $\Theta(a - x')$ will hold:

$$\begin{aligned}\Theta(b - x') &= 1 - \Theta(x' - b) \\ \Theta(a - x') &= 1 - \Theta(x' - a)\end{aligned}$$

and the integral, in turn, takes the form:

$$\int_{-\infty}^{\infty} \mathcal{A}^*(2\alpha - x') [\Theta(x' - b) - \Theta(x' - a)] \mathcal{A}(x') dx'. \quad (4.39)$$

Consequently, the LP operator is Hermitian.

Unitarity of the LP operator

The LP operator $\hat{\Pi}_{s_n}^{\mathcal{D}_n}$ which acts on the wave field $\mathcal{A}(x)$ in the n -th subdomain \mathcal{D}_n is defined in Eq. (4.24), which can be written in the following form:

$$\begin{aligned}\hat{\Pi}_s^{\mathcal{D}_n} \mathcal{A}(x) &= [\Theta(x - a) - \Theta(x - b)] \mathcal{A}(2\alpha - x) \\ &+ s [\Theta(a - x) + \Theta(x - b)] \mathcal{A}(x), \quad s = \pm 1\end{aligned} \quad (4.40)$$

A subsequent action of $\hat{\Pi}_{s_n}^{\mathcal{D}_n}$ on Eq. (4.40) leads to:

$$\begin{aligned}\left(\hat{\Pi}_s^{\mathcal{D}_n}\right)^2 \mathcal{A}(x) &= [\Theta(x - a) - \Theta(x - b)] \mathcal{A}(x) \\ &+ s^2 [\Theta(a - x) + \Theta(x - b)] \mathcal{A}(x)\end{aligned} \quad (4.41)$$

and consequently:

$$\left(\hat{\Pi}_s^{\mathcal{D}_n}\right)^2 \mathcal{A}(x) = [\Theta(x - a) - \Theta(x - b) + \Theta(a - x) + \Theta(x - b)] \mathcal{A}(x) \quad (4.42)$$

Finally, using the Heaviside Theta function property $\Theta(-x) = 1 - \Theta(x)$ we are led to:

$$\left(\hat{\Pi}_s^{\mathcal{D}_n}\right)^2 \mathcal{A}(x) = \mathcal{A}(x), \quad (4.43)$$

which in turn implies that the operator $\hat{\Pi}_{s_n}^{\mathcal{D}_n}$ is involutory as the global parity operator:

$$\left(\hat{\Pi}_s^{\mathcal{D}_n}\right)^2 = \hat{I} \Rightarrow \hat{\Pi}_s^{\mathcal{D}_n} = \left(\hat{\Pi}_s^{\mathcal{D}_n}\right)^{-1}, \quad (4.44)$$

Since $\hat{\Pi}_{s_n}^{\mathcal{D}_n}$ is Hermitian $\left(\hat{\Pi}_{s_n}^{\mathcal{D}_n}\right)^\dagger = \hat{\Pi}_{s_n}^{\mathcal{D}_n}$, then from Eq. (4.44) we conclude that the operator $\hat{\Pi}_{s_n}^{\mathcal{D}_n}$ is also unitary:

$$\left(\hat{\Pi}_{s_n}^{\mathcal{D}_n}\right)^\dagger = \left(\hat{\Pi}_{s_n}^{\mathcal{D}_n}\right)^{-1}, \quad (4.45)$$

CHAPTER 5

LOCAL PARITY AND SCATTERING IN APERIODIC MEDIA

5.1 Introduction

As it has already been mentioned in the previous chapters, transport properties and their control in inhomogeneous media has developed into a field of intense study. Systems with complex geometric structure [61] by suitably manipulating their characteristics, may demonstrate a large variety of applications to quantum [81, 121], photonic [122], acoustic [20] and magnonic [123] systems. Quasi-periodic and aperiodic systems possess a central role both in understanding the fundamental concepts which govern the transitions from perfectly periodic order to randomness and in the development and design of devices with controllable transport properties, which we will discuss in detail in the next chapter.

Here we show how LP symmetry, can serve as a tool for the interpretation and classification of perfect transmission resonances (PTRs) in globally non-symmetric systems and specifically, in systems with quasi-periodicity and aperiodicity. We explain in detail the role of multiple LP symmetry scales in the existence of PTRs and propose a framework providing a link between the PTR classification introduced in [14] for photonic multilayers and the physical properties originating from the local parity symmetries of the potential. However, our analysis extends so that it is applicable to a wide range of wave scattering, inhomogeneous devices (e.g. i.e. quantum, photonic and acoustic), offering the unique possibility to relate geometrical characteristics with transmission properties in a direct manner. Typical examples are systems possessing quasi-periodic Fibonacci [57–59], fractal Cantor [91–93] or even more general geometry [124] leading to scaling and self-similarity of the corresponding transmission spectra.

We also extend the use of the symmetry induced invariants, introduced in Chapter 2 and show how they can impose a geometric interpretation of PTRs in the complex plane.

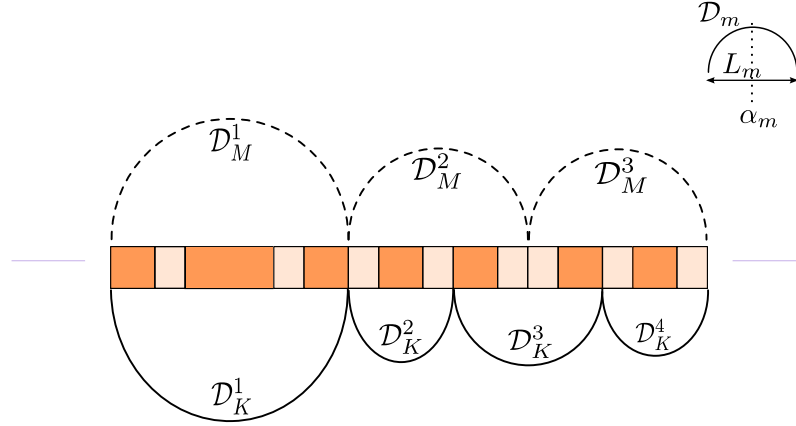


FIGURE 5.1: Aperiodic, completely local parity symmetric setup. Each different color layer stands for a different (LP symmetric) scatterer, corresponding to i.e. a quantum or a photonic system. The dashed and solid arcs depict 3 and 4 LP symmetric domains \mathcal{D}_M and \mathcal{D}_K for two different decompositions, respectively. As an example, a single domain \mathcal{D}_m has length L_m and extends around the local symmetry axis α_m .

This, in turn, facilitates an alternative PTR classification.

5.2 Symmetry scales in aperiodic systems

The decomposition of a completely LP symmetric setup in LP symmetric domains, may occur in more than one ways and a setup which offers this possibility is regarded as one with *multiple symmetry scales*. For reasons of clarity, we consider an aperiodic device consisted of N scatterers. These scatterers can be grouped in M LP symmetric domains \mathcal{D}_M around the corresponding LP symmetry axes, which, in turn, cover the entire device. Nevertheless, the N scatterers can be also grouped in K LP symmetric domains \mathcal{D}_K , around new LP symmetry axes, again covering the entire device. To be concrete, Fig. 5.1 illustrates such a system. Each different color layer stands for a different (LP symmetric) scatterer. In a quantum system these could correspond to barriers or wells whether in photonic systems to dielectrics of different refractive index. The arcs delimit the LP symmetric domains, comprising each decomposition. Particularly, the dashed and solid arcs denote two possible -but not the only- different decompositions in LP symmetric domains, consisting of 3 and 4 LP symmetric domains (\mathcal{D}_M , \mathcal{D}_K). Note, that in each decomposition the domains which constitute it, should be non-overlapping.

In the following sections we will show how the multitude of the possible decompo-

sitions of a completely LP symmetric device, can affect its transmission properties and specifically the emergence of PTRs.

5.2.1 Global properties emerging from local invariants

Let us return to the definition of the first complex locally invariant quantity Q , which was introduced in Chapter 2. Here we restrict ourselves to parity transforms ($F(x) = 2\alpha - x$), where α is the position of the symmetry axis of the parity symmetric domain.

$$Q = \mathcal{A}(2\alpha - x)\mathcal{A}'(x) - \mathcal{A}'(2\alpha - x)\mathcal{A}(x). \quad (5.1)$$

For a completely LP symmetric setup which is decomposable in N LP symmetric domains, there exist N , generally different, invariants Q_m , $m = 1, \dots, N$, each one corresponding to the domain $\mathcal{D}_m = [x_{m-1}, x_m]$. Note here the values of the Q_m depend on the considered local symmetry decomposition and on the input generalized energy ϵ .

The importance of the invariants Q and \tilde{Q} was revealed in Chapter 2 with the generalization of Bloch and parity theorems [105]. Here we will show how they enable the classification of a perfect transmission resonance according of the corresponding field configurations in terms of local (parity) symmetries. For this purpose we evaluate Q_m

$$Q_m = \mathcal{A}(2\alpha_m - x)\mathcal{A}'(x) - \mathcal{A}'(2\alpha_m - x)\mathcal{A}(x) \quad (5.2)$$

for $x = x_m$, which correspond to the boundaries of each domain \mathcal{D}_m , so that:

$$Q_m = \mathcal{A}(x_{m-1})\mathcal{A}'(x_m) - \mathcal{A}'(x_{m-1})\mathcal{A}(x_m). \quad (5.3)$$

By dividing Eq. (5.3) with the product $\mathcal{A}(x_{m-1})\mathcal{A}(x_m)$ we arrive at:

$$\frac{\mathcal{A}'(x_{m-1})}{\mathcal{A}(x_{m-1})} + \frac{\mathcal{A}'(x_m)}{\mathcal{A}(x_m)} = \frac{Q_m}{\mathcal{A}(x_{m-1})\mathcal{A}(x_m)}, \quad m = 1, 2, \dots, N \quad (5.4)$$

and set the right-hand side as:

$$\mathcal{V}_m \equiv \frac{Q_m}{\mathcal{A}(x_{m-1})\mathcal{A}(x_m)}. \quad (5.5)$$

The scaled currents \mathcal{V}_m , at a given energy ϵ , involve information exclusively for the corresponding sub-domains \mathcal{D}_m , since the Q_m characterizes the specific sub-domain and the wave fields in the denominator are computed at its boundaries. In the resulting system of the N Eqs. (5.4), we subtract the first two and add the result to the third. The resulting equation is subtracted from the fourth and so on. This procedure finally yields:

$$\frac{\mathcal{A}'(x_0)}{\mathcal{A}(x_0)} - (-1)^N \frac{\mathcal{A}'(x_N)}{\mathcal{A}(x_N)} = \sum_{m=1}^N (-1)^{m-1} \mathcal{V}_m \equiv \mathcal{L} \quad (5.6)$$

which depends only on the field at the set-up's *global* boundaries x_0, x_N . Having in mind that we want to study the influence of LP symmetry on the transmission properties and especially on PTRs, it is convenient to express the field $\mathcal{A}(x)$ in its polar representation, in order to involve its module $u(x)$,

$$\mathcal{A}(x) = |\mathcal{A}(x)|e^{i\varphi(x)} \equiv u(x)e^{i\varphi(x)}, \quad (5.7)$$

so that Eq. (5.6) becomes

$$\begin{aligned} \mathcal{L} = i & [\varphi'(x_0) - (-1)^N \varphi'(x_N)] \\ & + \left[\frac{u'(x_0)}{u(x_0)} - (-1)^N \frac{u'(x_N)}{u(x_N)} \right] \end{aligned} \quad (5.8)$$

In the following sections we will ascertain that the global quantity \mathcal{L} when it is combined with the local quantities \mathcal{V}_m , utilize a categorization of the scattering states of the system employing their geometric interpretation.

5.3 Scattering from piecewise constant setups

We now turn to the effects that LP symmetry induces to scattering from a completely LP symmetric 1-D (generalized) potential of the form

$$\mathcal{W}(x) = \sum_{m=1}^N \mathcal{W}_m(x) \Theta(L_m/2 - |x - \alpha_m|), \quad (5.9)$$

where $\mathcal{W}(x)$ is of compact support. Thereby, the scattering potential $\mathcal{W}(x)$ is consisted of N , non-overlapping units, symmetric about the LP axis at $x = \alpha_m$, with widths L_m , which are denoted as $\mathcal{W}_m(x)$. The complex wave field $\mathcal{A}(x)$ which satisfies the Helmholtz equation is uniquely determined by its boundary conditions at the ends x_0, x_N of the potential. In the cases which we will consider, symmetric and asymmetric asymptotic conditions are imposed with plane waves of the form:

$$\mathcal{A}(x) = Ae^{i\kappa x} + Be^{-i\kappa x} \quad (5.10)$$

where κ is the wave number, determined by the wave incident (generalized) energy ϵ . Note, that the term ‘‘generalized’’ is used to include both, energies for quantum mechanical particles and frequencies for optical or acoustic setups. There are two different kinds of asymptotic conditions in such scattering set-ups: (i) symmetric asymptotic conditions (SAC), where the wave incidence occurs both from the lhs and the rhs of the potential, with equal amplitudes and (ii) asymmetric asymptotic conditions (AAC), where

the incidence occurs only from one side of the potential. The corresponding asymptotic ingoing amplitudes are linked to the outgoing ones via the S -matrix

$$S = \begin{pmatrix} r & t \\ t & \tilde{r} \end{pmatrix} \quad (5.11)$$

which as we saw in Chapter 3 is unitary due to current conservation and symmetric due to time-reversal symmetry. Accordingly, in the transfer matrix (TM) representation, the plane wave amplitudes in the lhs of the potential are related to those in the rhs.

$$M = \begin{pmatrix} t^{*-1} & rt^{-1} \\ -t^{-1}r' & t^{-1} \end{pmatrix} \quad (5.12)$$

5.3.1 Scattering under SAC in locally symmetric media

In an aperiodic -though completely LP symmetric set-up- we impose SAC, so that incoming waves of the same amplitude arrive on either side of $\mathcal{W}(x)$. We consider a solution $\mathcal{A}(x)$ which satisfies the Helmholtz equation and also is locally parity symmetric in every LP symmetric domain of the particular decomposition. In other words, the wave field $\mathcal{A}(x)$ is a simultaneous eigenstate of the Helmholtz

$$\hat{\Omega} = \frac{d^2}{dx^2} + \mathcal{W}(x), \quad (5.13)$$

and the total LP operator

$$\hat{\Pi} = \prod_{m=1}^N \hat{\Pi}^{\mathcal{D}_m}, \quad (5.14)$$

This occurs under the validity of the *weak commutation* relation (see Appendix A')

$$\left[\hat{\Omega}, \hat{\Pi} \right] \mathcal{A}(x) = 0, \quad (5.15)$$

from which it stems that for an LP definite $A(x) = u(x)e^{i\varphi(x)}$ where $u(x) = |\mathcal{A}(x)|$ it holds that:

$$u(2\alpha_m - x) = u(x) \quad (5.16)$$

and

$$\varphi(2\alpha_m - x) = \varphi(x), \quad (5.17)$$

for each LP symmetric domain \mathcal{D}_m . This implies that the phase derivative $\varphi'(x)$ should be locally antisymmetric. Next, by replacing the polar form of the field

$$\mathcal{A}(x) = u(x)e^{i\varphi(x)},$$

into the current equation

$$J = \mathcal{A}^*(x)\mathcal{A}'(x) - \mathcal{A}(x)\mathcal{A}'^*(x), \quad (5.18)$$

we arrive at

$$J = u(x)\varphi'(x), \quad (5.19)$$

which expresses the probability current in the quantum mechanical case or energy density current in wave mechanical systems, e.g. optics. The current J , however, is a constant, positive quantity and the field magnitude $u(x)$ is positive and LP definite within the domain \mathcal{D}_m . Consequently, the phase slope $\varphi'(x)$ should be also symmetric, which is contradictory to the fact that the LP symmetry of $\mathcal{A}(x)$ leads to symmetric $\varphi(x)$ and antisymmetric $\varphi'(x)$. This incompatibility is lifted only in the case where $\varphi'(x) = 0$ and the phase $\varphi(x)$ is constant. There are interesting implications based on this result. The phase $\varphi(x)$ is locally constant within $\mathcal{W}(x)$ regions, where $\mathcal{A}(x)$ doesn't change sign. The occurrence of this effect is attributed to the alternating sign of the field $\mathcal{A}(x)$. Since the module $u(x)$ is always greater than or equal to zero, the wave function can only change sign due to the phase $\varphi(x)$. Thereby, in every point where $\mathcal{A}(x) = 0$ (and also $u(x) = 0$), the phase changes by $\pm\pi$, inducing in this manner a minus sign ($e^{i\pi}$) in front of the phase factor $e^{i\varphi(x)}$. Thus, $\varphi(x)$ behaves as a Θ -function and $\varphi'(x)$ as a δ -function, whenever the field changes sign ($\mathcal{A}(x) = 0$) and consequently, any possible irregularities in the continuity equation appear there ($\mathcal{A}(x) = 0$) and not to the interfaces between adjacent barrier or domains.

An interesting property of states with completely LP symmetric field profile is that, since it holds $\varphi'(x) = 0$, Eq. (5.19) yields that $J = 0$. In other words, states with LP symmetric $\mathcal{A}(x)$ profile in every LP symmetric domain, carry zero current. We will refer to these states as *zero-current states* (ZCS). Such states provide a link between the concept of LP and an observable as the current J , when SAC are imposed. Note, that in such states the inversion symmetry is retained $\forall x \in \mathbb{R}$ and the space invariant Q vanishes. Nevertheless, definite LP is not a necessary condition for a ZCS emergence. As an example we can consider the case of perfect transmission under asymmetric asymptotic condition where the incidence of the wave occurs from only one side of the potential. In such a state, by imposing SAC we recover a ZCS, which however is not LP definite within the interaction region.

5.3.2 Asymptotic conditions and symmetry breaking

With the most common scattering case in mind, we turn now to wave incidence only from the lhs of the potential $\mathcal{W}(x)$. Thereby, since the amplitudes of the incoming plane waves are now $\begin{pmatrix} 1 \\ 0 \end{pmatrix}$, in the $|\pm\rangle$ -space, the symmetry of the system is explicitly broken.

Particularly, the wave functions on either side of the (generalized) potential, are given by the plane wave expressions:

$$\mathcal{A}_L(x) = e^{i\kappa x} + r e^{-i\kappa x} \quad (5.20)$$

and

$$\mathcal{A}_R(x) = t e^{i\kappa x}. \quad (5.21)$$

The current J is non-zero, except from the trivial case of total reflection, which we will not consider here. Nonetheless, since $J \neq 0$, the LP condition in Eq. (5.16) is violated in the following manner: Assuming that Eq. (5.16) holds, we have from the spatial invariance of the current:

$$\begin{aligned} J(x) = J(2\alpha_m - x) &\Rightarrow \\ u(x)\varphi'(x) = u(2\alpha_m - x)\varphi'(2\alpha_m - x). \end{aligned} \quad (5.22)$$

From Eq. (5.16) we get that $\varphi(x) = \varphi(2\alpha_m - x)$ and therefore $\varphi'(x) = -\varphi'(2\alpha_m - x)$, which combined with Eq. (5.22) suggests that

$$u(x) = -u(2\alpha_m - x) = 0, \quad (5.23)$$

since the module of the field is always positive definite. Necessarily then, we conclude that, under AAC, the LP symmetry can be fulfilled in the module $u(x)$, though this is not possible for the phase. Obviously then, under AAC, it is impossible to get a LP definite field $\mathcal{A}(x)$.

5.3.3 Perfect transmission in locally symmetric media

The manifestation of the aforementioned symmetry of $u(x)$, has a significant role in the transmission properties of a *completely LP symmetric medium* and particularly in the emergence of perfect transmitting resonances (PTRs). In a lossless medium, as the one under consideration, the transmission T and reflection R coefficients are related via the relation $R + T = 1$ due to energy conservation. In the quantum mechanical case this equation expresses the conservation of probability (unitarity).

As the incident wave propagates through a composite, inhomogeneous medium with varying scatterers $\mathcal{W}_m(x)$, it is multiply scattered and the counter-propagating waves interfere into the stationary scattering state. Although the various parts of the medium may all exhibit finite reflection, the interference at *resonant* (generalized) energies ϵ occurs in such manner so that peaks appear in the transmission spectrum.

Of particular interest is the case of perfect transmission ($T = 1$) through an aperiodic multilayer. There is a wide class of examples supporting that mirror symmetry of photonic multilayers (e.g. Cantor) leads to perfectly transmitting resonances (PTRs) while

the lack of such a symmetry is usually accompanied by the absence of perfect transmission. A transparent example of this scenario is the emergence of PTRs in multilayers with Fibonacci geometry after appropriate symmetrization [15, 16, 100, 125]. These results indicate the direct link between global mirror symmetry and PTRs. Generally, in globally parity symmetric set-up, an isolated [126] resonance at energy ϵ can be shown [127] to have symmetric $u(x)$ and, therefore, be perfectly transmitting. The global symmetry of $u(x)$ at a PTR expresses the fact that the probability density of a perfectly transmitting state cannot reveal the direction of incidence in a reflection symmetric potential.

However, recent results report the presence of PTRs in devices without mirror symmetry [14, 65, 128, 129] indicating that the global mirror symmetry is a sufficient but not necessary condition for the appearance of perfect transmission. In some cases the occurrence of PTRs in such devices has been attributed to ‘internal’ [15] or ‘hidden’ [65] symmetries. Also in [14], the appearance of PTRs in an aperiodic, hybrid Fabry-Pérot-photonic crystal device is reported. These works have significantly impelled our understanding in resonant scattering off inhomogeneous media in 1-D. However, up to now, the link between transmission properties and the symmetries of the generalized potential $\mathcal{W}(x)$ is not yet fully understood.

Nevertheless, there is crucial remark which should be made for the aforementioned set-ups. In every case of these, even though being globally non-symmetric, mirror symmetry was retained on a local scale. Specifically, they could be decomposed in smaller, non-overlapping domains with *mirror symmetric* structure which cover the entire device. Even their simplest units $\mathcal{W}_m(x)$ as shown in Eq. (5.9) (e.g. a dielectric slab or a barrier) are piecewise constant. Thereby, they possess LP symmetry even in their most trivial decomposition, that is when the set-up is decomposed in every single contained scatterer. It has been stressed that such completely LP symmetric systems can possibly be decomposed in a multitude of ways. So, depending on the set-up, there can exist a several possible LP decompositions, emerging at different scales and about different axes. Thus, the question to be posed is, whether and how, these local mirror symmetric decompositions can affect the transmission properties, with respect to PTRs, in the absence of global mirror symmetry.

Since the scattering occurs under AAC, a first attempt would be to impose the LP condition on the field module, so that Eq. (5.16) holds in every LP symmetric domain of the selected decomposition, and seek its possible impact on the transmission properties. The outcome indicates that there are two possible cases for the overall probability amplitude (see Appendix B’ for the proof):

$$r = 0 \tag{5.24}$$

or

$$r = -e^{i\kappa x_0} \tag{5.25}$$

where x_0 is the start of the device. The former case obviously is the one of a PTR, while the latter corresponds to the trivial case of total reflection. Consequently, there is an explicit relation between the LP fulfilment on the level of the field module and the occurrence of PTRs. Particularly, whenever $u(x)$ is *completely LP symmetric* in a certain decomposition of a completely symmetric set-up, *the state is perfectly transmitting*.

In the rest of our analysis we will consider only set-ups employing mirror symmetric piecewise constant units which are commonly used in the current literature. In fact, the majority of the current literature indicates that the occurrence of a PTR in a completely non-parity symmetric set-up in 1-D scattering, would be extremely rare. Thus, we will assume that PTRs occur mainly in completely local parity symmetric potentials and any other case - if it exists - will be regarded as accidental.

To elaborate more the notion of symmetry scales, let us consider an 1-D set-up which is comprised of two or more kinds of scatterers \mathcal{W}_m . Each scatterer has an axis of mirror symmetry, transferring this property also to the total potential \mathcal{W} , though now as a local symmetry. As a consequence, all potentials belonging to this class are completely LP symmetric. Assuming that the characteristics of each scatterer (potential strength and width) are such that each of them can resonate at a given fixed energy ϵ then, within every scatterer, the magnitude of the wave field $u_\epsilon(x)$ will be LP symmetric as has been shown in Ref. [66,67]. The index ϵ indicates the corresponding energy where the specific profile of the module $u(x)$ occurs. This is the most immediate realization of a complete decomposition in LP symmetric units, for a potential in this class. However, more decompositions in LP symmetric units could manifest, as shown in Fig. 5.1. Notice, that each such unit may contain several scatterers. Obviously, different LP decompositions may have different number and/or structures of such LP symmetric units.

5.3.4 Geometric interpretation and classification of PTRs

When a PTR occurs at energy ϵ it holds that $u_\epsilon(x_0) = u_\epsilon(x_N) = 1$ for every $x \leq x_0$, $x \geq x_N$. Thus, the derivatives of $u_\epsilon(x)$ in Eq. (5.8) are zero and we can write

$$\mathcal{L} = i(\varphi'(x_0) - (-1)^N \varphi'(x_N)) \quad (5.26)$$

According to whether the setup can be decomposed in N even or odd LP symmetric units Eq. (5.26) becomes:

$$\sum_{m=1}^N (-1)^{m-1} \vec{v}_m = \begin{cases} 0, & N \text{ even} \\ 2iJ, & N \text{ odd} \end{cases}, \quad (5.27)$$

or

$$\mathcal{L} = iJ[1 - (-1)^N] = \begin{cases} 0, & N \text{ even} \\ 2i\kappa, & N \text{ odd} \end{cases} \quad (5.28)$$

where, we remind that:

$$\mathcal{V}_m = \frac{Q_m}{\mathcal{A}(x_m) \mathcal{A}(x_{m+1})} \quad ; \quad \kappa = \varphi'(x_0) = \varphi'(x_N). \quad (5.29)$$

κ is the wave number of the incident wave and

$$J \equiv u^2(x)\varphi'(x) = \kappa T. \quad (5.30)$$

We write the left-hand side of the Eq. (5.4) as the logarithmic derivative of the field.

$$\mathcal{V}_m = \frac{d}{dx} \left[\log \left(\frac{u(x_{m-1})}{u(x_m)} \right) \right] \quad (5.31)$$

This expression, together with its equivalent Eq. (5.5), consists entirely of quantities which refer to a single LP symmetric domain \mathcal{D}_m , thus describing specifically \mathcal{D}_m without inducing couplings with other domains. The substitution of the polar form of the wave field for the case of an s -PTR, where $u(x_{m-1}) = u(x_m) = 1$, leads to $\mathcal{V}_m = i(\varphi'(x_{m-1}) + \varphi'(x_m))$. We know, though, from Eq. (5.19), that in an s -PTR

$$\varphi'(x) = \varphi'(2\alpha - x) = J = \kappa.$$

Thus, in an s -PTR, the possible vectors which represent each resonator, degenerate to the vector $\mathcal{V}_m = 2i\kappa$, lying on the imaginary axis.

Beyond \mathcal{V}_m , for odd number of LP symmetric units (Eq. (5.27)), appears the global parameter J which is constant along the device. Equation (5.28) allow PTRs to acquire a geometric character if we interpret \mathcal{V}_m as a vector in the complex plane. Each LP symmetric domain \mathcal{D}_m is characterized by a single vector \mathcal{V}_m . The sum \mathcal{L} of the complex plane ‘vectors’ \mathcal{V}_m in Eq. (5.6), allows to categorize scattering states employing a relevant symmetry based argumentation. This classification distinguishes between the formation of open and closed trajectories on the complex plane, emerging from the summation of all the vectors \mathcal{V}_m , each one corresponding to an LP symmetric domain of the respective decomposition. Therefore, we have:

(i) *symmetric PTR*. We call symmetric PTR (s -PTR) a resonance which occurs if and only if $u_\epsilon(x)$ (at the resonance energy ϵ) is completely LP symmetric within the spatial extent of the device. In such states, reflectionless transmission occurs in every LP symmetric sub-domain \mathcal{D}_m of a selected decomposition. We will refer to each LP symmetric sub-domain \mathcal{D}_m which transmits with $T_m = 1$ (T_m is the transmission coefficient through \mathcal{D}_m alone) as *resonator*. Vectors \mathcal{V}_m become collinear and lie on the imaginary axis with values $(-1)^m 2iJ$. Therefore, the corresponding trajectory is thus restricted to the imaginary axis and taking values 0 for odd (Fig. 5.2(a)) and $2i\kappa$ for even number of LP symmetric sub-domains (Fig. 5.2(b)).

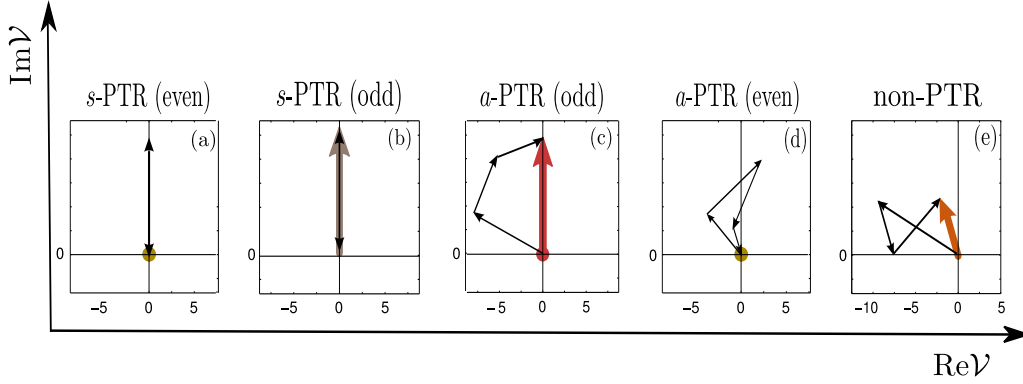


FIGURE 5.2: Geometric representation of a s -PTR in a set-up decomposed in an odd (a) and even (b) number of LP symmetric domains (resonators). Accordingly, a -PTR for an odd (c) and even (d) decomposition. A non-PTR state is shown in (e). The vectors \mathcal{V}_m (in black) correspond to each LP symmetric sub-domain \mathcal{D}_m . From their addition emerges the vector (in color) \mathcal{L} .

(ii) *asymmetric PTR*. An asymmetric PTR state (a -PTR) has $T = 1$. The field magnitude $u(x)$ is *not* completely LP symmetric [66], i.e. it doesn't follow the mirror symmetries of the domains of a certain set-up decomposition. If the decomposition consists of an odd number of LP symmetric domains N , the addition of \mathcal{V}_m forms a trajectory is open and ends on the imaginary axis, at $2i\kappa$ (Fig. 5.2(c)). If the decomposition is comprised of an even number of LP symmetric domains N , then the addition of \mathcal{V}_m leads to a closed trajectory in the complex plane, starting and ending at the origin (Fig. 5.2(d)).

(iii) *non-PTR*. Here $T < 1$. The sequence of the added 'vectors' forms an open trajectory in the complex plane since they lead to a complex 'vector' $\mathcal{L} \neq 0, 2i\kappa$ (see Fig. 5.2(i)).

In general, if a completely LP set-up which possesses a PTR, can be decomposed e.g. in two parts, possessing an a -PTR and a s -PTR respectively, then in the complex plane there will coexist both, a closed trajectory corresponding to the part exhibiting the a -PTR and collinear vectors $\mathcal{V}_j = (-1)^j 2iJ$ on the imaginary axis, corresponding to the part with the s -PTR.

An alternative geometric interpretation of PTR states emerges when we add \mathcal{V}_m in the complex plane so that they form a closed polygon. In this sense, in the general case of a PTR, vectors \mathcal{V}_m form a closed polygon in the complex plane, with number of sides equal to the number of LP symmetric domains of the decomposition. For an even number N of LP symmetric domains, the polygon is formed by the N vectors \mathcal{V}_m . For

odd N the polygon needs also the vector $2iJ$ to close. Thus, always the polygon has an even number of sides. For any non-PTR scattering state, the sum \mathcal{L} which appears in Eq. (5.6), does not lead to a closed polygon, unless a vector depending on the values of the field $u(x)$ on the boundaries of the interaction region is added. Figure (5.3) illustrates a qualitative example of this alternative scattering state representation, based on the formation of polygons. The solid and dashed orange vectors form closed polygons, thus representing a -PTRs for even and odd number of LP symmetric units, respectively. The solid purple vector lying on the imaginary axis represents a set of collinear vectors $\mathcal{V}_m = 2iJ$, corresponding to an s -PTR and finally, the blue dashed vectors, to a non-PTR scattering state.

On the other hand, \mathcal{L} is a global quantity, which characterizes the device as a whole. Assuming asymptotic conditions given by Eqs. (5.20), (5.21) on either side of device (computed at $x = x_0$ and $x = x_N$, respectively) and substituting them in Eq. (5.6) we get:

$$\mathcal{L} = -\frac{2i\kappa r}{1+r} \quad ; \quad N \text{ even} \quad (5.32)$$

and

$$\mathcal{L} = \frac{2i\kappa}{1+r} \quad ; \quad N \text{ odd}, \quad (5.33)$$

for even and odd number of LP symmetric domains \mathcal{D}_m , respectively. In the case of a PTR ($r = 0$) \mathcal{L} vanishes for even N or, for odd N , becomes $\mathcal{L} = 2i\kappa$ which is its maximum value (for fixed κ). Also, the separation of the real and imaginary parts yield:

$$\mathcal{L} = \frac{2i\kappa r_I}{[u(x_0)]^2} - i \left[\frac{2\kappa r_R + 2\kappa R}{[u(x_0)]^2} \right] \quad ; \quad N : \text{ even} \quad (5.34)$$

and

$$\mathcal{L} = \frac{2i\kappa r_I}{[u(x_0)]^2} + i \left[\frac{2\kappa + 2\kappa R}{[u(x_0)]^2} \right] \quad ; \quad N : \text{ odd}, \quad (5.35)$$

which shows that the expressions for \mathcal{L} for a decomposition with even or odd number of LP symmetric domains, retain their real part and differ only with respect to the imaginary.

Equations (5.32), (5.33) allow to prove that the proposed classification is unambiguous in the sense that for a PTR state, there is no LP decomposition so that it appears as being a non-PTR. Conversely, a non-PTR cannot appear as a PTR, for any LP decomposition. This can be shown by considering that the incident and outgoing waves have the following plane wave form:

$$\mathcal{A}(x) = e^{i\kappa x} + r e^{-i\kappa x} \quad (5.36)$$

$$\mathcal{A}(x) = r e^{i\kappa x}, \quad (5.37)$$

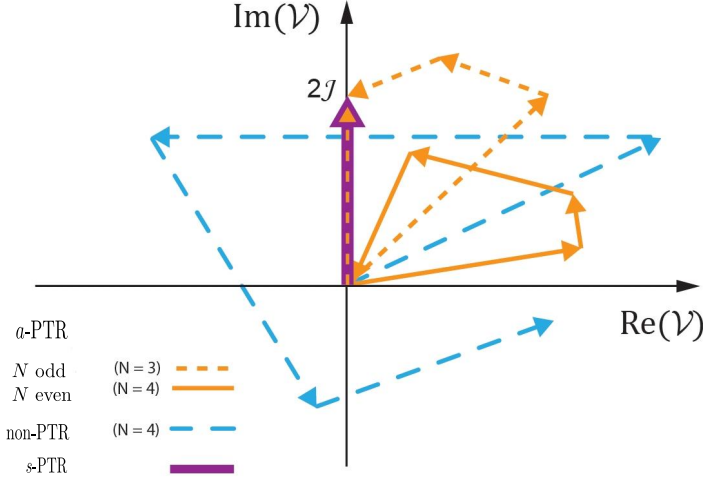


FIGURE 5.3: Geometric representation of any possible scattering state, expressed with respect to vectors \mathcal{V}_m . The closed polygons correspond to a -PTR states. The orange solid (dashed) curve represents a a -PTR state in a set-up comprised of an even (odd) number of LP symmetric units. The purple collinear, degenerate vectors $\mathcal{V}_m = 2iJ$ correspond to a s -PTR state and the blue dotted curve represents a non-PTR state.

where r and t are the reflection and transmission amplitudes, we get the following expressions for \mathcal{L} :

$$\mathcal{L}_{\text{even}} = -\frac{2i\kappa r}{1+r} \quad (5.38)$$

$$\mathcal{L}_{\text{odd}} = \frac{2i\kappa}{1+r} \quad (5.39)$$

depending on whether the setup can be decomposed is *even* or *odd* number of LP symmetric domains, respectively. Equation (5.38) clearly indicates that if $r = 0$ (PTR) then $\mathcal{L}_{\text{even}} = 0$ and inversely, if $\mathcal{L}_{\text{even}} = 0$ then $r = 0$. On the other hand, Eq. (5.39) when $r = 0$ becomes $\mathcal{L}_{\text{odd}} = 2i\kappa$. Inversely, if $\mathcal{L}_{\text{odd}} = 2i\kappa$, then:

$$2i\kappa = \frac{2i\kappa}{1+r} \Rightarrow 1+r = 1 \Rightarrow r = 0 \quad (5.40)$$

We will close this subsection with a detailed investigation of the case of two setups with one ($N = 1$) and two ($N = 2$) LP symmetric domains respectively, both in a a -PTR state. The first is trivial since the whole setup is globally symmetric. Equation (5.27)

yields that

$$\frac{|Q|^2}{u(x_{m-1}) u(x_m)} = 4J^2$$

and since $u(x_{m-1}) = u(x_m) = 1$ we obtain that $|Q| = 2J$. In the second case for domains $\mathcal{D}_1, \mathcal{D}_2$, Eq. (5.27) leads to $|Q_1| = |Q_2| > 2J$. According to Eq. (5.27), these two vectors are, apart of equal magnitude, also collinear with zero sum. For $N > 2$ the above mentioned closed trajectories (or polygons) begin to manifest in the complex plane, connecting each domain to the other in a more complicated, though well determined and transparent manner. The result for $N = 1$ can be generalized to hold for every resonator at an s -PTR. This is due to the fact that they behave in a completely independent manner. For instance, we could permute two or more resonators and still obtain the same result. Note, that in this case and for N resonators holds that $|Q_0| = |Q_1| = \dots = |Q_{N-1}| = 2J$, rendering the magnitude of the conserved, two-point current $|Q|$ equal to two times the probability current.

The equality in the magnitudes $|Q|$ of the invariant currents implies a higher degree of symmetry preservation in the case of an s -PTR. As it has been mentioned in Chapter 2, the symmetry breaking of a global, discrete symmetry leaves remnants in the form of the non-vanishing invariant current Q . In the case of an s -PTR, even though the global inversion symmetry is broken, the field magnitude retains its inversion symmetry on a local level. This is reflected to the equality between the $|Q|$ s of each LP symmetric sub-domain. On the other hand, in an a -PTR where no symmetry is reflected to $u(x)$, the respective $|Q|$ s are not equal. Therefore, we see that the invariant quantities Q reflect the extend to which a global symmetry is broken.

5.4 Transmission properties of an aperiodic set-up

Having described in detail the effect of different LP symmetry scales, we turn now to a specific aperiodic setup, in order to demonstrate how the aforementioned notions can be implemented and also how they can be utilized for the deeper comprehension of PTR properties. In Subsection 5.4.1 we use a photonic multilayer comprised of dielectric slabs with piecewise constant refraction index $n(x)$ and study thoroughly its transmission properties. It is commonly met in the literature to describe photonic multilayers by slabs with piecewise constant refractive indices as shown in Fig. 5.1. This allows the decomposition of this class of devices in a multitude of ways which, in turn, leads to the possible coexistence of multiple symmetry scales within the same set-up. In Subsection 5.4.2 we consider the quantum version of the above system and look into the behaviour of the global quantity \mathcal{L} .

Regardless of the inherent local symmetry and the feasible decomposition in multiple symmetry scales, aperiodic photonic (quantum) systems with piecewise constant

refraction index $n(x)$ (rectangular barriers $V(x)$) are also analytically tractable. The combination of these properties renders them an ideal choice for implementing the proposed concepts on the transmission properties of aperiodic systems. In larger systems, binary aperiodic order (in case of multilayers, of two kinds of slabs A and B) can be shown to feature local symmetries with arbitrarily large ranges and high density, and with remarkable symmetry axis distributions [102].

5.4.1 PTRs in an aperiodic photonic multilayer

Remaining to the 1-D case, we turn to the specific case of light wave scattering. Therefore, we drop the general notation used up to now, by introducing the following correspondences:

- $\mathcal{A}(x) \rightarrow E(x)$
- $\epsilon \rightarrow \omega$
- $\mathcal{W}(x) \rightarrow \frac{n(x)\omega}{c}$
- $\kappa \rightarrow k$

The electric component of a monochromatic plane light wave of frequency ω in 3-D obeys the equation [30]

$$\nabla \times \nabla \times \vec{E}(\vec{r}, t) = \left(\frac{\omega^2}{c^2} \right) n^2(\vec{r}) \vec{E}(\vec{r}, t), \quad (5.41)$$

where $n(\vec{r})$ is the refractive index which varies spatially.

We consider light propagation in an aperiodic medium which is inhomogeneous as a whole, nevertheless the dielectric materials which constitute it, are homogeneous in the yz -plane. The refractive index then, varies only in the x -direction, $n(\vec{r}) \rightarrow n(x)$. Further, we restrict the wave to normal incidence on the yz -plane, so that it propagates everywhere along the x -axis, which renders the problem effectively 1-D. The field can then be written as

$$\vec{E}(\vec{r}, t) = E(x)e^{-i\omega t} \hat{x},$$

where $E(x)$ the complex field amplitude. Such a system is illustrated in Fig. 5.4.

Considering only the stationary case, we drop the time-dependence term and Eq. (5.41) acquires the (Helmholtz) form

$$\hat{\Omega}(x, \omega)E(x) = \frac{\omega^2}{c^2}E(x) \quad (5.42)$$

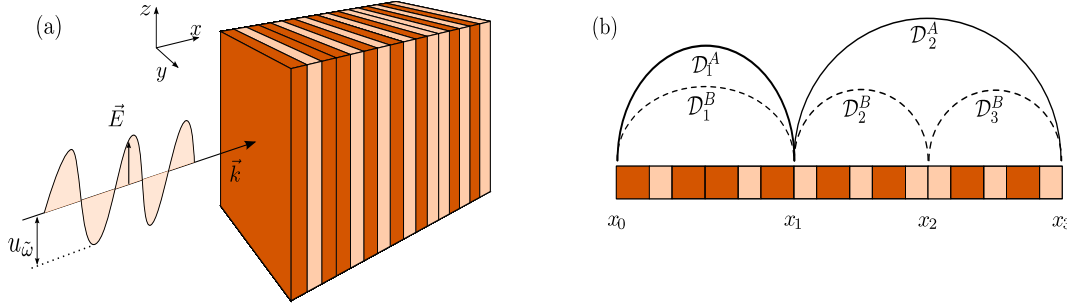


FIGURE 5.4: (a) Schematic of an aperiodic multilayer comprised of 16 planar slabs of materials A and B . The electric field amplitude E propagates only along the x -axis, rendering the medium effectively 1-D. (b) 1D representation of the multilayer with 2 different LP symmetric decompositions, depicted by the solid and dashed arcs.

where, however, the differential operator

$$\hat{\Omega}(x, \omega) = -\frac{d^2}{dx^2} + [1 - n^2(x)] \frac{\omega^2}{c^2}. \quad (5.43)$$

depends simultaneously on $n(x)$ and ω , which, as we shall see below, has significant consequences on the corresponding transmission profile.

We consider a photonic multilayered device comprised of two different materials A and B . The refraction indices and the widths of the (piecewise constant) slabs are n_A , d_A and n_B , d_B respectively, so that for the optical length nd the quarter-wave condition [30]):

$$n_A d_A = n_B d_B = \lambda_0/4 \quad (5.44)$$

is valid. The central wavelength λ_0 is a central wavelength, around of which the transmission spectrum is symmetric, when Eq. (5.44) holds [57, 131]. The corresponding values for the refraction indices are $n_A = 2.12$ and $n_B = 1.45$ while $\lambda_0 = 600 \text{ nm}$. In the Appendix Γ we explain why the quarter wave condition is often a choice in light transmission experiments [70, 99, 132, 133]. The set-up is shown in Fig. 5.4.

The total device is represented symbolically by

$$S_5 \rightarrow ABAABABABABBABAB.$$

This modified quasi-periodic dielectric array was first studied in Ref. [65] and is constructed by the juncture of the j -th generation of the Fibonacci sequence F_j , followed by the respective conjugate structure C_j . In the case of S_5 the emerging array has the form $ABAABABABABBABAB$, where $F_5 = ABAABABA$ and $C_5 = BABBABAB$. We

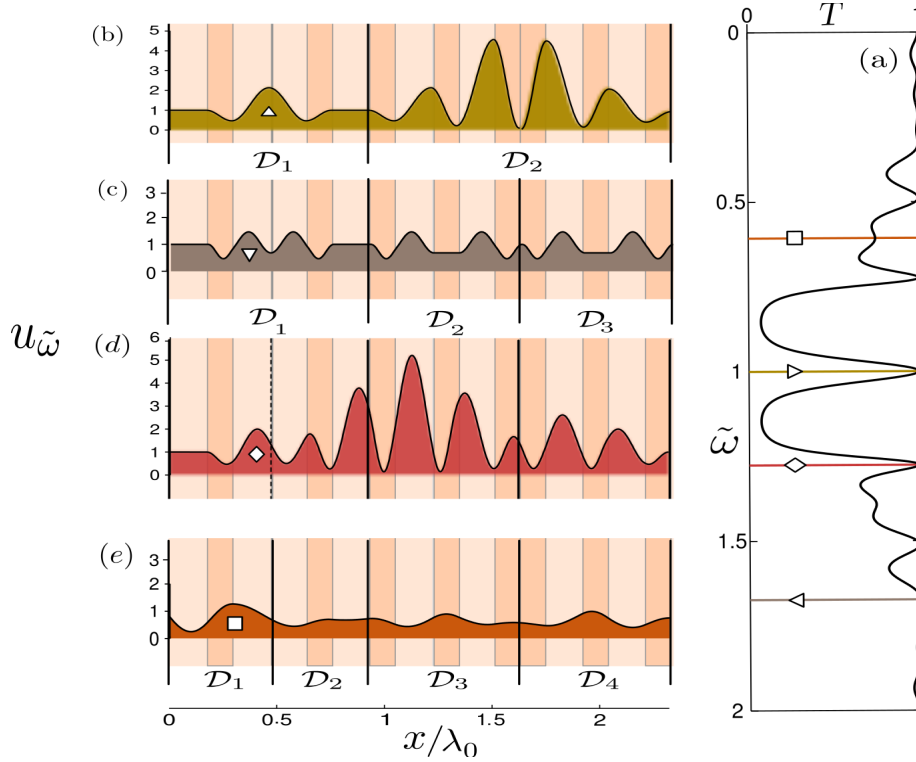


FIGURE 5.5: (a) Transmission coefficient T as function of $\tilde{\omega}$ for the photonic multilayer shown in Fig. 5.4, where slabs A and B have refractive indices $n_A = 2.12$ and $n_B = 1.45$. Field magnitude $u_{\tilde{\omega}}(x)$ across the multilayer at the frequencies marked in (a), corresponding to (b) a s -PTR at frequency $\tilde{\omega}_\Delta = 1$, (c) a s -PTR at frequency $\tilde{\omega}_\nabla = 1.673$ and (d) an a -PTR at $\tilde{\omega}_\diamond = 1.276$. Finally, at frequency $\tilde{\omega}_\square = 0.607$ a non-PTR state is shown. The background shows the corresponding slabs along the device, and the vertical lines depict the considered decomposition into LP symmetric subdomains of the device.

choose this set-up because, even though it doesn't have any global symmetry, it exhibits multiple resonances, covering both cases of our classification.

Figure 5.5(a) illustrates the transmission spectrum T of the device versus the incident light's frequency. Since the quarter wave condition is valid it is symmetric around the central frequency $\omega_0 = 2\pi c/n_0\lambda_0$. Notice that n_0 is the refractive index of the ambient medium which in this case coincides with n_A . Figures 5.5(b) and (c) show the wave field module $u(x)$ at two different frequencies ($\tilde{\omega}_\Delta = 1$ and $\tilde{\omega}_\nabla = 1.6732$) in which s -PTRs occur. It is obvious that $u(x)$ in these s -PTRs follows the symmetries

of the two corresponding (different) decompositions, in LP symmetric domains, namely $\mathcal{D}_1=ABAABA$, $\mathcal{D}_2=BABABBABAB$ in (b) and $\mathcal{D}_1=ABAABA$, $\mathcal{D}_2=BABAB$, $\mathcal{D}_3=BABAB$ in (c). With $\tilde{\omega}$ we denote the dimensionless frequency $\tilde{\omega} = \frac{\omega}{\omega_0}$. In both cases the s -PTR manifestation is due to the fact that the moduli $u_{\tilde{\omega}}(x)$ of the electric fields fulfil exactly the LP symmetry within the multilayer and follow the corresponding symmetries of the resonators which constitute the respective decompositions of the potential. Note also, that according to the LP decomposition which is satisfied by $u_{\tilde{\omega}}(x)$ one can enhance or detract localization strength $u_{\tilde{\omega}}(x)$ peaks in the device. This can be seen in the decomposition illustrated in Fig. 5.5 (b), where $u_{\tilde{\omega}}(x)$, in \mathcal{D}_2 , is about three times more enhanced than in the respective region in Fig. 5.5 (c). The same mechanism underlies the existence of the PTR at $\tilde{\omega} = 0.3268$ which is the mirror symmetric of $\tilde{\omega}_{\nabla}$ with respect to $\tilde{\omega}_{\Delta}$.

On the other hand Fig. 5.5 (d) illustrates an a -PTR, at $\tilde{\omega}_{\diamond} = 1.2761$. Obviously, here the module $u_{\tilde{\omega}}(x)$ of the electric field is not LP symmetric within any possible decomposition of the set-up. However, the selected set-up decomposition determines the way that this resonance will be represented in the complex plane according to the proposed classification scheme. Finally, for reasons of completeness, we show in Fig. 5.5 (e) a non-PTR state ($T < 1$), occurring at $\tilde{\omega}_{\square} = 0.607$. As it is expected no local symmetries are fulfilled by the corresponding $u_{\tilde{\omega}}(x)$ in the LP subdomains of the device.

Figures 5.6 (a), (b) refer to the same set-up, showing the behaviour of the magnitude of the invariant quantity Q and of the ‘vectors’ \mathcal{V}_m for each case. For the two s -PTRs at frequencies ω_{Δ} and ω_{∇} , $|Q|$ is constant in the whole spatial extent of the device, indicating the higher degree of the (retained) symmetry. Particularly each $|Q_m|$ corresponding to a resonator is equal to $2J$. Accordingly, the sum \mathcal{L} oscillates on the imaginary axis, becoming $\mathcal{L} = 0$ for the PTR at ω_{Δ} which follows a decomposition in two resonators and $\mathcal{L} = 2ik_{\Delta}$ for the second case where it follows a decomposition in three resonators.

Since for the third resonance (\diamond) the field has also no local symmetry the respective $|Q_m|$ s will vary within each different domain \mathcal{D}_m . Regarding the behaviour of the vectors \mathcal{V}_m , this resonance, can be represented in the complex plane according to the selected decomposition in LP symmetric domains. For instance, two possible decompositions in LP symmetric domains are: ABA, ABA, ABABA, ABABA, where the sum of \mathcal{V}_m form a trajectory ending at $2ik_{\diamond}$ and ABAABA, ABABA, ABABA where the sum of \mathcal{V}_m form a trajectory ending at the origin. The non-PTR state at frequency ω_{\square} has -as it was expected- non equal $|Q_m|$ s in any chosen decomposition and for the sum \mathcal{L} holds that $\mathcal{L} \neq 0, 2ik_{\square}$, shown by the coloured vector.

Apart from the s -PTRs at ω_{Δ} , at ω_{∇} and its mirror symmetric frequency, all other PTRs in the plotted spectrum are a -PTRs, following the classification rules that we have demonstrated. Note that, for the chosen parameters, the left half $ABAABABA$ of the setup does not feature PTRs, as shown in Ref. [65]. It does, however, possess local

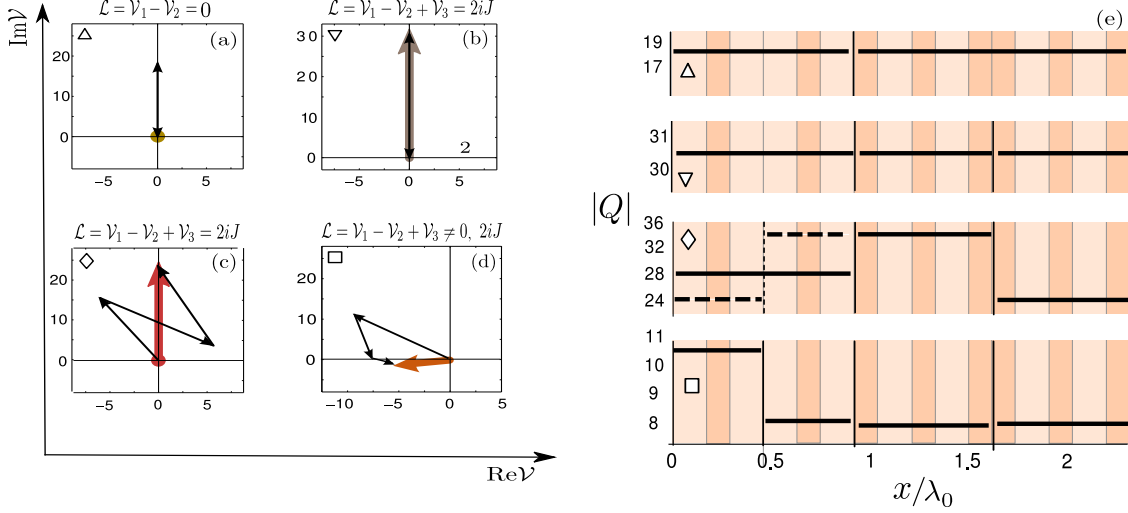


FIGURE 5.6: The alternating sum \mathcal{L} (thick colored arrows) of the \mathcal{V}_m for each considered decomposition in Fig. 5.5, represented as a trajectory (thin black arrows) in the complex plane. In (a) and (b) corresponds to s -PTRs for even and odd decompositions, respectively. (c) For the a -PTR an odd ($N = 3$) decomposition is considered. However, as shown from (e) an even ($N = 4$) decomposition (dashed lines) can be used also. This would end at the origin. (e) The module $|Q_m|$ corresponding to each subdomain D_m are plotted as thick solid or dashed lines.

symmetries, and a suitable tuning of the $d_{A,B}$ and $n_{A,B}$ would render it transparent at certain frequencies (in the form of a - or s -PTRs). However, there are then less available LP decompositions, so that the occurrence of *multiple* PTRs is relatively limited compared to the present multilayer. The significance of a large parameter space for the emergence of PTRs in multiple frequencies, will be discussed thoroughly in the next chapter.

Closing this analysis we stress that the representative set-up which we studied here illustrates in a direct way how the local symmetry analysis of both the device and the resonant field profiles, elucidate the underlying mechanisms for PTR occurrence.

5.4.2 PTRs in an aperiodic quantum system

We consider now the quantum mechanical version of the aforementioned setup, which consists of 16 adjacent rectangular barriers A , B with potential strength $V_A = 2.45$ and $V_B = 3.12$ and widths $d_A = 0.3$ and $d_B = 0.6$, respectively. Similarly to the photonic case, we identify the different symmetry scales and select two of them in order to study

the behaviour of the magnitude of \mathcal{L} , especially in relation to the transmission coefficient T . The suggested decompositions are

- $ABAABA \mid BABAB \mid BABAB$
- $ABAABA \mid BABABBABAB$

in order to have both even and odd number of LP symmetric domains.

Figure (5.7) illustrates transparently the close relation between $|\mathcal{L}|$ and the transmission coefficient T , which is indicated with the red line. Let us first consider the case of $N = 3$ resonators. From Eq. (5.33) we find the magnitude of \mathcal{L} is

$$|\mathcal{L}|^2 = \frac{4k^2}{1 + R + 2\text{Re}[r]}, \quad N : \text{ odd} \quad (5.45)$$

which is illustrated with the blue line. Obviously, it has an increasing trend, following the trend of the doubled wave-number of the incident particle, which is shown with the green curve. When a PTR occurs, $|\mathcal{L}| = 2k$ and consequently the two curves intersect, indicating the PTR value. However, it is ambiguous whether or not this is a PTR, since $|\mathcal{L}| = 2k$ also when $R = -2\text{Re}[R]$.

When the decomposition is comprised of an even number of LP symmetric domains, $|\mathcal{L}|$ acquires more interesting properties. As it is given by

$$|\mathcal{L}|^2 = \frac{4k^2 R}{1 + R + 2\text{Re}[r]}, \quad N : \text{ even}, \quad (5.46)$$

easily one ascertains that in the case of PTR, it becomes zero. Also, the existence of R in the numerator indicates the competition with the respective terms in the denominator and as a result, $|\mathcal{L}|$ in this case does not follow an increasing trend (see black curve in Fig. (5.7)). However, it follows a pattern, particularly consistent with the transmission spectrum. At every T maximum, $|\mathcal{L}|$ minimizes and vice-versa. Obviously, in the PTR case ($T = 1$), $|\mathcal{L}| = 0$. An interesting feature can be seen in the inset of Fig. (5.7). The transmission peak near $\epsilon \simeq 7.75$ seems to be perfectly transmitting. Nevertheless, a closer look to the inset reveals that the transmission is not perfect. This very small deviation from the perfect transmitting case, however is significantly magnified in the corresponding $|\mathcal{L}(\epsilon)|$ plot. Therefore, $|\mathcal{L}(\epsilon)|$ could possibly act as a ‘magnifying glass’ in situations where there is ambiguity on whether a state corresponds to a PTR or not.

Having studied a set-up with the same geometry, both in its photonic and in its quantum versions, we can stand to the striking differences between the two transmission spectra. As the parameter ω is varied, the transmission spectrum $T(\omega)$ has fundamental differences from the quantum counterpart, since it starts from $T = 1$, while in the quantum case it starts from $T = 0$. Moreover, in the quantum case as ϵ increases,

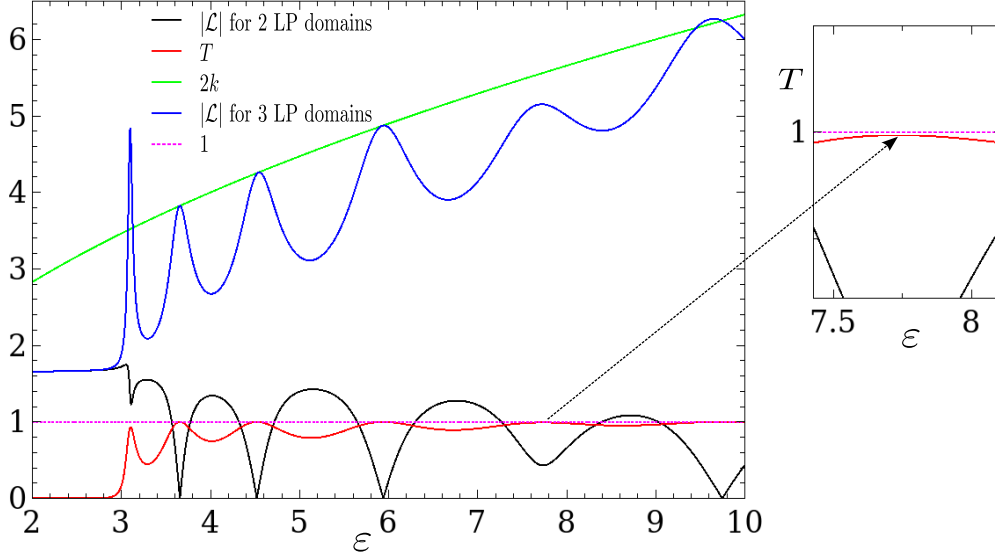


FIGURE 5.7: The blue curve shows $|\mathcal{L}(\epsilon)|$ for the decomposition ∇ shown in Fig 5.6 which is comprised of 3 LP symmetric domains. The green curve corresponds to $2k$ (k is the wave number of the incident particle) and the red curve to the transmission coefficient T . The black curve illustrates $|\mathcal{L}(\epsilon)|$ for the decomposition Δ which consists of an even number of LP symmetric domains ($N = 2$) in Fig 5.6. Note how a very small deviation from $T = 1$ (as shown in the inset), is magnified under the prism of $|\mathcal{L}(\epsilon)|$.

the transmission tends to unity, as the particle ‘feels’ the potential weakly. On the contrary this is not the case in the photonic counterpart since in the wave number k in Eq. (5.42), the refractive index $n(x)$ is multiplied by ω . This means that as ω increases, the ‘effective potential’ $n(x)$ becomes ‘stronger’. Therefore, classical light will always ‘feel’ the presence of the scatterer, whereas a quantum particle becomes gradually insensitive to it at higher energies ($T(\epsilon \rightarrow \infty) \rightarrow 1$).

5.5 Relation to alternative approaches

Having demonstrated how the concept of local symmetries enable the ‘geometric’ classification of resonant scattering for aperiodic and quasi-periodic devices, we will comment on its relation to other approaches which also consider PTRs. Several different theoretical approaches have been proposed in the literature and have significantly con-

tributed in the understanding regarding occurrence of PTRs in such systems [18, 134]. A particularly relevant approach is given by Zhukovsky in Ref. [14], where the PTRs of combined photonic multilayers are classified with respect to the transmissions of their parts to which they can be decomposed. Most of these works, however, focus more on the *conditions* for the occurrence of PTRs and less on the understanding of their *origin* from fundamental principles. The latter is captured here, on the level of the field magnitude, within the classification of PTRs on (local) symmetry grounds.

In a recent work, appeared in Ref. [14], using the Airy formulas [87, 88], showed that PTRs can be incorporated in two categories. In this approach, each mixed dielectric medium can be decomposed in two subdomains \mathcal{D}_1 and \mathcal{D}_2 , which are not necessarily LP symmetric, and possesses a PTR either when

$$T_1 = T_2 = 1 \quad (5.47)$$

or

$$T_1 = T_2 \neq 1 \quad ; \quad \phi_1 + \phi_2 = 2m\pi \quad (5.48)$$

where ϕ_1 and ϕ_2 are the phases of the reflection coefficients r_1 and r_2 , for the domains \mathcal{D}_1 and \mathcal{D}_2 respectively. The bar above 1 means that \mathcal{D}_1 is traversed in the opposite direction ($-x$) [14]. The former of these two cases indicates that substructures \mathcal{D}_1 , \mathcal{D}_2 behave individually, while in the latter case the PTR occurs when \mathcal{D}_1 , \mathcal{D}_2 are treated in an interwoven manner.

The conditions described in [14] that lead to a PTR, refer to general potential arrays where no symmetry considerations have been taken into account. Under this prism it provides a valid classification of PTRs. However, in the case of completely LP symmetric set-ups, this classification allows for an overlap between the two PTR categories, namely *a*-PTRs and *s*-PTRs, for $N > 2$ decomposition domains $\tilde{\mathcal{D}}_m$. Let us assume that a set-up w_A with reflectionless transmission at a frequency $\tilde{\omega}_r$, can be decomposed in two subdomains w_A^1 and w_A^2 according to the second kind of PTRs described in [14]. Then we consider a different set-up w_B with the same properties, also resonant at $\tilde{\omega}_r$. A total potential $w_A w_B$ can then be considered to belong to both PTR categories, according to the selected decomposition. That is, if decomposed in w_A and w_B then it belongs to the first kind ($T_{w_A} = T_{w_B} = 1$) but if decomposed in w_A^1 , w_A^2 , w_B^1 , w_B^2 , it belongs to the second kind. The approach proposed in this paper avoids this overlapping since it treats PTRs exclusively with respect to the symmetry properties of the corresponding potential and the electric field's magnitude $u_{\tilde{\omega}}(x)$ ⁴. In other words, for $N > 2$ decomposition domains $\tilde{\mathcal{D}}_m$ (not necessarily reflection symmetric) there is no one-to-one mapping between the conditions in Eqs. (5.47), (5.48) and the *s*- and *a*-PTRs.

⁴The second PTR category in the classification proposed in [14] is valid for PTRs in setups which cannot be decomposed in domains which transmit resonantly ($T = 1$)

CHAPTER 6

PERFECT TRANSMISSION CONTROL: A LOCAL PARITY APPROACH

6.1 Introduction

This chapter focuses on the power of LP symmetry, as a tool to manipulate certain transmission features of a scattering system. As it was discussed in the previous chapter, the identification of the LP symmetry scales of a device possesses a significant role both on the emergence of PTRs and on their kind. Here, we develop a *construction principle* which takes advantage of the simultaneous LP symmetries at different scales and show how they can be utilized to design aperiodic set-ups with PTRs at prescribed energies. The proposed method is applicable to a wide class of 1-D systems, involving quantum aperiodic potential arrays, photonic multilayers and acoustic media. Here, we will consider the analytically tractable case of set-ups comprised of piecewise constant building blocks and δ -function barriers. However, there are possibilities for applications in a wider range of barrier forms if the corresponding transfer matrices can be obtained.

6.2 Quantum, optical and acoustic engineering

As the technological progress dictates the transition to tiny electronic devices, rapidly moving from the micro to the nano scale, the quantum phenomena can no longer be neglected. In turn, the peculiarity of the quantum world leads to devices with extraordinary properties and applications which were unattainable within the regime of classical physics. Thereby, new theoretical ideas and adequate experimental techniques are required to exploit the potential of quantum effects. The quantum control [135] and quantum engineering [136] have turned into a broad field of study, mainly exploiting solid state structures which can stay coherent in a controlled manner [137] and consequently fabricating devices with very specialized properties. A controllable han-

dling of quantum effects in such devices would have significant impact i.e. on quantum information processing [138], nano-electronics [139] and nano-photonics [140].

The concept of LP allows to make a step towards the design of aperiodic quantum devices with prescribed PTR properties [66, 67]. As a matter of fact, its applicability is much wider -extending from the quantum to the classical regime- since it can be used for the design of optical media in the length scale of nano-meters and even for macroscopic acoustic wave tubes with length scales in the order of meters [141, 142].

Let us now briefly outline which transmission properties of piecewise constant potentials are known. The single rectangular barrier (when we refer to a rectangular barrier $V(x)$ we also include the case of a single slab with constant refraction index) has PTRs for certain energies, totally determined by its width and strength. Also no PTR occurs for classically forbidden energies ($E < V(x)$). A double barrier on the other hand, allows for resonant tunnelling, giving rise to PTRs both for $E > V(x)$ and in the classically forbidden region $E < V(x)$. The tunnelling induced PTR usually is isolated and occurs in relatively low energies compared to the transmission spectrum background where $T \rightarrow 1$. Isolated resonances are narrower, signifying a large life time. An array of N equidistant, identical barriers lead to $N - 1$ closely positioned PTRs followed by a region of low transmission and so on. As the number of N increases, the number of PTRs also increases and becomes denser, constituting precursors of the band structure of the fully periodic case. Finally, multiple different barriers, aperiodically placed, will exhibit resonant structure, however in the majority of cases they will not be perfectly transmitting.

The aforementioned structures possess filtering capabilities, offering the possibility to create devices which transmit resonantly in certain energies. However, a single rectangular barrier would do so only in a certain energy, which would be near the background where $T(E)$ fluctuates around 1. A locally periodic structure, on the other hand, would possess more PTRs, although once we would determine -based on the characteristics of the unit cell- the desirable energy of one PTR, the rest would be pre-determined, according to the Kronig-Penney equation (see Eq. (1.28)).

The question posed here is, whether and how could we design devices exhibiting PTRs in more than one desirable energies. The key concept to this, as we shall see in next subsections, is the aperiodicity of the set-up, accompanied by complete LP symmetry in multiple scales.

6.3 Local parity based design of PTR states

6.3.1 s -PTR construction principle

Here we will explain in detail, how several LP symmetric decompositions of a set-up can be exploited for the occurrence of multiple PTRs at pre-selected frequencies. This

‘construction principle’ was introduced in Ref. [66,67] and can lead to s -PTRs. We consider a completely LP symmetric set-up comprised of N_S parity symmetric scatterers. The scatterer is assumed to be the smallest and not decomposable part of the device, for example a rectangular barrier or dielectric slab. The total unimodular transfer matrix (TM) which connects the wave fields $\mathcal{A}(x)$ on either side of the multilayer is given by the product:

$$M = \begin{pmatrix} w & z \\ z^* & w^* \end{pmatrix} = \prod_{m=1}^{N_S} M_m(k; \mathcal{W}_m, d_m) \quad (6.1)$$

where $M_m(k; \mathcal{W}_m, d_m)$ is the single-scatterer unimodular TM, corresponding to the m -th scatterer, characterized by a generalized potential \mathcal{W}_m and width d_m . Let’s now assume that there exist N_D different decompositions in LP symmetric units and the constituent units of each decomposition cover the entire set-up. In the i -th decomposition, the N_S scatterers are grouped into $N_{\mathcal{R}}^{(i)} \leq N_S$ LP symmetric units -which we will refer to as *resonators*- and the l -th LP symmetric unit (which is comprised of $N_{\mathcal{P}}$ scatterers) of this decomposition has the corresponding TM

$$M = \begin{pmatrix} w_l & z_l \\ z_l^* & w_l^* \end{pmatrix} = \prod_{m=1}^{N_{\mathcal{P}}} M_m(k; \mathcal{W}_m, d_m) \quad (6.2)$$

This LP symmetric unit will transmit with $T_l = 1$ if the matrix element $z_l^* = 0$. Thus, in order to construct a set-up with a pre-selected PTR frequency, one has to solve the equation system emerging from the demand that all the matrix elements z^* which correspond to every LP symmetric unit (resonator) of the i -th decomposition, are zero. To do so, the desired frequency ω_r is fixed, along with other parameters depending on the extent of the parameter space. Finally, we leave as unknowns as many parameters as the number of the $z^* = 0$ equations. The solution of this system provides us with the parameters of a set-up, that is potential strengths \mathcal{W}_l and widths d_l , which will be transparent at (generalized) energy ϵ_r . It is therefore shown how the desired PTR can in principle be constructed with the aid of the derived one-to-one correspondence to LP symmetry.

However, a single PTR can be easily achieved with much simpler set-ups. The significance of this approach is revealed when it comes to the construction of devices possessing multiple PTRs at desired frequencies. Then a complex geometry is necessary to take advantage of the possible multiple LP symmetry decompositions.

Let us now consider two of the N_D possible decompositions i.e. the l -th and j -th, which consist of N_l and N_j resonators, respectively. We can then obtain two different PTR energies ϵ_{r_1} and ϵ_{r_2} by asking the l -th and j -th decompositions to be transparent

in ϵ_{r_1} and ϵ_{r_2} respectively. This can be done by the simultaneous solution of:

$$\begin{aligned} z_l^{(1)}(\epsilon_{r_1}) = 0, z_l^{(2)}(\epsilon_{r_1}) = 0, \dots, z_l^{(N_l)}(\epsilon_{r_1}) = 0 \\ z_j^{(1)}(\epsilon_{r_2}) = 0, z_j^{(2)}(\epsilon_{r_2}) = 0, \dots, z_j^{(N_j)}(\epsilon_{r_2}) = 0 \end{aligned} \quad (6.3)$$

Consequently, we fix the desired frequency values as well as all the other parameters leaving $N_l + N_j$ unknowns to be determined from the system solution. This solution, if it exists, will provide a set-up with the proper parameters to transmit with $T = 1$ at ϵ_{r_1} and ϵ_{r_2} . The existence of more decompositions in LP symmetric units would allow the occurrence of more PTRs in selected energies. Nevertheless, as the number of desired PTRs increase, the set-ups have to become more complex, with increasing parametric space, so that there are enough unknowns to be determined from the solution of the system. Such calculations, however, may be rendered cumbersome.

The key concept in the above procedure lies in the fact that the LP symmetry - by considering only space domains where the potential is LP symmetric - causes a significant reduction to the space of the possible decompositions which are suitable for allowing a s -PTR. Without taking into consideration the possible LP symmetric decompositions, the parametric space where one should look for appropriate combinations of parameters (e.g potential strengths and widths), so that the emerging equations would support PTRs, would be double. Those are now restricted by considering only locally symmetric decompositions, relying on the one-to-one correspondence between s -PTRs and LP symmetry.

6.3.2 a -PTR construction principle

The implementation of conditions shown in Eqs. (5.47), (5.48) proposed in [14] allows also for the construction of a -PTRs. To this aim one has to construct two sub-devices, which don't need to be LP symmetric, however, when treated separately, their transmission spectra should exhibit a common value for some energy. Then, using their combination and altering their distance so to fulfil condition of Eq. (5.48), we can achieve an a -PTR at the selected energy. However, it is not straightforward whether it is feasible to construct more than one a -PTRs in desired energies in a systematic manner.

In any case, the combination of above proposed techniques can lead to device with very specialized PTR properties. Also the increased complexity of such set-ups, give rise to transmission spectra with modifiable gap and band precursors, though in a rough manner.

6.4 *s*-PTR construction in quantum mechanical systems

Let us now discuss some examples which illustrate the above concepts and their implementation more explicitly, in the case of quantum mechanical scattering in 1-D from an aperiodic barrier array consisted of rectangular barriers.

Before proceeding to particular examples it is useful to refer briefly to a classification of resonators in quantum mechanical set-ups, according to the PTRs that they can support:

- a single (rectangular) barrier, supporting above-barrier resonances (ABRs)
- a homogeneous array of identical equidistant barriers, supporting tunneling resonances and ABRs
- an inhomogeneous barrier array, supporting isolated PTRs for appropriate combinations of barrier strengths and widths [126]. Such PTRs can be either tunnelling or ABRs.

Note also that the magnitude of the field $u_\epsilon(x)$ (the index ϵ denotes the incident energy of the quantum particle) of a PTR state for a specific decomposition may be LP symmetric within smaller sub-domains than those depicted in the specific decomposition. If the system resonates within such smaller constituents (scatterers or gaps) covering the LP symmetric domain, we refer to the state as *reducible* within this domain. If, on the other hand, $u_\epsilon(x)$ follows exactly the symmetry of the domain, without resonating into smaller constituents (of the domain), then we refer to it as *irreducible*. For *s*-PTRs, the resonating LP symmetric units can be interchanged without affecting the perfect transmission. In this sense also resonators are independent constituents of the scatterer array at PTRs [143].

Figure 6.1 shows the occurrence of a zero-current state and an irreducible PTR in an asymmetric double-barrier set-up. Such a system can be regarded as the simplest case breaking explicitly the global parity of the potential. The transmissions spectrum $T(\tilde{\epsilon})$ displays a multi-ABR structure, but only the peak zoomed in the inset is an actual *s*-PTR state. The ZCS appears at $\tilde{\epsilon}_{ZCS} = 8.7$ and the *s*-PTR at $\tilde{\epsilon}_{PTR} = 4.6$, where $\tilde{\epsilon}$ is a dimensionless energy. We remind the reader that the ZCS occurs under SAC whether the PTR under AAC.

Figure 6.2 demonstrates an aperiodic set-up of $N_{\mathcal{R}} = 2$ resonators, although now the resonators have a more complex structure. This complexity, supported by the fact that the resonator \mathcal{R}_2 allows resonant tunnelling, lead to two close PTRs at low energies, well below the background energies where the $T(\tilde{\epsilon})$ oscillates around one. Regarding the reducibility of the probability density, $u_\Delta(x)$ at $\tilde{\epsilon}_\Delta = 7.46$ is irreducible in both \mathcal{R}_1 and \mathcal{R}_2 , while $u_\nabla(x)$ at $\tilde{\epsilon}_1 = 7$ is irreducible in \mathcal{R}_1 but reducible in \mathcal{R}_2 . This is shown by the vertical dotted lines. The flat parts of $u_{\tilde{\epsilon}_1}$ in the last resonator indicates only

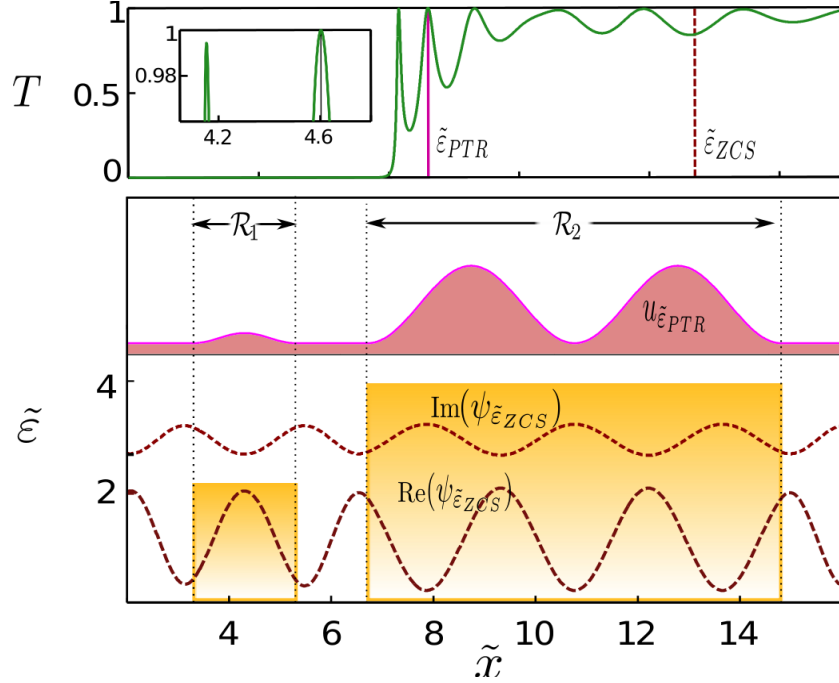


FIGURE 6.4: Transmission spectrum of an LP-symmetric set-up consisted of two rectangular barriers. The real and imaginary parts of $\psi_{\tilde{\varepsilon}}(x)$ are shown for a zero-current state at $\tilde{\varepsilon}_{ZCS} = 8.7$ and the module $u_{\tilde{\varepsilon}}(x)$ for a s -PTR at $\tilde{\varepsilon}_{PTR} = 4.6$.

forward (reflectionless) propagating wave. This is an example of LP being fulfilled at two different scales in the same system, as it is clearly shown by the probability distribution in resonator \mathcal{R}_2 . This s -PTR occurs under AAC and illustrates explicitly that the LP symmetry followed by the wave function amplitude at s -PTRs can be regarded as a remnant of the symmetry which breaks with AAC. The occurrence of the PTR at $\tilde{\varepsilon}_{\Delta}$ requires that the positioning of scattering units in \mathcal{R}_2 supports LP symmetry at a new spatial scale, in accordance with the general construction principle described above. A different positioning, where the LP symmetry would not be fulfilled in the spatial extent of \mathcal{R}_2 would support the PTR at $\tilde{\varepsilon}_{\nabla}$ (provided that the three equidistant barriers would remain unaffected), however the PTR at $\tilde{\varepsilon}_{\Delta}$ would cease to exist due to the vanishing of the second LP symmetry scale. We also point out that the setup remains resonant for arbitrary combinations of \mathcal{R}_1 and \mathcal{R}_2 , with repeated corresponding patterns in $u_{\tilde{\varepsilon}_{\Delta}, \nabla}$.

In Fig. 6.3 we show the manifestation of a ZCS at energy $\tilde{\varepsilon} = 7.354$, for a wave which propagates in a set-up of five LP symmetric domains. However, if the symmetry is broken by the asymptotic conditions and turn to AAC, this state exhibits a transmission

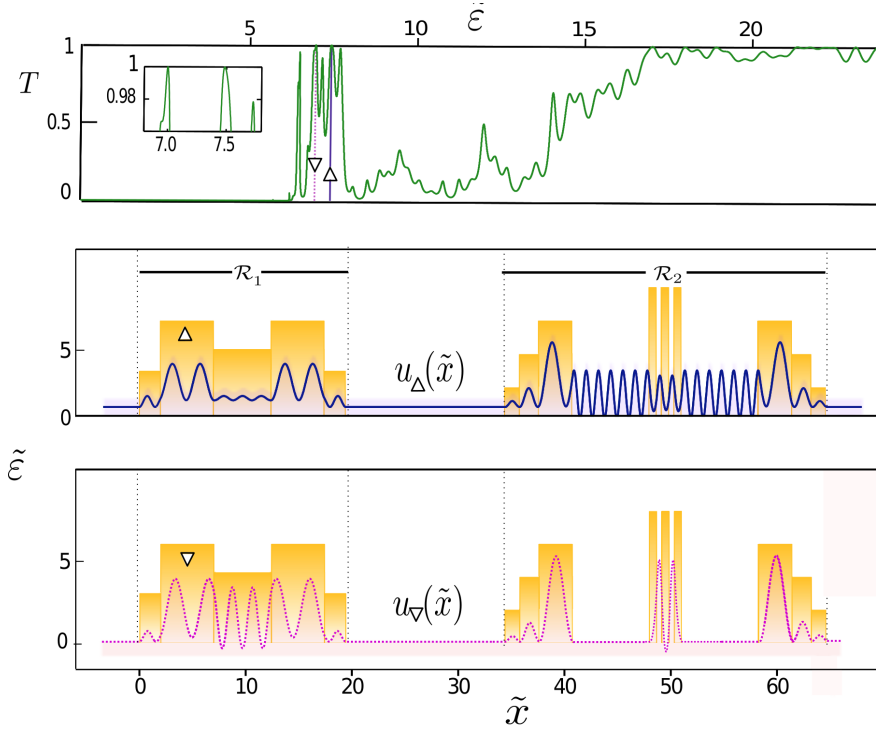


FIGURE 6.2: Set-up comprised of two resonators \mathcal{R}_1 and \mathcal{R}_2 . The transmission spectrum exhibits two isolated, tunneling *s*-PTRs at $\tilde{\epsilon}_1 = 7$ and $\tilde{\epsilon}_2 = 7.46$. The respective probability densities illustrate transparently the two different symmetry scales due to which the two *s*-PTRs are constructed.

value slightly lower than one. This small reflection, as seen in the figure, comes from the \mathcal{R}_1 . Its removal turns the state into a *s*-PTR. As can be seen, the corresponding wave field module is irreducible, and more localized within \mathcal{R}_4 . Notice that this PTR is independent of the width of the central barrier in \mathcal{R}_5 , within which the wave propagates only forwardly with constant magnitude $u_{\tilde{\epsilon}}(x) > 1$. Such a property could be utilized for the flexible design of efficiently transmitting non-symmetric devices.

Finally, in Fig. 6.4 we investigate the role of defects in a finite periodic array, under the prism of the possible LP symmetries. In this case the defects are two (rectangular) barriers with deviating strength and width compared to the rest of the array. Without the defects, the transmission properties of the locally periodic array are determined by its unit cell [24] and the transmission spectrum would exhibit $N - 1 = 11$ PTR peaks in the precursor of each energy band. The presence of aperiodicity [144] distorts these

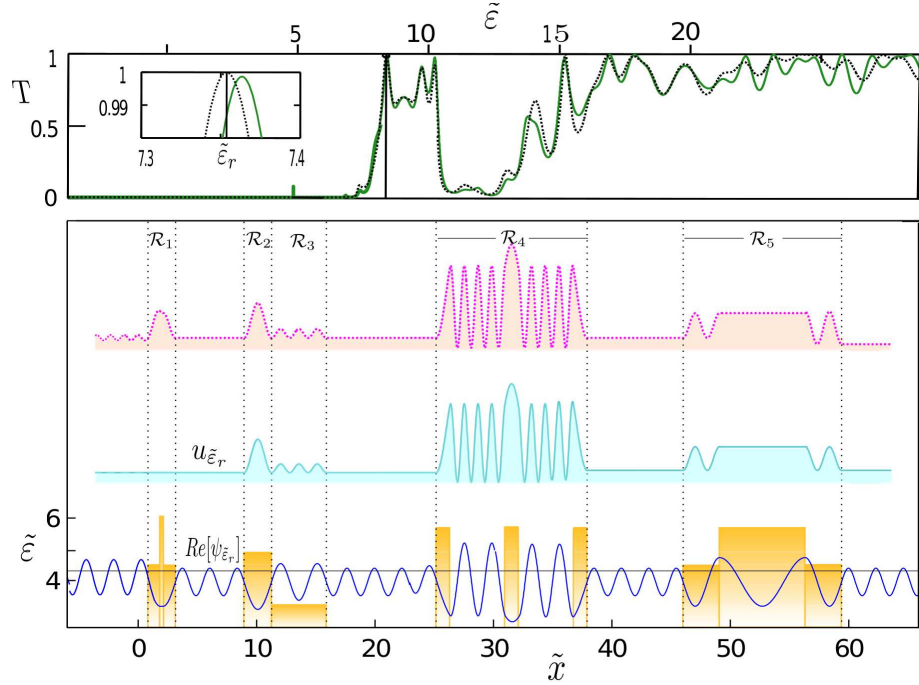


FIGURE 6.3: Rectangular barrier array decomposed into $N_{\mathcal{R}} = 5$ LP symmetric domains. Under SAC, in the energy $\tilde{\varepsilon} = 7.354$, a zero-current state appears. The removal \mathcal{R}_1 and the imposition of AAC renders the state a s -PTR at the same energy. The probability density of the latter is illustrated with the dashed line.

precursors [22, 145] and in principle the resonance peaks at the transmission spectrum are below unity, due to the induced asymmetry [19]. Nevertheless, the identification of the possible LP symmetry scales and subsequently the decomposition into suitable LP symmetric domains, not only reveals the possibility of multiple s -PTRs, but also allows for their manifestation in prescribed energies. In the particular example we identify two different symmetry scales. The implementation of the construction principle yields two s -PTR: one ABR at $\tilde{\varepsilon} = 8.47$ and one tunnelling resonance at $\tilde{\varepsilon} = 5$.

6.4.1 s -PTR construction in aperiodic photonic multilayers

Having considered several quantum mechanical examples of aperiodic, effectively 1-D systems, we turn now to their photonic counterparts, to verify whether and in what way the construction principle can be implemented for classical light waves. Here, we will focus on how parametric tuning can enable the construction of s -PTRs in a photonic

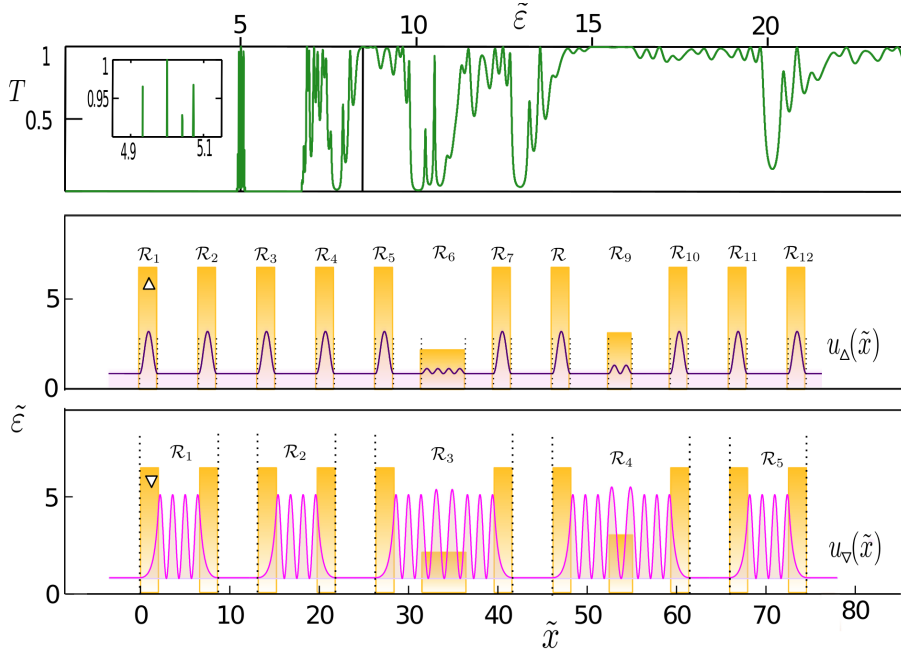


FIGURE 6.4: Finite periodic array of $N_S = 12$ rectangular barriers with two defects. The role of defects have two of the barriers which deviate from the rest with respect to their width and strength. The array is decomposed into $N_{\mathcal{R}}^{(1)} = 5$ and $N_{\mathcal{R}}^{(2)} = 12$ resonators, depicted by the vertical dotted lines in the u_{ε} profiles.

multilayer at *prescribed* frequencies ω , making use of its local symmetries. We choose the setup $BABABC_1BABABABAC_2ABA$ shown in Fig. 6.5, which is a slight geometrical modification of a multilayer studied in Ref. [14], where two dielectric slabs C_1 and C_2 of different widths d_{C_1} and d_{C_2} have been inserted. Without the inserted slabs, this structure features a single PTR over a wide frequency range [14], and we will now demonstrate the occurrence of two PTRs in the modified setup. Essentially, the local symmetries of the device are exploited to reduce the space of available parameters. In the present case the parameters corresponding to the dielectric slabs A and B are $n_A = 2.15$, $\tilde{d}_A = 0.08426$ and $n_B = 1.43$, $\tilde{d}_B = 1.01348$ respectively, where \tilde{d} is a dimensionless length $\tilde{d} = d/\lambda_0$ and $\lambda_0 = 700$ nm is the central wavelength chosen, around which the transmission spectrum is contracted. The slab parameters $n_{A,B}$, $\tilde{d}_{A,B}$ are determined from a set of coupled transfer matrix equations for different LP decompositions, as described above in the construction principle. On the other hand, the parameter space

must initially be sufficiently large in order to achieve the formation of s -PTRs at desired frequencies. This is ensured here by the inclusion of the slabs $C_{1,2}$, which increase the parameter space to the required extent. In our case, $C_{1,2}$ are vacuum gaps with $n_{C_1} = n_{C_2} = 1$. Also, here the ambient medium is the vacuum. We stress here that without referring to the decomposition of the device into locally symmetric sub-domains, there is no obvious way to control the frequencies where light s -PTRs would occur, exactly as in the quantum mechanical case. Therefore, we identify the following two decompositions, consisting of two

$$(BABABC_1BABAB \mid ABAC_2ABA)$$

and four

$$(BABAB \mid C_1 \mid BABAB \mid ABA \mid C_2 \mid ABA)$$

LP symmetric domains, respectively. We will refer to these domains as ‘resonators’, since each one in the respective decomposition transmits resonantly with $T = 1$. The two decompositions are distinguished by denoting the first with the symbol (Δ) and the second with (∇), while the vertical line \mid is used as a guide to the eye to separate the corresponding resonators. In the former decomposition the $C_{1,2}$ constitute parts of the resonators, while in the latter they intervene between the four resonators. All these are clearly demonstrated in Fig. 6.5, where the different colours in the background correspond to the different slabs used.

Figure 6.5(a) illustrates the transmission spectrum of the set-up. The two s -PTRs at the pre-selected frequencies are marked with Δ and ∇ . Note that although there are a multitude of resonant frequencies, only the aforementioned have exactly $T = 1$, within the plotted frequency. Also, the spectrum is no longer symmetric around ω_0 as in Fig. 5.5(a), since the quarter-wave condition used previously, is now relaxed. We remind that the quarter-wave condition dictates that $n_A d_A = n_B d_B = \frac{\lambda_0}{4}$, which does not hold here.

Here we will describe in detail the implementation of the *construction principle* in this particular example. As indicated in Fig. 6.5, we choose two, among all possible decompositions. The first is comprised of two LP symmetric units, namely, \mathcal{D}_1 and \mathcal{D}_2 . Accordingly, the LP symmetric units which constitute the second decomposition are \mathcal{D}_1 , \mathcal{D}_2 , \mathcal{D}_3 and \mathcal{D}_4 , along with the two intervening gaps $C_{1,2}$. Note that in this case the ambient medium gaps are not parts of the LP symmetric units which will act as resonators. According to the above described procedure, firstly we compute the TM of each LP symmetric unit in both decompositions. Thus, we have six transfer matrices and consequently, a system of six algebraic equations emerging from the demand that $z^* = 0$ for each TM. The ten parameters which determine the set-up are the refraction indices n_{A,B,C_1,C_2} , the corresponding widths d_{A,B,C_1,C_2} and the desired frequencies $\tilde{\omega}_\nabla$, $\tilde{\omega}_\Delta$. By fixing the values $\tilde{\omega}_\nabla = 1.38$, $\tilde{\omega}_\Delta = 0.67$ and $n_{C_{1,2}} = 1$ we are left with six unknown

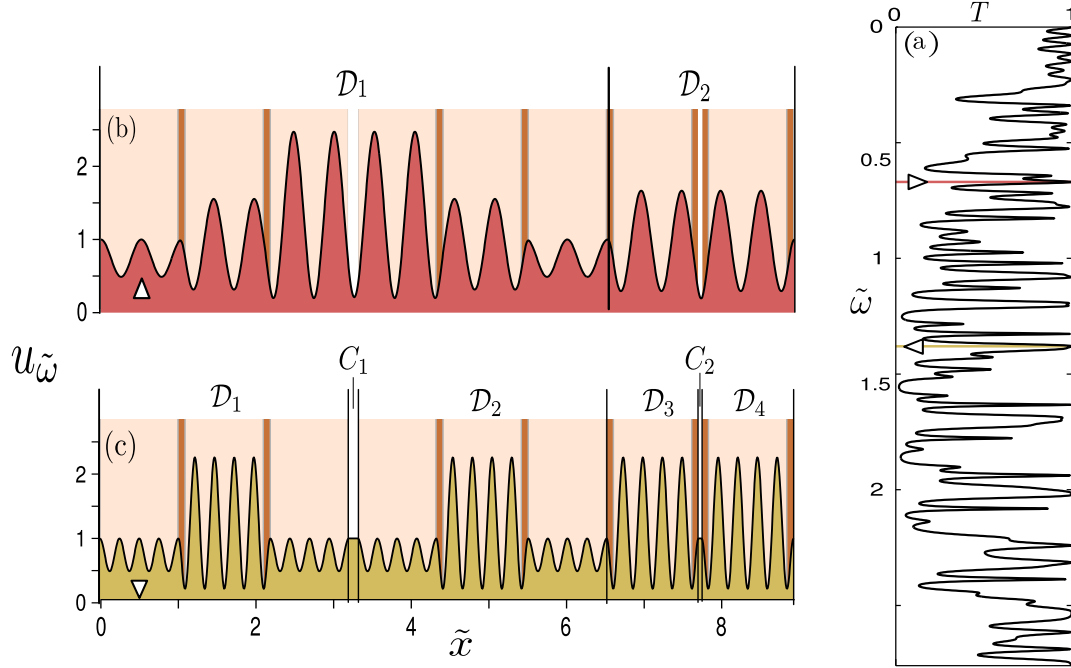


FIGURE 6.5: (a) Transmission spectrum of a photonic multilayer consisting of two different kinds of slabs A with $n_A = 2.15$, $\tilde{d}_A = 0.08426$ and B with $n_B = 1.43$, $\tilde{d}_B = 1.01348$. Within the device there are also two gaps C_1 and C_2 of the ambient medium, which in this case is vacuum ($n_{C_1} = n_{C_2} = 1$). The corresponding widths are $\tilde{d}_{C_1} = 0.1146 \lambda_0$ and $\tilde{d}_{C_2} = 0.04236$. (b) Field magnitudes at the *s*-PTR frequencies $\tilde{\omega}_\Delta = 0.67$ and $\tilde{\omega}_\nabla = 1.38$ marked in (a). The background shows the media A , B and C along the device, and vertical lines are used to depict the respective LP decompositions into resonators.

values, namely n_A , n_B , \tilde{d}_A , \tilde{d}_B , \tilde{d}_{C_1} and \tilde{d}_{C_2} , which are determined from the solution of the system. We emphasize here on the fact that if the ambient medium gaps were not induced in the set-up and the exact same geometry, as in Ref. [14] was retained, then exactly six parameters (n_A , n_B , \tilde{d}_A , \tilde{d}_B , $\tilde{\omega}_\nabla$, $\tilde{\omega}_\Delta$) would have to be determined from six equations. Thus, the solution, if it existed, would be unique and neither we would have the freedom to choose the two PTR frequencies nor we could tune some extra parameter(s) in order to achieve valid values for the materials, i.e. refraction indices. Note also, that the choice of the intervening slabs C_1 , C_2 was based on the minimal intervention on the set-up used in Ref. [14]. One could use more layers with different refraction indices, to broaden the parameter space and obtain more PTR choices.

Thus, according to the way they were constructed both resonances are of s -PTR type. As it is suggested by Fig. 6.5(b), the field $u_{\tilde{\omega}}$ profiles follow the local symmetries of the device, according to the indicated resonator decompositions. The fact that the second PTR (∇) is independent of the width $\tilde{d}_{C_{1,2}}$ of the gaps becomes evident from the corresponding plateaus of the field ($u_{\tilde{\omega}}(x) = 1$ along the gaps in Fig. 6.5(b). This indicates, reflectionless (only in forward direction), wave propagation within the gaps. In this sense, if we set $\tilde{d}_{C_1} = \tilde{d}_{C_2} = 0$, this PTR (∇) would survive and would be the equivalent to the single PTR, as found in Ref. [14]. However, the PTR at $\tilde{\omega}_{\Delta}$ would disappear. We see here that, by inserting a third type of slab in the multilayer, the local symmetries of the device can be exploited to design a new s -PTR, which would not be possible without the modification. Further, the new resonant field at $\tilde{\omega}_{\Delta}$ is localized on a *different spatial scale*, as seen in Fig. 6.5(b), from the fields' moduli within the respective \mathcal{D}_1 at $\tilde{\omega}_{\Delta}$ and $\tilde{\omega}_{\nabla}$. Additionally, since the PTR at $\tilde{\omega}_{\nabla}$ is invariant with respect to the gap widths $\tilde{d}_{C_{1,2}}$, the LP construction principle can be utilized for the flexible spatial design of resonantly transparent multilayer devices.

6.4.2 PTR construction in aperiodic acoustic waveguides

Finally we will employ the LP concept to manipulate the transmission properties of classical waves in macroscopic acoustic waveguides. This implementation is of special interest, since the proposed construction principle is going to be utilized as the theoretical framework for the design of experimental set-ups with prescribed acoustic wave transmission properties. The experiments are conducted by a collaborating research group in *LAUM (Laboratoire d'Acoustique de l'Université du Maine), Le Mans, France*. Thereby, being significantly confined by the experimental constraints, we try to theoretically design a waveguide, with optimized PTR properties. The optimization lies on the emergence s - and a -PTRs at desired frequencies and on the other hand on their maintenance during the experiment. For instance, a very narrow PTR peak in low frequencies, is highly possible to be significantly lowered or even disappear during the experimental measurement.

The main factor which hinders the coincidence between the experimental and the theoretically anticipated results are the losses. Losses can occur either due to frictional phenomena or due to escape of radiation. In this case, obviously we can't expect perfect transmitting resonances to be maintained. Nevertheless, a part of the optimization process would be the determination of the circumstances, under which losses can be minimized. As we shall see in the following, this control can be partly achieved by varying the geometrical parameters of the set-up, such as the total length or the diameter of the tube.

A worth-mentioning aspect is the existence of invariant quantities even in systems with losses. This was theoretically proven in Chapter 2, where it was shown from the

equations:

$$\begin{aligned}\frac{d}{dx}(q_1 - q_4) &= 0 \Rightarrow \\ q_1 - q_4 &= \text{const}\end{aligned}\quad (6.4)$$

and

$$\begin{aligned}\frac{d}{dx}(q_2 + q_3) &= 0 \Rightarrow \\ q_2 + q_3 &= \text{const},\end{aligned}\quad (6.5)$$

that $q_1 - q_4$ and $q_2 + q_3$ remain spatially invariant. This result is expected to be verified by the experiments.

The experimental apparatus consists of a cylindrical waveguide where the wave propagation occurs. On the top of the tube there are holes which act as the potential barriers. Particularly, up a frequency $f \simeq 2000$ Hz, the scattering properties induced by the holes, can be described by δ -function barriers, with strength given by:

$$V = \frac{R_n^2}{R^2(l_n + l_{eff})} \quad (6.6)$$

where R_n and l_n are the radius and the length of the ‘neck’ of the corresponding hole, respectively, R is the radius of the tube and l_{eff} an effective length induced by the radiation losses out of each hole. Finally, for the transmission measurement, the tube is not rigidly terminated. Instead, an anechoic, 10m long tube is used. The latter is partially filled with a plastic porous foam material to suppress the back propagating waves, which alter measured signal. The acoustic wave source is a piezo-electric device placed in the start of the waveguide [141]. Finally, the measurement of the transmission coefficient is achieved by the suitable placement of a microphone to the end of the waveguide and particularly its distance from the last hole is equal to the distance between the source and the first hole.

The experimental set-up design is subject to several geometrical constraints which have to be considered during the theoretical calculations. In order to minimize losses, the total length of the cylindrical waveguide should be the smallest possible. Also, as the number of barriers (holes) increases, the radiation induced losses are also increased. This effect is enhanced as the radius of each hole -and effectively the barrier strength- is increased. Thereby, for a realistic set-up, the total length of the cylindrical waveguide should not exceed the 1.5 m and the R_n should optimally be $2.5\text{cm} < R_n < 3.5\text{cm}$. A final remark is that the holes should be separated by a distance at leach $d = 5$ cm, since closer placement induces coupling in the propagating modes.

Let us now proceed to the implementation of the construction principle to the waveguide set-up. As it was mentioned, the piecewise constant barriers (refraction index slabs)

which were used in the quantum (photonic) case, are replaced by δ barriers. Since, in each inter-barrier region the wave propagation is described by a superposition of plane waves (expressing the pressure):

$$P_n(x) = A_n e^{ikx} + B_n e^{-ikx}, \quad (6.7)$$

the procedure to solve this scattering problem remains almost the same. The pressure $P_n(x)$ is continuous in every point of the x -axis, however the δ barriers induce a discontinuity in the derivative of $P_n(x)$ at the points where they are located:

$$\left. \frac{dP(x)}{dx} \right|_{x=x_n^+} - \left. \frac{dP(x)}{dx} \right|_{x=x_n^-} = V_n P(x_n), \quad (6.8)$$

where x_n is the position of the δ -barrier.

Figure 6.6(a) illustrates such a set-up. As it is clearly shown, there are two possible different LP symmetry decompositions m and n , which in turn can be used for the construction of two s -PTRs at desired frequencies. The solid and dashed arcs delimit the LP symmetric units $\mathcal{D}_{m,n}^i$ which constitute each decomposition, i.e. m and n involve 4 and 2 LP symmetric units, respectively. The implementation of the construction principle provides the suitable device characteristics so that two s -PTR occur: one in frequency $f_1 = 545\text{Hz}$, where the LP symmetric domains \mathcal{D}_m^i , $i = 1, 4$ behave as resonators and and the other in frequency $f_2 = 938.6\text{Hz}$ where now the resonating units are the LP symmetric domains \mathcal{D}_2^i , $i = 1, 2$. Therefore, the transfer matrix calculations for each resonator lead to the following characteristics: $V_1 = 5.518$, $V_2 = 4.167$ corresponding to hole radii $R_n = 0.023\text{m}$ and $R_n = 0.018\text{m}$, respectively and $L_1 = 0.1\text{m}$, $L_2 = 0.0949\text{m}$, $L_3 = 0.2792\text{m}$, $L_4 = 0.1781\text{m}$, $L_5 = 0.1323\text{m}$, $L_6 = 0.1845\text{m}$. Note also that the radius of the cylindrical waveguide has the fixed value $R = 0.05\text{m}$, $l_n = 0.005\text{m}$ and $l_{eff} = 1.45R_n$.

The additional a -PTR was constructed as follows: We identify two parts of the device (\mathcal{R}_1 , \mathcal{R}_2), where their distance can be altered without affecting the already existing s -PTRs. Then, we calculate separately the transmission spectra of \mathcal{R}_1 and \mathcal{R}_2 and check for the existence of a frequency with common transmission. In our case this occurs in $f_3 = 287,6\text{Hz}$. Finally, we combine again \mathcal{R}_1 and \mathcal{R}_2 , searching for the proper distance which satisfies the phase condition in Eq. (5.48).

The theoretically computed transmission spectra, with and without losses are demonstrated in the same figure. The losses cause a decrease of the order of $\simeq 30\%$ in the transmission. However, the narrow, isolated a -PTR is significantly decreased ($\simeq 80\%$). The experimentally anticipated spectrum we expect to be close to the corresponding theoretical with losses. It is interesting to investigate under which conditions the narrow PTRs at low frequencies can be maintained.

Figure 6.6(b) demonstrates an alternative, shorter set-up which consists of 7 δ -barriers. A small device length leads to decreased losses during the experiment. However, the smaller length comes at the expense of the absence of the second LP symmetry

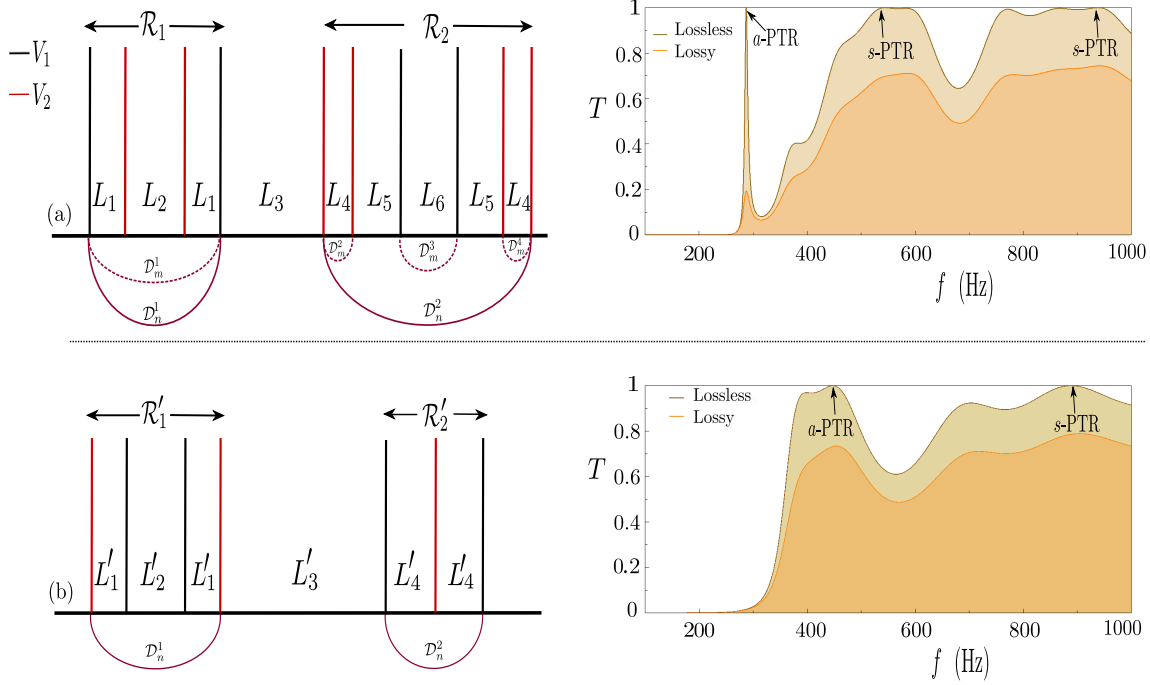


FIGURE 6.6: (a) Schematic of an LP based design, exhibiting 1 *a*- and 2 *s*-PTRs, proposed for the experimental set-up. The set-up is comprised of 10 δ -barriers, shown in black and red lines, corresponding to two δ -barriers with different strengths V_1, V_2 . Each L_i denotes the width separating the adjacent barriers. The solid and dashed arcs depict the two different LP symmetry scales of the device and $\mathcal{D}_{m,n}^i$ represent the resonating LP symmetric domains of each decomposition. In the right, the corresponding theoretical calculation of the transmission coefficient - with and without losses - is shown. (b) Alternative LP based, waveguide design for a 7 δ -barrier array. The smaller size of the cylinder reduced the losses. However, the absence of the second LP symmetry scale, doesn't allow for the emergence of a second *s*-PTR.

scale and consequently of the absence of the second *s*-PTR. Indeed, this set-up supports one decomposition in LP symmetric units, namely \mathcal{D}_n^i . The δ -barrier strengths remain the same as in the first example, while the distances between adjacent barriers are $L'_1 = 0.08m$, $L'_2 = 0.1968m$, $L'_3 = 0.0798m$, $L'_4 = 0.1566m$.

The preceding examples showed in a direct and transparent manner that the identification of local symmetries on scales larger than the elementary (e.g. a single barrier) building blocks provides a new viewpoint on the description of systems with structural

complexity. Different decompositions in LP symmetric domains for the same setup correspond to possible different PTR states, according to the proposed construction principle. Therefore, local symmetry considerations prove to have a fundamental role in understanding and even controlling the properties of aperiodic, complex systems of stationary wave propagation.

CHAPTER 7

CONCLUSIONS AND PERSPECTIVES

We have studied the concept of global, discrete symmetry breaking in one-dimensional systems. Particularly we have focused on the effects of the remnants of broken global symmetries when retained in local scales, as principally occurs in aperiodic, non-symmetric scattering systems, where the wave propagation in their time-independent version can be described by the Helmholtz equation. The linear symmetry transformations which can occur in one-dimension are the translation by a certain length and the reflection through an point. In the generic case, these symmetries are global and the corresponding linear transformations are applicable $\forall x \in \mathbb{R}$. From the global translation invariance, Bloch states emerge, while global reflection symmetry leads to eigenstates with even or odd parity. However, under the occurrence of a symmetry breaking, the corresponding theorems cease to hold. In the simplest case the symmetry breaking occurs due to the asymmetry in the asymptotic boundary condition, while the potential retains its symmetry. Then a pair of two - symmetry induced - spatially invariant quantities, in the form of non-local currents, (Q, \tilde{Q}) emerge. On the other hand, apart from the asymptotic conditions, the symmetry can be broken also in the level of the potential. If however, it is retained on a local scale, that is in domains \mathcal{D}_m of finite extent, we show that pairs of the aforementioned invariants (Q_m, \tilde{Q}_m) emerge for each symmetric domain \mathcal{D}_m . These currents are identified as remnants of the corresponding broken global symmetry and provide a mapping for the wave field from a *source* to a *target* domain which are related with the corresponding symmetry transform. Therefore the identification of the invariants (Q_m, \tilde{Q}_m) lead to a generalization of the Bloch and parity theorems for systems where the symmetry is preserved locally. In the limit of the global symmetry restoration Q vanishes and \tilde{Q} becomes a phase, identified as the Bloch phase of the infinite system. In this sense, a non-vanishing Q is the key to describe a globally broken symmetry.

Due to the Helmholtz-Schrödinger isomorphism, waves in the classical and quantum regime can be described in the same framework. Therefore, we investigated quantum,

photonic and acoustic systems under a unified formalism, notwithstanding their essential differences with respect to their dimensions and general properties. We considered non-symmetric, aperiodic scattering set-ups which are completely decomposable to domains where the LP is fulfilled, i.e. the LP domains cover the entire device. Focusing on the parity transformation when applied to finite mirror symmetric domains, we introduced the concept of local parity (LP) and the corresponding operator. The symmetry-based treatment of such set-ups revealed the impact of LP on their transport properties and particularly on perfect transmission resonances (PTRs). With emphasis on the manifestation of PTRs, we used the local invariants Q , \tilde{Q} for every LP domain appearing in the decomposition (divided by the product of the wave field's values at the limits of the LP domain) and proposed a geometric representation of scattering states, on the complex plane. This, in turn, led to a classification of scattering states and particularly of PTRs. Thus we showed that there exist:

- (i) symmetric PTRs (s -PTRs), where the magnitude of the wave field is exactly LP symmetric within the scattering device, following the symmetries of the units in which the set-up can be decomposed. s -PTRs are represented in the complex plane by collinear vectors and of equal magnitude and lie upon the imaginary axis.
- (ii) asymmetric PTRs (a -PTRs), where the magnitude of the wave field is non-symmetric in the scattering region and can be represented, in the complex plane, by vectors which form closed trajectory. For a decomposition in even (odd) number of LP symmetric domains, it closes to the origin (to $2iJ$) where J describes the energy current.
- (iii) non-PTRs, where local invariants are different among the sub-domains of a considered decomposition of the scattering device, forming an arbitrary trajectory in the complex plane.

This classification in a - and s -PTRs lifts certain overlaps of alternative approaches and provides an unambiguous distinction between resonances based on fundamental (local) symmetry principles.

The above concepts were demonstrated in an inhomogeneous, aperiodic set-up, with a spatially varying generalized potential, which exhibited in a representative manner all the above features. Focusing on the transmission properties we elucidated the emergence of perfect transmission on symmetry ground and contributed to the clarification of the PTR mechanism in non-symmetric devices -a not resolved issue up to now. Further, it was shown how the simultaneous existence of different LP symmetry scales in the same set-up, can be utilized to design aperiodic wave mechanical devices with prescribed PTR properties. To this aim, we developed and proposed a construction principle for completely LP symmetric devices, which utilizes the -possibly multiple- symmetry scales to

determine the characteristics of the set-up, so that it transmits resonantly at pre-selected frequencies. The proposed construction principle was implemented on quantum, photonic and acoustic systems, indicating its applicability in diverse systems.

The study of one-dimensional systems under the prism of their local symmetries revealed a plethora of new properties, starting from the fundamental occurrence of the spatially invariant quantities (Q , \tilde{Q}) (emerging from discrete symmetries) to the utilization of the different LP symmetry scales for the construction of devices with PTRs at prescribed energies. In a first extension of the present work one could study the effect of local symmetries to systems of higher dimensionality. Since such a system would be subject to more symmetry transforms, it would be interesting to see whether the respective invariants remain and if new emerge. Also, in this Thesis we focused on linear symmetry transformations. The influence, however, of non-linear transformations could possibly lead to interesting, novel phenomena.

Another path, relevant to the local symmetry concept, is the implementation of the above notions to one-dimensional systems with \mathcal{PT} -symmetry. In such systems the Hamiltonian ceases to be Hermitian. However, if the combination of parity and time reversal symmetries is fulfilled, then there are conditions where the energy eigenvalue spectrum becomes real. This indicates a phase transition. Such systems -also realized in photonics- describe a balanced gain and loss. The question to be posed is whether -and how- this symmetry could be globally broken and implemented on local domains and what would the effect be. Also, how such a symmetry breaking could affect the phase transition.

Finally, a very interesting task would be to implement the introduced ideas to interacting systems. As a first step, we have considered the two-dimensional Ising model with first neighbour interaction, under the influence of an sinusoidal magnetic field. Breaking the symmetry of the Hamiltonian by restricting the field to act on confined cells, we find interesting phenomena regarding the stochastic resonance and the hysteresis loop.

APPENDIX A

Here we will calculate in detail the commutator $[\hat{\Omega}, \hat{H}_s^{\mathcal{D}}]$ of the LP operator $\hat{H}_s^{\mathcal{D}}$ in an LP symmetric domain \mathcal{D} with the Helmholtz operator

$$\hat{\Omega} = \frac{d^2}{dx^2} + \mathcal{W}(x).$$

We will act on the wave field $\mathcal{A}(x)$ with the commutator and derive the conditions for the *weak* commutation of the corresponding operators. The action of the local parity (LP) operator, within an LP symmetric domain \mathcal{D} , on $\mathcal{A}(x)$ is defined as follows:

$$\begin{aligned} \hat{H}_s^{\mathcal{D}} \mathcal{A}(x) = & \Theta \left(\frac{L}{2} - |x - \alpha| \right) \mathcal{A}(2\alpha - x) \\ & + s \Theta \left(|x - \alpha| - \frac{L}{2} \right) \mathcal{A}(x), \quad s = \pm 1 \end{aligned} \quad (\text{A'.1})$$

where $L = b - a$ is the width of \mathcal{D} and $\alpha = \frac{a+b}{2}$ is the position of the LP axis. Substituting L and α we obtain the following expression:

$$\hat{H}_s^{\mathcal{D}} \mathcal{A}(x) = [\Theta(x - a) - \Theta(x - b)] \mathcal{A}(2\alpha - x) + s [\Theta(a - x) - \Theta(b - x)] \mathcal{A}(x). \quad (\text{A'.2})$$

The action of the commutator on $\mathcal{A}(x)$ is:

$$\left[\hat{\Omega}, \hat{H}_s^{\mathcal{D}} \right] \mathcal{A}(x) = \hat{\Omega} \hat{H}_s^{\mathcal{D}} \mathcal{A}(x) - \hat{H}_s^{\mathcal{D}} \hat{\Omega} \mathcal{A}(x) \quad (\text{A'.3})$$

and we set

$$\mathcal{I}_1 = \hat{\Omega} \hat{H}_s^{\mathcal{D}} \mathcal{A}(x) \quad (\text{A'.4})$$

$$\mathcal{I}_2 = \hat{H}_s^{\mathcal{D}} \hat{\Omega} \mathcal{A}(x) \quad (\text{A'.5})$$

To facilitate the calculation we will first calculate \mathcal{I}_1 and subsequently \mathcal{I}_2 .

$$\begin{aligned}
\mathcal{I}_1 &= \hat{\Omega} \hat{\Pi}_s^{\mathcal{D}} \mathcal{A}(x) \\
&= \hat{\Omega} ([\Theta(x-a) - \Theta(x-b)] \mathcal{A}(2\alpha-x) + s [\Theta(a-x) + \Theta(x-b)] \mathcal{A}(x)) \\
&= -\frac{d^2}{dx^2} ([\Theta(x-a) - \Theta(x-b)] \mathcal{A}(2\alpha-x)) + \mathcal{W}(x) [\Theta(x-a) - \Theta(x-b)] \mathcal{A}(2\alpha-x) \\
&\quad -\frac{d^2}{dx^2} ([\Theta(a-x) + \Theta(x-b)] \mathcal{A}(x)) + \mathcal{W}(x) ([\Theta(a-x) + \Theta(x-b)] \mathcal{A}(x)) \\
&= -\mathcal{A}''(2\alpha-x) [\Theta(x-a) - \Theta(x-b)] + 2\mathcal{A}'(2\alpha-x) [\delta(x-a) - \delta(x-b)] \\
&\quad -\mathcal{A}(2\alpha-x) [\delta'(x-a) - \delta'(x-b)] + \mathcal{W}(x) [\Theta(x-a) - \Theta(x-b)] \mathcal{A}(2\alpha-x) \\
&\quad -s \mathcal{A}''(x) [\Theta(a-x) + \Theta(x-b)] -s 2\mathcal{A}'(x) [\delta(x-a) - \delta(x-b)] \\
&\quad -s \mathcal{A}(x) [\delta'(x-a) - \delta'(x-b)] +s \mathcal{W}(x) [\Theta(a-x) + \Theta(x-b)] \mathcal{A}(x)
\end{aligned}$$

where the prime denotes differentiation with respect to x and we have used the properties:

$$\Theta'(x) = \delta(x) \quad , \quad \delta(-x) = \delta(x)$$

Thus, the first part of the commutator, \mathcal{I}_1 becomes:

$$\begin{aligned}
\mathcal{I}_1 &= -\mathcal{A}''(2\alpha-x) [\Theta(x-a) - \Theta(x-b)] + 2\mathcal{A}'(2\alpha-x) [\delta(x-a) - \delta(x-b)] \\
&\quad -\mathcal{A}(2\alpha-x) [\delta'(x-a) - \delta'(x-b)] + \mathcal{W}(x) [\Theta(x-a) - \Theta(x-b)] \mathcal{A}(2\alpha-x) \\
&\quad -s \mathcal{A}''(x) [\Theta(a-x) - \Theta(b-x)] -s 2\mathcal{A}'(x) [\delta(x-a) - \delta(x-b)] \\
&\quad -s \mathcal{A}(x) [\delta'(x-a) - \delta'(x-b)] +s \mathcal{W}(x) [\Theta(a-x) - \Theta(b-x)] \mathcal{A}(x)
\end{aligned}$$

Next we compute \mathcal{I}_2 .

$$\begin{aligned}
\mathcal{I}_2 &= \hat{\Pi}_s^{\mathcal{D}} \hat{\Omega} \mathcal{A}(x) = \hat{\Pi}_s^{\mathcal{D}} (-\mathcal{A}''(x) + \mathcal{W}(x)\mathcal{A}(x)) \\
&\quad -\mathcal{A}''(2\alpha-x) [\Theta(x-a) - \Theta(x-b)] + \mathcal{W}(2\alpha-x) \mathcal{A}(2\alpha-x) [\Theta(x-a) - \Theta(x-b)] \\
&\quad -\mathcal{A}''(x) [\Theta(a-x) + \Theta(x-b)] + \mathcal{W}(x)\mathcal{A}(x) [\Theta(a-x) + \Theta(x-b)]
\end{aligned}$$

which leads to the second part of the commutator

$$\begin{aligned}
\mathcal{I}_2 &= -\mathcal{A}''(2\alpha-x) [\Theta(x-a) - \Theta(x-b)] + \mathcal{W}(2\alpha-x) \mathcal{A}(2\alpha-x) [\Theta(x-a) - \Theta(x-b)] \\
&\quad -s \mathcal{A}''(x) [\Theta(a-x) + \Theta(x-b)] + s \mathcal{W}(x) \mathcal{A}(x) [\Theta(a-x) + \Theta(x-b)]
\end{aligned}$$

The sum $\mathcal{I}_1 + \mathcal{I}_2$ yields:

$$\begin{aligned}
\mathcal{I}_1 + \mathcal{I}_2 &= \mathcal{A}''(2\alpha - x) [\Theta(x - a) - \Theta(x - b)] + 2\mathcal{A}'(2\alpha - x) [\delta(x - a) - \delta(x - b)] \\
&\quad - \mathcal{A}(2\alpha - x) [\delta'(x - a) - \delta'(x - b)] + \mathcal{W}(x) [\Theta(x - a) - \Theta(x - b)] \mathcal{A}(2\alpha - x) \\
&\quad - s \mathcal{A}''(x) [\Theta(a - x) - \Theta(b - x)] - s 2\mathcal{A}'(x) [\delta(x - a) - \delta(x - b)] \\
&\quad - s \mathcal{A}(x) [\delta'(x - a) - \delta'(x - b)] + s\mathcal{W}(x) [\Theta(a - x) - \Theta(b - x)] \mathcal{A}(x) \\
&\quad - \mathcal{A}''(2\alpha - x) [\Theta(x - a) - \Theta(x - b)] + \mathcal{W}(2\alpha - x) \mathcal{A}(2\alpha - x) [\Theta(x - a) - \Theta(x - b)] \\
&\quad - s\mathcal{A}''(x) [\Theta(a - x) + \Theta(x - b)] + s\mathcal{W}(x) \mathcal{A}(x) [\Theta(a - x) + \Theta(x - b)]
\end{aligned}$$

The above equation can be significantly simplified and the final form of the commutator $[\hat{\Omega}, \hat{\Pi}_s^{\mathcal{D}}]$ when acting on the field $\mathcal{A}(x)$ becomes:

$$\begin{aligned}
[\hat{H}, \hat{\Pi}_s^{\mathcal{D}}] \mathcal{A}(x) &= \frac{1}{2} (\delta'(x - a) - \delta'(x - b)) \{ \mathcal{A}(2\alpha - x) - s\mathcal{A}(x) \} - \quad (\text{A'.6}) \\
&\quad (\delta(x - a) - \delta(x - b)) \{ \mathcal{A}'(2\alpha - x) + s\mathcal{A}'(x) \}, \quad s = \pm 1
\end{aligned}$$

APPENDIX B

We show here that if the field module $\mathcal{A}_0(x)$ of a propagating wave $\mathcal{A}(x)$ is completely LP symmetric within every LP symmetric domain of a particular decomposition, at an energy ϵ , then this state corresponds to a s -PTR. We prove it here for two arbitrary LP symmetric barriers, as shown in Fig. B.1, however the generalization for N barriers is straightforward.

We begin with the assumption that the field module $\mathcal{A}_0(x)$ is LP symmetric in each barrier. Thus, on either side of \mathcal{W}_1 it holds that

$$u^L(a) = u^{\mathcal{W}_2}(b), \quad (\text{B'.1})$$

where L denotes the potential free region $x < \alpha$ on the left hand side of \mathcal{W}_1 . Substituting the known plane wave form of the incident wave we get:

$$1 + |r|^2 + re^{-2i\kappa a} + r^*e^{2i\kappa a} = u^{\mathcal{W}_2}(b). \quad (\text{B'.2})$$

Also, from the LP conditions Eq. (4.30), we have for the derivative:

$$u'^L(a) = -u'^{\mathcal{W}_2}(b), \quad (\text{B'.3})$$

which leads to

$$-2i\kappa (re^{-2i\kappa a} - r^*e^{2i\kappa a}) = -u'^{\mathcal{W}_2}(b). \quad (\text{B'.4})$$

For \mathcal{W}_3 the respective relations yield:

$$u^{\mathcal{W}_2}(c) = |t|^2 \quad (\text{B'.5})$$

and from the derivative:

$$u'^{\mathcal{W}_2}(c) = 0 \quad (\text{B'.6})$$

Then, in the barrier \mathcal{W}_3 holds that

$$u^{\mathcal{W}_2}(b) = u^{\mathcal{W}_2}(c) \quad ; \quad u'^{\mathcal{W}_2}(b) = -u'^{\mathcal{W}_2}(c), \quad (\text{B'.7})$$

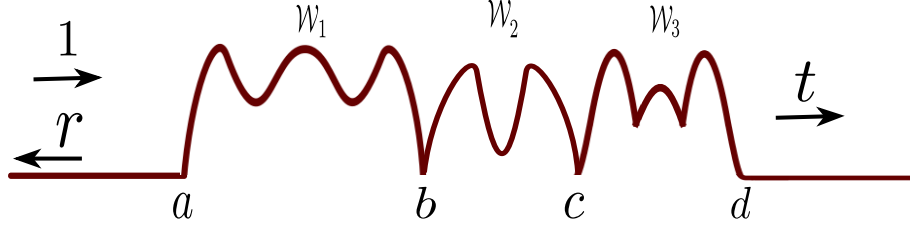


FIGURE B'.1: Schematic of a 1-D potential array, comprised of two arbitrary LP symmetric barriers. In the potential free regions the field $\mathcal{A}(x)$ is a superposition of left- and rightwards propagating plane waves.

which in turn leads to

$$1 + |r|^2 + re^{-2i\kappa a} + r^*e^{2i\kappa a} = |t|^2 \quad (\text{B'.8})$$

and

$$-2i\kappa (re^{-2i\kappa a} - r^*e^{2i\kappa a}) = 0. \quad (\text{B'.9})$$

Equation (B'.9) clearly states that $re^{-2i\kappa a} \in \mathbb{R}$, consequently Eq. (B'.8) becomes

$$1 + |r|^2 + 2re^{-2i\kappa a} = |t|^2. \quad (\text{B'.10})$$

Substituting the unitarity relation $|t|^2 + |r|^2 = 1$ in Eq. (B'.10), we get

$$|r|^2 + re^{-2i\kappa a} = 0 \quad (\text{B'.11})$$

or

$$r(r^* + e^{-2i\kappa a}) = 0. \quad (\text{B'.12})$$

Thus, for the case where the field module $u(x)$ is completely LP symmetric in a certain decomposition of a completely LP symmetric setup, there are the following two possibilities:

- $r = 0$
- $r^*e^{2i\kappa a} = -1$.

The first corresponds to the case of perfect transmission $|t| = 1$, while the second to the trivial case of total reflection $|t| = 0$, where there is no wave penetration in the potential array. The latter, can be easily shown by substituting $|t|^2 + |r|^2 = 1$ and $r^*e^{2i\kappa a} = -1$ into Eq. B'.8, finally yielding $|t| = 0$.

APPENDIX Γ

A *quart-wave stack* is a multilayer dielectric mirror, which is comprised of alternating materials with different refraction indices. The quarter-wave condition leads to total reflection of waves with a proper wavelength, due to the partial reflection on each layer interface. If the device is periodic (1D photonic crystal), the multiple reflection of the incident wave leads to destructive interference, thereby preventing the wave propagation.

The quarter-wave condition in the a photonic crystal has significant effects on the size of the band gap. We consider a periodic structure with alternating slabs with refraction indices n_1 , d_1 and n_2 , d_2 , respectively. However, both materials have equal optical lengths:

$$n_1 d_1 = n_2 d_2 = \frac{\lambda_0}{4}, \quad (\Gamma.1)$$

each one equal to a quarter wavelength of $\lambda_0 = 2\pi c/\omega_0$, which is called the mid-gap wavelength. For this reason, such a multilayered device is referred as *quart-wave stack*. The basic property that this condition induces is the maximization of the photonic band gap in the edge of the Brillouin zones. The reason for this maximisation is that the reflected waves from each layer are in phase at the mid-gap frequency ω_0 . Also, when the quarter wave condition holds, the possible band gaps at $k = 0$ (center of the Brillouin zone) becomes zero. Thus, in the case of a periodic device, the photonic band gap is maximized in the edge of the Brillouin zones and becomes zero for $k = 0$.

In aperiodic structures (aperiodic, quasi-periodic, fractal) the notion of the quarter-wave condition is also widely used. Namely, every periodic or non-periodic quarter-wave multilayer possesses a transmission spectrum which is periodic with period $2\omega_0$ and symmetric with respect to ω_0 , where ω_0 is equal to

$$\omega = \frac{2\pi c}{\lambda_0} = \frac{\pi c}{2n_1 d_1} = \frac{\pi c}{2n_2 d_2}. \quad (\Gamma.2)$$

ΠΕΡΙΛΗΨΗ

Εισαγωγή

Η περιγραφή της φύσης είναι άρρηκτα συνδεδεμένη με τον εντοπισμό και τη χρήση συμμετριών. Η χρήση συμμετριών αποτελεί τη βάση της Φυσικής από τις απαρχές της καθώς ο ρόλος τους είναι θεμελιώδης για την κατανόηση οποιουδήποτε συστήματος. Συχνά, προκειμένου να περιγράψουμε ένα σύστημα, τουλάχιστον ως προς τις φαινομενολογικές του ιδιότητες, είναι σύνηθες να υιοθετούμε ένα μοντέλο καθολική συμμετρία η οποία θα καθορίσει τελικά και τις ιδιότητες αυτές.

Ως παραδείγματα μπορούμε να αναφέρουμε ένα δυναμικό με καθολική συμμετρία αντιστροφής (inversion), όπου οι αντίστοιχες ιδιοκαταστάσεις έχουν άρτια ή περιττή ομοτιμία ή την περίπτωση ενός άπειρου, περιοδικού δυναμικού, που περιγράφει τη διάδοση ηλεκτρονίων σε έναν κρύσταλλο. Η δεύτερη περίπτωση δείχνει χαρακτηριστικά την επίδραση των συμμετριών καθώς, μόνο λόγω της θεώρησης της (καθολικής) συμμετρία μετάθεσης, προκύπτουν οι ενεργειακές ζώνες μέσω του θεωρήματος Bloch.

Παρ' όλα αυτά, η καθολική ικανοποίηση μιας συμμετρίας αποτελεί ένα ιδεατό σενάριο, το οποίο δε μπορεί να εφαρμοστεί συνήθως σε αρκετά πραγματικά φυσικά συστήματα. Στην πραγματικότητα, η πλειονότητα των δομών που εμφανίζονται στη φύση συνδέεται στενά με μηχανισμούς που οδηγούν στο σπάσιμο κάποιας καθολικής ή και τοπικής συμμετρίας. Μία τέτοια διαδικασία συνήθως οδηγεί στην εμφάνιση νέων συμμετριών, πιθανότατα σε διαφορετικές κλίμακες. Πέραν των συστημάτων που εμφανίζονται στη φύση, το σπάσιμο καθολικών συμμετριών - και μάλιστα με συγκεκριμένους τρόπους- επιβάλλεται και σε τεχνητές διατάξεις, λόγω τεχνολογικών περιορισμών και λειτουργικών απαιτήσεων. Κατά συνέπεια, συχνά κανείς έρχεται αντιμέτωπος με συστήματα τα οποία, παρά το γεγονός ότι δεν παρουσιάζουν κάποια καθολική συμμετρία, διατηρούν συμμετρίες τοπικά, σε χωρικά διαστήματα μικρότερα από το συνολικό μήκος της διάταξης. Τέτοιες περιπτώσεις συναντώνται σε μεγάλα μόρια, οιονεί-κρυστάλλους (quasi-crystals), ακόμα και σε συστήματα με (μερική) αταξία. Η ύπαρξη τοπικών συμμετριών σε αυτού του είδους τις δομές έχει σημαντικές επιπτώσεις στις ιδιότητες, οι οποίες εντοπίζονται, από την ύπαρξη διατηρουμένων μεγεθών προερχόμενα από τη θεωρούμενη συμμετρία, ως την ερμηνεία ενδιαφερου-

σών καταστάσεων σκέδασης, όπως οι συντονισμοί πλήρους διέλευσης. Ωστόσο, αν και τέτοιου είδους τοπικές συμμετρίες - συνυπάρχουσες στο ίδιο σύστημα αλλά σε διαφορετικές κλίμακες - είναι ευρύτατα διαδεδομένες, δεν υπάρχει κάποια θεωρία που να τις αντιμετωπίζει με συστηματικό τρόπο.

Στην παρούσα εργασία αναπτύσσουμε ένα θεωρητικό πλαίσιο για την αντιμετώπιση καταστάσεων κυματικής σκέδασης σε μονοδιάστατα συστήματα με συμμετρία αντιστροφής και μετατόπισης, μέσα σε πεπερασμένα ή άπειρα, connected/disconnected, χωρία. Αναζητούμε κατάλοιπα της σπασμένης καθολικής συμμετρίας τα οποία να μπορούν να καθορίσουν τη δομή του σκεδαζόμενου κύματος. Υπό αυτό το πρίσμα, αναζητούμε - αν υπάρχει - τη μορφή που θα μπορούσαν να αποκτήσουν τα γνωστά θεωρήματα Bloch και ομοτιμίας για περιπτώσεις σπασμένης καθολικής συμμετρίας μετατόπισης και αντιστροφής, αντιστοίχως.

Υιοθετώντας ένα συμβολισμό, που να περιγράφει με γενικό τρόπο κυματικά συστήματα, είτε κβαντικά είτε κλασικά, αποδεικνύουμε την ύπαρξη χωρικά αναλλοίωτων ποσοτήτων, με τη μορφή ρευμάτων, που επιφέρει η εκάστοτε συμμετρία (μετατόπισης, αντιστροφής) και τα οποία διατηρούνται σε χωρία που ισχύει η συμμετρία. Στη συνέχεια δείχνουμε πώς αυτές οι αναλλοίωτες ποσότητες μπορούν να χρησιμοποιηθούν για να απεικονιστεί η αντίστοιχη κυματική συνάρτηση από ένα χωρίο σε ένα άλλο το οποίο συνδέεται με το προηγούμενο μέσω ενός μετασχηματισμού συμμετρίας. Αυτή η απεικόνιση αποτελεί τη γενίκευση των θεωρημάτων Bloch και ομοτιμίας για συστήματα με σπασμένη την αντίστοιχη καθολική συμμετρία. Στο όριο που η καθολική συμμετρία αποκαθίσταται ανακτούμε τα θεωρήματα Bloch και ομοτιμίας.

Αναλλοίωτα μη-τοπικά ρεύματα

Στο ενοποιημένο θεωρητικό πλαίσιο που θα χρησιμοποιήσουμε, θα θεωρήσουμε την σκέδαση ενός κυματικού πεδίου $\mathcal{A}(x)$ περιγράφεται από την εξίσωση Helmholtz

$$\mathcal{A}''(x) + \mathcal{W}(x)\mathcal{A}(x) = 0. \quad (\Gamma.3)$$

Το γενικευμένο δυναμικό $\mathcal{W}(x) = \kappa^2(x)$ περιγράφει την ανομοιογένεια του υλικού στο οποίο γίνεται η διάδοση του κύματος.

Στη συνέχεια θεωρούμε τη χωρική συμμετρία του δυναμικού $\mathcal{W}(x)$ κάτω από τους δύο προαναφερθέντες γραμμικούς μετασχηματισμούς: την αντιστροφή μέσω ενός σημείου a και τη μετατόπιση κατά ένα μήκος L . Οι μετασχηματισμοί αυτοί περιγράφονται μέσω των σχέσεων:

$$F(x) = \sigma x + \rho \quad ; \quad \text{with} \quad \begin{cases} \sigma = -1 & ; \quad \rho = 2a \quad (\text{parity}) \\ \sigma = +1 & ; \quad \rho = L \quad (\text{translation}) \end{cases} \quad (\Gamma.4)$$

και προσδίδουν στο δυναμικό την ιδιότητα:

$$\mathcal{W}(x) = \mathcal{W}(F(x)), \quad (\Gamma.5)$$

$\forall x$ στην περιοχή του χωρίου \mathcal{D} . Επειδή η Εξ. (Γ.3) ικανοποιείται για κάθε x στο \mathbb{R} θα πρέπει να ικανοποιείται επίσης για τα αντίστοιχα x κάτω από το μετασχηματισμό F :

$$\mathcal{A}''(F(x)) + \mathcal{W}(F(x))\mathcal{A}(F(x)) = 0. \quad (\Gamma.6)$$

Η (τοπική) συμμετρία του δυναμικού που εκφράζεται από την Εξ. (Γ.5) μπορεί να οδηγήσει στην κατασκευή ποσοτήτων, που είναι χωρικά αναλλοίωτες στο εύρος που ικανοποιείται η συμμετρία. Πολλαπλασιάζοντας την Εξ. (Γ.3) με $\mathcal{A}(F(x))$, την Εξ. (Γ.6) με $\mathcal{A}(x)$ και στη συνέχεια αφαιρώντας, λαμβάνοντας υπ' όψιν την Εξ. (Γ.5), καταλήγουμε στην ακόλουθη έκφραση:

$$\mathcal{A}(F(x))\mathcal{A}''(x) - \mathcal{A}''(F(x))\mathcal{A}(x) = 0, \quad (\Gamma.7)$$

η οποία με ολοκλήρωση οδηγεί στην ποσότητα:

$$Q = \frac{1}{2i} [\sigma\mathcal{A}(x)\mathcal{A}'(F(x)) - \mathcal{A}(F(x))\mathcal{A}'(x)], \quad (\Gamma.8)$$

που είναι χωρικά αναλλοίωτη στο συμμετρικό χωρίο \mathcal{D} . Αντίστοιχα, θεωρώντας τη μιγαδική συζυγή της Εξ. (Γ.3) και ακολουθώντας την ίδια διαδικασία οδηγούμαστε σε μία νέα, ανεξάρτητη, χωρικά σταθερή - στο συμμετρικό \mathcal{D} - ποσότητα:

$$\tilde{Q} = \frac{1}{2i} [\sigma\mathcal{A}^*(x)\mathcal{A}'(F(x)) - \mathcal{A}(F(x))\mathcal{A}'^*(x)]. \quad (\Gamma.9)$$

Αφαιρώντας τα μέτρα (στο τετράγωνο) των Q , \tilde{Q} οδηγούμαστε στο ρεύμα πιθανότητας ή ενέργειας

$$J = \frac{1}{2i} [\mathcal{A}'(x)\mathcal{A}^*(x) - \mathcal{A}'^*(x)\mathcal{A}(x)] \quad (\Gamma.10)$$

για την περίπτωση υλικών ή ηλεκτρομαγνητικών κυμάτων, αντίστοιχα. Η σχέση που συνδέει τα Q , \tilde{Q} , J είναι:

$$\sigma (|\tilde{Q}|^2 - |Q|^2) = J^2, \quad (\Gamma.11)$$

Γενίκευση των θεωρημάτων Bloch και ομοτιμίας

Μπορούμε τώρα να χρησιμοποιήσουμε τα Q , \tilde{Q} προκειμένου να βρούμε μία σχέση η οποία να συνδέει το κυματικό πεδίο $\mathcal{A}(x)$ σε ένα σημείο x με την απεικόνισή του $\mathcal{A}(F(x))$ μετά από το μετασχηματισμό συμμετρίας $F(x)$. Θα διαπιστώσουμε ότι αυτή η σχέση αποτελεί τη γενίκευση του θεωρήματος Bloch ή του θεωρήματος της ομοτιμίας όταν οι καθολικές συμμετρίες μετατόπισης και αντιστροφής, αντίστοιχα, έχουν σπάσει. Λύνοντας το σύστημα των Εξ. (Γ.8), (Γ.9) ως προς το πεδίο στη θέση $F(x)$, βρίσκουμε ότι:

$$\mathcal{A}(F(x)) = \frac{\tilde{Q}}{J}\mathcal{A}(x) - \frac{Q}{J}\mathcal{A}^*(x) \quad (\Gamma.12)$$

και

$$\mathcal{A}'(F(x)) = \sigma \left(\frac{\tilde{Q}}{J} \mathcal{A}'(x) - \frac{Q}{J} \mathcal{A}'^*(x) \right). \quad (\Gamma.13)$$

Οι παραπάνω εξισώσεις ισχύουν για οποιοδήποτε τύπο χωρίου \mathcal{D} (για $J \neq 0$) και οδηγούν άμεσα στο πεδίο $\mathcal{A}(F(x))$ στο χωρίο $\bar{\mathcal{D}}$ που συνδέεται με το \mathcal{D} μέσω του μετασχηματισμού συμμετρίας F . Συγκεκριμένα, το πεδίο $\mathcal{A}(F(x))$ εκφράζεται ως γραμμικός συνδυασμός του πεδίου στη θέση x και του μιγαδικού συζηγού του, μέσω των αναλλοίωτων μεγεθών Q , \tilde{Q} , J . Δηλαδή, τα Q , \tilde{Q} δημιουργούν μία απεικόνιση ανάμεσα στα πλάτη των πεδίων, σε σημεία που συνδέονται με τον εκάστοτε μετασχηματισμό συμμετρίας. Αυτός ο γενικευμένος μετασχηματισμός του πεδίου μπορεί να θεωρηθεί ως κατάλοιπο της (σπασμένης) καθολικής συμμετρίας.

Δυναμικά με καθολική συμμετρία

Προκειμένου να εξηγήσουμε το μηχανισμό σπασίματος της συμμετρίας ορίζουμε τον τελεστή \hat{O}_F ο οποίος δρα πάνω στο $\mathcal{A}(x)$ ως εξής:

$$\hat{O}_F \mathcal{A}(x) = \mathcal{A}(F(x)), \quad (\Gamma.14)$$

όπου ο δείκτης F υποδηλώνει μετασχηματισμό μετατόπισης ή αντιστροφής. Υλοποίηση της καθολικής συμμετρίας F έχουμε όταν ο \hat{O}_F μετατίθεται με τον τελεστή Helmholtz:

$$\Omega = \frac{d^2}{dx^2} + \mathcal{W}(x), \quad (\Gamma.15)$$

οπότε το γενικευμένο δυναμικό $\mathcal{W}(x)$ μετασχηματίζεται συνολικά κάτω από το μετασχηματισμό F και το πεδίο $\mathcal{A}(x)$ είναι ιδιοσυνάρτηση του \hat{O}_F με ιδιοτιμή λ_F :

$$\hat{O}_F \mathcal{A}(x) = \lambda_F \mathcal{A}(x). \quad (\Gamma.16)$$

Το απλούστερο σενάριο για να σπάσουμε την καθολική συμμετρία είναι να εξακολουθεί να ισχύει η μετάθεση

$$[\Omega, \hat{O}_F] = 0$$

αλλά το πεδίο $\mathcal{A}(x)$ να μην είναι πλέον ιδιοσυνάρτηση του \hat{O}_F , έχοντας παραβιάσει τη συμμετρία της ασυμπτωτικής συμπεριφοράς του $\mathcal{A}(x)$. Αυτή είναι μία τυπική περίπτωση σκέδασης από το δυναμικό $\mathcal{W}(x)$ όπου τα προσπίπτοντα κύματα φτάνουν μόνο από τη μία μεριά του δυναμικού.

Από τις Εξ. (Γ.12), (Γ.14) μπορούμε να γράψουμε:

$$\hat{O}_F \mathcal{A}(x) = \frac{\tilde{Q}}{J} \mathcal{A}(x) - \frac{Q}{J} \mathcal{A}^*(x) \quad ; \quad \forall x \in \mathbb{R} \quad (\Gamma.17)$$

η οποία υποδεικνύει ότι ένα μη μηδενικό Q μία εκδήλωση της σπασμένης καθολικής συμμετρίας κάτω από μετασχηματισμούς μετατόπισης ή αντιστροφής.

Ανάκτηση των θεωρημάτων Bloch και ομοτιμίας

Ο μηδενισμός του Q έχει ενδιαφέρουσες επιπτώσεις στο πεδίο $\mathcal{A}(x)$. Εδώ θα δείξουμε πώς μπορούμε να ανακτήσουμε τα θεωρήματα Bloch και ομοτιμίας όταν η καθολική συμμετρία αποκαθίσταται.

Αντιστροφή ($\sigma = -1$)

Στην περίπτωση της αντιστροφής, για $Q = 0$, ολοκληρώνουμε την Εξ. (Γ'.8) και καταλήγουμε στις σχέσεις:

$$\mathcal{A}(2\alpha - x) = c\mathcal{A}(x) \quad ; \quad \mathcal{A}'(2\alpha - x) = -c\mathcal{A}'(x) \quad (\text{Γ'.18})$$

όπου c είναι μία σταθερά ολοκλήρωσης η οποία υπολογίζεται πηγαίνοντας στο κέντρο της αντιστροφής $x = \alpha$, αφού η Εξ. (Γ'.8) γίνεται $\mathcal{A}(\alpha)\mathcal{A}'(\alpha) = 0$. Υποθέτοντας ότι $\mathcal{A}(\alpha) \neq 0$ και $\mathcal{A}'(\alpha) = 0$ βρίσκουμε $c = 1$ ενώ αν $\mathcal{A}(\alpha) = 0$ και $\mathcal{A}'(\alpha) \neq 0$ καταλήγουμε ότι $c = -1$. Συνεπώς για $Q = 0$ η κυματική συνάρτηση $\mathcal{A}(x)$ γίνεται ιδιοσυνάρτηση του τελεστή της καθολικής ομοτιμίας $\hat{O}_F \equiv \hat{\Pi}_\alpha$ του οποίου η δράση προκαλεί μια αντιστροφή γύρω από το σημείο στο α . Επίσης για $Q = 0$, η Εξ. Γ'.11 γίνεται:

$$\left| \tilde{Q} \right|^2 = -J^2,$$

και η οποία υποδεικνύει ότι $\tilde{Q} = J = 0$. Κατά συνέπεια για τη συμμετρία της ομοτιμίας το σενάριο της καθολικής συμμετρίας υλοποιείται είτε σε προβλήματα δέσμιων καταστάσεων είτε σε προβλήματα σκέδασης στα οποία το ρεύμα είναι μηδενικό. Τέτοιες καταστάσεις, διατηρούν την καθολική συμμετρία και περιγράφονται στο Κεφ. (5).

Μετάθεση ($\sigma = 1$)

Στην περίπτωση της καθολικής συμμετρίας μετάθεσης, για $\sigma = 1$ και $Q = 0$ η Εξ. (Γ'.17) παίρνει τη μορφή εξίσωσης ιδιοτιμών. Τότε, από την Εξ. (Γ'.11) προκύπτει ότι:

$$\left| \frac{\tilde{Q}}{J} \right| = 1 \quad (\text{Γ'.19})$$

και κατά συνέπεια ο όρος $\frac{\tilde{Q}}{J}$ γίνεται μια φάση, το οποίο είναι σύμφωνο με το γεγονός ότι είναι ιδιοτιμή του τελεστή μετατόπισης $\hat{O}_F \equiv \hat{T}_L$.

Η καθολική συμμετρία μετατόπισης προϋποθέτει ένα άπειρο, περιοδικό σύστημα του οποίου το δυναμικό ικανοποιεί $\mathcal{W}(x) = \mathcal{W}(x + L)$ για κάθε $x \in \mathbb{R}$. Είναι τότε εμφανές ότι θα ισχύει και η σχέση $\mathcal{W}(x) = \mathcal{W}(x + nL)$ με $n \in \mathbb{Z}$. Σε ένα πεπερασμένο σύστημα τα \tilde{Q} θα διαφέρουν μεταξύ τους ανάλογα με το μέγεθος της μετατόπιση που

εκφράζεται με το n . Ως εκ τούτου εισάγουμε το μέγεθος \tilde{Q}_{nL} το οποίο υποδηλώνει ότι αντιστοιχεί σε μετατόπιση nL . Έτσι Η Εξ. (Γ.12) γενικεύεται ως:

$$\begin{aligned} \mathcal{A}(x+L) &= e^{i\theta(L)} \mathcal{A}(x) & ; & & \theta(L) &= \theta_{\tilde{Q}_L} \\ \tilde{Q}_L &= \pm |J| e^{i\theta_{\tilde{Q}_L}} \end{aligned} \quad (\Gamma.20)$$

Εξαιτίας της άπειρης περιοδικότητας το \tilde{Q}_L θα είναι το ίδιο για κάθε $x \in \mathbb{R}$. Με τη βοήθεια της Εξ. (Γ.12) μπορούμε να συσχετίσουμε την τιμή του πεδίου $\mathcal{A}(x+nL)$ με την αντίστοιχή στο x $\mathcal{A}(x)$ είτε μέσω n μετατοπίσεων κατά L η με μία μετατόπιση κατά nL . Η μοναδικότητα της κυματοσυνάρτησης τότε απαιτεί:

$$\begin{aligned} \mathcal{A}(x+nL) &= e^{i\theta(nL)} \mathcal{A}(x) = (e^{i\theta(L)})^n \mathcal{A}(x) \\ \Rightarrow \theta(nL) &= n\theta(L) \end{aligned} \quad (\Gamma.21)$$

απ' όπου προκύπτει ότι $\theta(L) = kL$ με k μια σταθερά διαστάσεων αντίστροφου μήκους. Ερμηνεύοντας τη σταθερά k ως την κρυσταλλική ορμή, έχουμε την ανάκτηση του θεωρήματος Bloch για το άπειρο, περιοδικό σύστημα.

Δυναμικά με τοπική συμμετρία

Το δεύτερο - και πιο απαιτητικό - σενάριο για το σπάσιμο της συμμετρίας επιτάσσει η συμμετρία του δυναμικού να μην ικανοποιείται σε όλο το χωρικό του εύρος, σε αντίθεση με την προαναφερθείσα περίπτωση που ίσχυε $\mathcal{W}(x) = \mathcal{W}(F(x))$ για κάθε x εντός του δυναμικού. Σε αυτή την περίπτωση ο τελεστής \hat{O}_F δε μετατίθεται με τον τελεστή $\hat{\Omega}$ και δε μπορούμε να αναζητήσουμε ιδιοκαταστάσεις του αντίστοιχου τελεστή, εκτός αν είναι δυνατή η τμηματική δράση ενός τελεστή τοπικής συμμετρίας - αν υφίσταται τέτοια - όπως περιγράφεται στο Κεφ. (4). Παρ' όλα αυτά, καταστάσεις σπασμένης συμμετρίας στο δυναμικό, η οποία διατηρείται σε τοπικό επίπεδο, μπορούν να αντιμετωπιστούν μέσω των αναλλοίωτων Q, \tilde{Q} , τα οποία συσχετίζουν με άμεσο τρόπο την επίδραση της συμμετρίας στα πλάτη των πεδίων $\mathcal{A}(x)$.

Στην ακραία περίπτωση που υπάρχει πλήρες σπάσιμο στη συμμετρία του δυναμικού, δηλαδή δεν υπάρχει κανένα χωρίο \mathcal{D}_n για το οποίο να υπάρχει κάποιο κατάλοιπο της καθολικής συμμετρίας στο δυναμικό $\mathcal{W}(x)$, τα Q, \tilde{Q} δε θα παραμένουν αναλλοίωτα σε καμία περιοχή, όπως αναμένουμε. Αν και θα υφίστανται ως συναρτήσεις της θέσης, η μη-διατηρησιμότητά τους δεν επιφέρει κάποιο πλεονέκτημα στην περιγραφή της σκέδασης.

Το ενδιαφέρον εντοπίζεται στις περιπτώσεις όπου σε ένα ή περισσότερα χωρία \mathcal{D}_n για τα οποία ισχύει $\mathcal{W}(x) = \mathcal{W}(F(x))$, $\forall x \in \mathcal{D}_n$, δηλαδή η αντίστοιχη συμμετρία ικανοποιείται τοπικά στα συγκεκριμένα χωρία, ως κατάλοιπο της σπασμένης καθολικής συμμετρίας. Στην περίπτωση αυτή, η προηγούμενη ανάλυση οδηγεί σε ένα

ζεύγος Q_n, \tilde{Q}_n για κάθε ένα χωρίο D_n , τα οποία με τη σειρά τους επιτρέπουν τον προσδιορισμό του πεδίου $\mathcal{A}(F(x))$ από το $\mathcal{A}(x) \forall x \in D_n$.

Η μέθοδος της τοπικής ομοτιμίας στη σκέδαση

Επικεντρωνόμαστε τώρα στη συμμετρία της ομοτιμίας όταν αυτή ικανοποιείται μόνο τοπικά, σε συγκεκριμένα χωρία. Συγκεκριμένα, μελετάμε διατάξεις οι οποίες αποσυντίθενται πλήρως σε πεπερασμένα χωρία στα οποία ικανοποιείται ξεχωριστά η συμμετρία της ομοτιμίας. Έτσι, έχουμε διατάξεις εν γένει απεριοδικές και μη συμμετρικές οι οποίες όμως διατηρούν ακριβείς συμμετρίες σε διαφορετικές, τοπικές κλίμακες. Η θεώρηση αυτή έχει ιδιαίτερες επιπτώσεις στις ιδιότητες διέλευσης του συστήματος και συγκεκριμένα στους συντονισμούς πλήρους διέλευσης (ΣΠΔ). Ο εντοπισμός των αναλλοίωτων μεγεθών Q_n, \tilde{Q}_n για κάθε τοπικά συμμετρικό τμήμα του δυναμικού στο αντίστοιχο χωρίο D_n επιτρέπει μία γεωμετρική ερμηνεία των ΣΠΔ στο μιγαδικό επίπεδο, η οποία με τη σειρά της οδηγεί σε μία κατηγοριοποίηση των καταστάσεων σκέδασης, γύρω από τους ΣΠΔ. Συγκεκριμένα μπορούμε να δείξουμε ότι υπάρχουν:

- i Συμμετρικοί ΣΠΔ, στους οποίους το μέτρο του πεδίου $\mathcal{A}(x)$ ακολουθεί ακριβώς τη συμμετρία της τοπικής ομοτιμίας στα (κατοπτρικά συμμετρικά) χωρία που μπορεί να χωριστεί η διάταξη. Αυτοί οι συντονισμοί μπορούν να αναπαρασταθούν στο μιγαδικό επίπεδο μέσω των Q_n ως συγγραμικά διανύσματα στον άξονα των φανταστικών.
- ii Μη-συμμετρικοί ΣΠΔ, στους οποίους το μέτρο του πεδίου $\mathcal{A}(x)$ δεν είναι συμμετρικό στις εκάστοτε συμμετρικές υποπεριοχές. Αυτοί οι συντονισμοί αναπαρίστανται (μέσω των Q_n) στο μιγαδικό επίπεδο ως κλειστές τροχιές.
- iii Καταστάσεις που δεν είναι ΣΠΔ. Αυτές οι καταστάσεις σχηματίζουν ανοιχτές τροχιές στο μιγαδικό επίπεδο.

Οι παραπάνω διαπιστώσεις έρχονται να διαφωτίσουν το μηχανισμό που υπόκειται κατά την εμφάνιση ΣΠΔ, ένα ζήτημα το οποίο δεν ήταν ξεκαθαρισμένο στην υπάρχουσα βιβλιογραφία. Επιπλέον, η προτεινόμενη κατηγοριοποίηση αποφεύγει αλληλοεπικαλύψεις που εμφανίζονται σε άλλες προσεγγίσεις.

Τέλος, διαπιστώνουμε πώς οι συνύπαρξη πολλαπλών κλιμάκων συμμετρίας στην ίδια διάταξη επιτρέπει το σχεδιασμό απεριοδικών διατάξεων κυματικής σκέδασης οι οποίες εμφανίζουν ΣΠΔ σε προεπιλεγμένες ενέργειες. Για το σκοπό αυτό αναπτύσσουμε και προτείνουμε μία “κατασκευαστική αρχή” οι οποία εκμεταλλεύεται τη συμμετρία της τοπικής ομοτιμίας μιας μη-συμμετρικής διάταξης και μέσω της οποίας καθορίζονται τα χαρακτηριστικά της ώστε να εμφανίζει ΣΠΔ στις επιθυμητές ενέργειες.

BIBLIOGRAPHY

- [1] A. Zee, *Fearful Symmetry: The Search for Beauty in Modern Physics*, Princeton University Press, New Jersey, USA, (2007).
- [2] D. J. Gross, Proc. Nat. Acad. Sci. U.S.A. **93**, 14256 (1996).
- [3] M. Kaku, *Quantum Field Theory, A modern Introduction*, Oxford University Press, New York, USA, (1993).
- [4] J. Echeverria, A. Carreras, D. Casanova, P. Alemany and S. Alvarez, Chem. Eur. J. **17**, 3359 (2011).
- [5] K. Grzeskowiak *et al* Biochemistry **32**, 8923 (1993).
- [6] R. A. Pascal, J. Phys. Chem. A **105**, 9040 (2001).
- [7] A-Li Chen, Yue-Sheng Wang and Chuanzeng Zhang, Physica B **407**, 324 (2012).
- [8] D. Shechtman, I. Blech, D. Gratias, and J. W. Cahn, Phys. Rev. Lett. **53**, 1951 (1984).
- [9] D. Levine and P. J. Steinhardt, Phys. Rev. Lett. **53**, 2477 (1984).
- [10] M. Widom, D. P. Deng and C. L. Henley, Phys. Rev. Lett. **63**, 310 (1989).
- [11] R. Lifshitz, Physica A **232**, 633 (1996).
- [12] P. Wochner *et al*, Proc. Natl. Acad. Sci. U.S.A. **106**, 11511 (2009).
- [13] E. Maciá, Rep. Prog. Phys. **69**, 397 (2006).
- [14] S. V. Zhukovsky, Phys. Rev. A **81**, 053808 (2010).
- [15] X. Q. Huang, S. S. Jiang, R. W. Peng, and A. Hu, Phys. Rev. B **63**, 245104 (2001).
- [16] R. W. Peng, X. Q. Huang, F. Qiu, Mu Wang, A. Hu, S. S. Jiang, and M. Mazzer, Appl. Phys. Lett. **80**, 3063 (2002).

- [17] R. W. Peng, Y. M. Liu, X. Q. Huang, F. Qiu, Mu Wang, A. Hu, S. S. Jiang, D. Feng, L. Z. Ouyang, and J. Zou, *Phys. Rev. B* **69**, 165109 (2004).
- [18] W. J. Hsueh, S. J. Wun, Z. J. Lin, and Y. H. Cheng, *J. Opt. Soc. Am. B* **28**, 2584 (2011)
- [19] D. K. Ferry and S. M. Goodnick, *Transport in Nanostructures* (Cambridge University Press, Cambridge, UK, 1997).
- [20] A. C. Hladky-Hennion, J. O. Vasseur, S. Degraeve, C. Granger, and M. de Billy, *J. Appl. Phys* **113**, 154901 (2013).
- [21] E. Maciá, *Rep. Prog. Phys.* **75**, 036502 (2012).
- [22] G.A. Luna-Acosta, F.M. Izrailev, N.M. Makarov, U. Kuhl and H.-J. Stöckmann, *Phys. Rev. B* **80**, 115112 (2009).
- [23] G. Couplier, C. Guthmann, Y. Noat, and M. Saint Jean, *Phys. Rev. E* **71**, 046105 (2005).
- [24] D.J. Griffiths and C.A. Steinke, *Am. J. Phys.* **69**, 137 (2001).
- [25] R.L. Kronig and W.G. Penney, *Proc. R. Soc. Lond. A.* **130**, 499 (1931).
- [26] N. W. Ashcroft and N. D. Mermin, *Solid State Physics*, Holt, Rinehart and Winston, New York, (1976).
- [27] G. Floquet, *Annales Scientifiques de l'E.N.S* **12**, 47 (1883).
- [28] F. Bloch, *Zeit. f. Phys.* **52**, 555 (1929).
- [29] E. Yablonovitch and T. J. Gmitter, *Phys. Rev. Lett.*, **63**, 1950 (1989).
- [30] J. D. Joannopoulos, S. G. Johnson, J. N. Winn, R. D. Meade, *Photonic Crystals Molding the Flow of Light*, Princeton University Press, New Jersey (2008).
- [31] K. Ohtaka, *Phys. Rev. B*, **19**, 5057 (1979).
- [32] J. W. Strutt (Lord Rayleigh), *Phil. Mag., S.*, **24**, 145 (1887).
- [33] J. W. Strutt, (Lord Rayleigh), *Phil. Mag., S.5*, **26**, 256 (1888).
- [34] M. Barbier, P. Vasilopoulos, and F. M. Peeters, *Phys. Rev. B* **80**, 205415 (2009).
- [35] M Ramezani Masir, P. Vasilopoulos and F. M. Peeters, *New J. Phys.* **11**, 095009 (2009).

- [36] S. Gattenlöhner, W. Belzig, and M. Titov, Phys. Rev. B **82**, 155417 (2010)
- [37] G. Bastard, *Wave Mechanics Applied to Semiconductor Heterostructures*, Halsted, New York, (1988).
- [38] Angel Sánchez, Enrique Maciá, and Francisco Domínguez-Adame, Phys. Rev. B **49**, 147 (1994)
- [39] F. M. Izrailev, A. A. Krokhin, and S. E. Ulloa, Phys. Rev. B **63**, 041102(R) (2001)
- [40] F. Domínguez-Adame, A. Sánchez, Phys. Lett. A, **159**, 153-157 (1991).
- [41] A. Alippi, A. Bettucci, and F. Craciun, *Ultrasonic waves in monodimensional periodic composites* in Physical Acoustics: Fundamentals and Applications, edited by O. Leroy and M. A. Breazeale, Plenum, New York, (1990)
- [42] M. Hammouchi, E. H. El Boudouti, A. Nougouai, B. Djafari-Rouhani, M. L. H. Lahlaouti, A. Akjouj, and L. Dobrzynski, Phys. Rev. B **59** (1999).
- [43] D. W. L. Sprung, H. Wu, and J. Martorell Am. J. Phys. **60**, 1118-1124 (1993).
- [44] M. Abramowitz and I. A. Stegun, *Handbook of Mathematical Functions* (Dover, New York, 1965), pp. 777, 782.
- [45] P. W. Anderson, Phys. Rev. **109**, 1492 (1958).
- [46] S. Fishman, D. R. Grempel, and R. E. Prange, Phys. Rev. Lett. **49**, 509 (1982)
- [47] G. Bergmann, Phys. Rep., **107**, 1-58 (1984)
- [48] F. Scheffold, R. Lenke, R. Tweert and G. Maret, Nature **398**, 206 (1999).
- [49] M. Kaveh, M. Rosenbluh, I. Edrei and I. Freund, Phys. Rev. Lett. **57**, 2049 (1986).
- [50] A. Z. Genack and J. M. Drake, Europhys. Lett. **11**, 331 (1990).
- [51] F. J. P. Schuurmans, M. Megens, D. Vanmaekelbergh and A. Lagendijk, Phys. Rev. Lett. **83**, 2183 (1999).
- [52] Sergey V. Gaponenko, *Introduction to Nanophotonics*, Cambridge University Press, Cambridge, UK (2010).
- [53] M. Imada, A. Fujimori, and Y. Tokura Rev. Mod. Phys. **70**, 1039 (1998).
- [54] M. Kohmoto, L. P. Kadanoff and C. Tang Phys. Rev. Lett. **50**, 1870 (1983).
- [55] M. Kohmoto, B. Sutherland and K. Iguchi, Phys. Rev. Lett. **58**, 2436 (1987).

- [56] M. Dulea, M. Severin, and R. Riklund, Phys. Rev. B **42**, 3680 (1990).
- [57] W. Gellermann, M. Kohmoto, B. Sutherland and P. C. Taylor, Phys. Rev. Lett. **72**, 633 (1994).
- [58] R. Merlin, K. Bajema, R. Clarke, F.Y. Juang and P. K. Bhattacharya, Phys. Rev. Lett. **55**, 1768 (1985).
- [59] E. Maciá, Appl. Phys. Lett. **73**, 3330 (1998).
- [60] E. Maciá, Phys. Rev. B **63**, 205421 (2001).
- [61] E. Maciá, Rep. Prog. Phys. **75**, 036502 (2012).
- [62] M.H. Tyc, W. Salejda, Physica A **303**, 493 (2002).
- [63] Luca Dal Negro, *Optics of Aperiodic Structures, Fundamentals and Device Applications*, Taylor and Francis (2014).
- [64] E. Maciá, *Aperiodic Structures in Condensed Matter: Fundamentals and Applications*, Taylor and Francis, London (2009).
- [65] R. Nava, J. Taguena-Martinez, J. A. del Rio, and G. G. Naumis, J. Phys.: Condens. Matter **21**, 155901 (2009).
- [66] P. A. Kalozoumis, C. Morfonios, F. K. Diakonov and P. Schmelcher, Phys. Rev. A **87**, 032113 (2013).
- [67] P. A. Kalozoumis, C. Morfonios, N. Palaiodimopoulos, F. K. Diakonov and P. Schmelcher, Phys. Rev. A **88**, 033857 (2013).
- [68] M. Senechal, *Quasicrystals and Geometry* Cambridge University Press (1996).
- [69] T. Janssen, G. Chapuis and M. De Boissieu, *Aperiodic Crystals: From Modulated Phases to Quasicrystals* Oxford University Press, USA (2007).
- [70] Z. Valy Vardeny, A. Nahata and A. Agrawal, Nat. Phot. **7**, 177 (2013).
- [71] M. Dulea, M. Johansson and R. Riklund, Phys. Rev. B **45**, 105 (1992).
- [72] Z. Cheng, R. Savit, and R. Merlin, Phys. Rev. B **37**, 4375 (1988).
- [73] N. Liu, Phys. Rev. B **55**, 3543 (1997).
- [74] W. Steurer and D. Sutter-Widmer, J. Phys. D **40**, R229 (2007).

- [75] E. Maciá and F. Dominguez-Adame, *Electrons, Phonons and Excitons in Low Dimensional Aperiodic Systems*, Editorial Complutense, Madrid (2000).
- [76] E. L. Albuquerque and M. G. Cottam, Phys. Rep. **376**, 225 (2003).
- [77] E. L. Albuquerque and M. G. Cottam, *Polaritons in Periodic and Quasiperiodic Structures*, Elsevier, Amsterdam (2004).
- [78] J. M. Dubois, *Useful Quasicrystals* World Scientific, Singapore (2005).
- [79] A. Endo and Y. Iye, Phys. Rev. B **78**, 085311 (2008).
- [80] P. Panchadhyayee, R. Viswas, C. Sinha C and P. K. Mahapatra, J. Phys.: Condens. Matter **20**, 445229 (2008)
- [81] W. J. Hsueh, C. H. Chen and J. A. Lai J, Eur. Phys. J. B **73**, 503 (2010).
- [82] K. Fradkin-Kashi and A. Arie, IEEE J. Quantum Electron **35**, (1649).
- [83] K. Fradkin-Kashi, A. Arie, P. Urenski and G. Rosenman, Phys. Rev. Lett. **88**, 023903 (2002).
- [84] R. Lifshitz, A. Arie and A. Bahabad, Phys. Rev. Lett. **95**, 133901 (2005).
- [85] B. B. Mandelbrot, *The Fractal Geometry of Nature*, Macmillan, New York, (1982).
- [86] J. Feder, *Fractals*, Plenum Press, New York, (1988).
- [87] D. L. Jaggard and X. Sun, Opt. Lett. **15**, 1428 (1990).
- [88] X. Sun and D. L. Jaggard, J. Appl. Phys. **70**, 2500 (1991).
- [89] C. Sibilia, I. S. Nefedov, M. Scalora and M. Bertolotti, J. Opt. Soc. Amer. B **15**, 1947 (1998).
- [90] S. V Zhukovsky, S. V Gaponenko and A. V Lavrinenko, Nonlinear Phenomena in Complex Systems **4**, 383 (2001).
- [91] A. V. Lavrinenko, S. V. Zhukovsky, K. S. Sandomirski, and S. V. Gaponenko, Phys. Rev. E **65**, 036621 (2002).
- [92] S. V. Zhukovsky, A. V. Lavrinenko, and S. V. Gaponenko, Europhys. Lett. **66**, 455 (2004).
- [93] S. V Zhukovsky, S. V Gaponenko and A. V. Lavrinenko, Bulletin Russ. Acad. Sci. (Physics) **68**, 29 (2004).

- [94] K. Machida and M. Fujita, Phys. Rev. B **34**, 7367 (1986).
- [95] M. Kohmoto and B. Sutherland, Phys. Rev. B **35**, 1020 (1987).
- [96] E. Maciá and F. Dominguez-Adame, Phys. Rev. Lett. **60**, 10032 (1996).
- [97] E. Maciá, Phys. Rev. B **60**, 10032 (1999).
- [98] A. Suto, J. Stat. Phys. **56**, 525 (1989).
- [99] L. Dal Negro, J. H. Yi, V. Nguyen, Y Yi, J. Michel, and L. C. Kimerling, Appl. Phys. Lett. **86**, 261 (2005).
- [100] X. Huang, Y.Wang, and C. Gong, J. Phys.: Condens. Matter **11**, 7645 (1999).
- [101] L. Moretti , I. Rea, L. De Stefano and I. Rendina, Appl. Phys. Lett. **90**, 191112 (2007)
- [102] C. Morfonios, P. Schmelcher, P. A. Kalozoumis and F. K. Diakonov, arXiv:1307.1838.
- [103] D. Colton and R. Kress, *Inverse Acoustic and Electromagnetic Scattering Theory*, Springer, New York (2013).
- [104] N. Zettili, *Quantum Mechanics Concepts and Applications*, John Wiley and Sons (2009).
- [105] P. A. Kalozoumis, C. Morfonios, F. K. Diakonov and P. Schmelcher, submitted to Phys. Rev. Lett. (<http://arxiv.org/pdf/1403.7149.pdf>).
- [106] S. Weinberg, Phys. Rev. Lett. **17**, 616 (1966).
- [107] G. L. Squires, *Introduction to the Theory of Thermal Neutron Scattering*, Cambridge University Press, New York (2012).
- [108] A. Guinier, *X-ray Diffraction in Crystals, Imperfect Crystals, and Amorphous Bodies*, Dover Publications Inc, New York (1994).
- [109] L. J. P. Ament, M. van Veenendaal, T. P. Devereaux, J. P. Hill and J.van den Brink, Rev. Mod. Phys. **83**, 705 (2011).
- [110] M. Shibayama, Polymer Journal **43**, 18 (2011).
- [111] M. V. Petoukho and D. I. Svergun, *Small Angle X-Ray Scattering/Small Angle Neutron Scattering as Methods Complementary to NMR, in NMR of Biomolecules: Towards Mechanistic Systems Biology* (eds I. Bertini, K. S. McGreevy and G. Parigi), Wiley-VCH Verlag GmbH and Co. KGaA, Weinheim, Germany (2012)

- [112] P. Markoš, C. M. Soukoulis, *Wave Propagation From Electrons to Photonic Crystals and Left-Handed Materials*, Princeton University Press, New Jersey (2008)
- [113] P.A. Mello and N. Kumar, *Quantum Transport in Mesoscopic Systems: Complexity and Statistical Fluctuations*, Oxford University Press, New York (2004).
- [114] G. J. Ferreira, M. N. Leuenberger, D. Loss, and J. C. Egues, *Phys. Rev. B* **84**, 125453 (2011).
- [115] O. Deparis, *Optics Letters*, **36**, 3962 (2011)
- [116] K. Verdière, R. Panneton, S. Elkoun, T. Dupont and P. Leclaire, *POMA* **19**, 065011 (2013).
- [117] L. L. Sánchez-Sotoa, J. J. Monzóna, A. G. Barriusoa, J. F. Cariñenab, *Phys. Rep.* **513**, 191 (2012).
- [118] F. S. Levin, *An Introduction to Quantum Theory*, Cambridge University Press, Cambridge, UK (2002).
- [119] H. Zabrodsky, S. Peleg, D. Avnir, *J. Am. Chem. Soc.* **114**, 7843 (1992).
- [120] M. Pinsky, D. Casanova, P. Alemany, S. Alvarez, D. Avnir, C. Dryzun, Z. Kizner, A. Sterkin, *J. Comput. Chem.* **29**, 190 (2008).
- [121] N. L. Chuprikov, O. D. Spiridonova, *J. Phys. A* **39**, L559 (2006).
- [122] M. Werchner, M. Schafer, M. Kira, S. W. Koch, J. Sweet, J.D. Olitzky, J. Hendrickson, B. C. Richards, G. Khitrova, H. M. Gibbs, A. N. Poddubny, E. L. Ivchenko, M. Voronov and M. Wegener, *Opt. Express* **17**, 6813 (2009).
- [123] W. J. Hsueh, C. H. Chen, R. Z. Qiu, *Phys. Lett. A* **377**, 1378 (2013).
- [124] S. V. Zhukovsky and S. V. Gaponenko, *Phys. Rev. E* **77**, 046602 (2008).
- [125] P. W. Mauriz, M. S. Vasconcelos, and E. L. Albuquerque, *Phys. Lett. A* **373**, 496 (2009).
- [126] H. Yamamoto, K. Tsuji and K. Taniguchi, *Phys. Stat. Sol. B* **188**, 679 (1995).
- [127] G. García-Calderón, *Solid State Commun.* **62**, 441 (1987); G. Garcia-Calderón
- [128] Ye Lu, R. W. Peng, Z. Wang, Z. H. Tang, X. Q. Huang, Mu Wang, Y. Qiu, A. Hu, S. S. Jiang, and D. Feng, *J. Appl. Phys.* **97**, 123106 (2005).
- [129] V. Grigoriev and F. Biancalana, *New J. Phys.* **12** 053041 (2010).

- [130] W. Chen and D. L. Mills, Phys. Rev. B **35**, 524 (1987)
- [131] D. S. Wiersma *et al.*, J. Opt. A: Pure Appl Opt. **7**, S190 (2005).
- [132] A. Poddubny and E. Ivchenko, Physica E **42**, 1871 (2010).
- [133] L. Dal Negro and S. V. Boriskina, Las. Phot. Rev. **6**, 178 (2012).
- [134] G. F. Karavaev, N. L. Chuprikov, Russ. Phys. J. **36**, 749 (1993)
- [135] H. Rabitz, R. de Vivie-Riedle, M. Motzkus, K. Kompa, Science **288**, 824 (2000).
- [136] R. Gilmore, *Elementary quantum mechanics in one dimension*, The Johns Hopkins University Press, Baltimore (2004).
- [137] D. Meshulach and Y. Silberberg, Nature **396**, 239 (1998).
- [138] S.B. Zheng and G.C. Guo, Phys. Rev. Lett. **85**, 2392 (2000).
- [139] D. Goldhaber-Gordon, V.A. McLean, M.S. Montemerlo, J.C. Love, G.J. Opiteck, J.C. Ellenbogen, Proceedings of the IEEE **85**, 521 (1997).
- [140] F.J.G. de Abajo, Science **339**, 917 (2013).
- [141] C.A. Macaluso and J.P. Dalmont, J. Acoust. Soc. Am **129**, 404 (2011).
- [142] O. Richoux and V. Pagneux, Europhys. Lett. **59**, 34 (2002).
- [143] R. Renner, Nat. Phys. **3**, 645 (2007).
- [144] J.C. Hernández-Herrejón, F.M. Izrailev and L. Tessieri, J. Phys. A **43**, 425004 (2010).
- [145] O. Dietz, U. Kuhl, J. C. Hernández-Herrejón and L. Tessieri, New J. Phys. **14** 013048 (2012).
- [146] R. Peierls, Nucl. Phys. A **265**, 443 (1976).
- [147] C. Morfonios, D. Buchholz and P. Schmelcher, Phys. Rev. B **80**, 035301 (2009).
- [148] S. Roche, Phys. Rev. Lett. **91**, 108101 (2003)
- [149] A. Nomata and S. Horie, Phys. Rev. B **76**, 235113 (2007)

This research has been co-financed by the European Union (European Social Fund – ESF) and Greek national funds through the Operational Program “Education and Lifelong Learning” of the National Strategic Reference Framework (NSRF) - Research Funding Program: Heracleitus II. Investing in knowledge society through the European Social Fund.



European Union
European Social Fund



MINISTRY OF EDUCATION & RELIGIOUS AFFAIRS, CULTURE & SPORTS
M A N A G I N G A U T H O R I T Y

Co-financed by Greece and the European Union

